Republic of Iraq

Ministry of Higher Education and Scientific Research

Kerbala University/College of Engineering

Civil Engineering Department

Reactive Powder Concrete- Filled Double Skin Tubular Column Subjected to Repeated Loading

A Thesis Submitted to the Department of Civil Engineering, University of Kerbala in Partial Fulfillment of the Requirements for the Degree of Master of Science in Civil Engineering

(Infrastructure Engineering)

By

Ahmed Wafi Abbas

BSc. in Civil Engineering-2017

Supervised by

Assist prof. Dr. Bahaa Hussain Mohammed

Prof. Dr. Ali Hameed Naser

2021, A.D. 1443, A.H.

بِسْمِ اللَّـهِ الرَّحْمَـٰنِ الرَّحِيمِ

{يَرْفَعِ اللَّهُ الَّذِينَ آمَنُوا مِنْكُمْ وَالَّذِينَ أُوتُوا الْعِلْمَ دَرَجَاتٍ}

صَدَقَ اللهُ العَلِيُّ العَظيم

(المجادلة–الآية 11)

Supervisors Certification

We certify that this thesis titled "**Reactive powder Concrete - Filled Double Skin Tubular Column Subjected to repeated Loading**" which is being submitted by "**Ahmed Wafi Abbas**" was prepared under our supervision at the University of Kerbala in partial fulfillment of the requirements for the degree of Master of Science in Civil Engineering "**INFRASTRUCTURE**".

Signature: Dr. Ali Hameed

Name: **Prof.** Dr. **Ali Hameed Naser**

Date: 27 / 10 / 2021

Signature:

Name: **Assist Prof.** Dr. **Bahaa Hussain Mohammed**

Date: 27 / 10 / 2021

LINGUISTIC CERTIFICATE

I certify that this thesis entitled " **Reactive powder Concrete - Filled Double Skin Tubular Column Subjected to repeated Loading**) " which is prepared by Ahmed Wafi Abbas under my linguistic supervision. It was amended to meet the English style.

Signature:

Linguistic Supervisor

Asst. Lecturer Noor Husam Jaber

Date: / / 2021

Examination Committee Certification

We certify that we have read this thesis titled " **Reactive powder Concrete - Filled Double Skin Tubular Column Subjected to repeated Loading** " and as an examining committee, we examined the student "**Ahmed Wafi Abbas**" in its content and that in our opinion, it meets the standard of a thesis for the degree of the Master of Science in Civil Engineering "**INFRASTRUCTURE**".

Member and Supervisor

Signature:

Name: **Prof.** Dr. **Ali Hameed Naser**

Data: / /2021

Member and Supervisor

Signature:

Name: **Assist Prof.** Dr. **Bahaa Hussain Mohammed**

Data: 27 / 10 /2021

Member

Signature:

Name: **Assist Prof.** Dr. **Ali Ghanim Abbas Al-Khafaji**

Data: / /2021

Member

Signature:

Name: **Assist. Prof.** Dr. **Muslim Abdul-Ameer Khudhair Al-Kannoon**

Data: / /2021

Chairman

Signature:

Name: Assist. **Prof.** Dr. **Sadjad Amir Hemzah**

Data: / /2021

Approved by the Head of Civil Engineering Department

Signature:

Name: Dr. **Raid R. A. Almuhanna**

Data: 27 / 10 /2021

Approved by the Dean of Collage of Engineering

Signature:

Name: **Assist. Prof. Dr. Laith Sh. Rasheed**

Data: / /2021

Acknowledgements

Firstly, my great thanks to ***ALLAH*** *for enabling me to complete my works.*

I would like to express my gratitude and thanks to our supervisors, Assist ***prof. Dr. Bahaa Hussain Mohammed*** *and* ***Prof. Dr. Ali Hameed Naser*** *for their great assistance, guidance and valuable suggestions throughout the research period.*

I would also like to thank ***Dr. Dhafer Mohsin*** *and* ***Dr. Aymen jameel*** *for their assistance to me on several occasions during the research period. Thanks also to the head and the staff in the Civil Engineering department, the construction materials laboratory and all those who stood with me to complete this work.*

A special thank and gratitude to my family especially ***My Father*** *and* ***My Mother*** *for their care, patience and encouragement throughout the research period.*

Finally, I would like to express my extreme love and appreciation to everyone who has supported this work.

Ahmed Wafi Abbas

Abstract

Double skin concrete filled column consist of two-tube steel section filled with Reactive Powder Concrete is one of the methods that combine the properties of concrete and steel and faster in construction with better load carrying capacity. The present method consists of welding two tubes of steel of different sections concentrically, then filling the gap between them with reactive powder concrete in this study. The current study consists of practical part that relates to casting fourteen a composite column included seven sections for circular and square type with different variables to know their axial performance. They were divided into three groups, the first group was not filled, the second group was filled with ordinary concrete and the third group was filled with reactive powder concrete. All columns had dimensions of cross section (100 *100) and (50*50) mm for outer and inner square section and a diameter of (100) and (50) mm for outer and inner circular section with a thickness of 2.2 mm. Lengths of the samples were 800 mm but only two of the columns were 700mm. The properties of the tube were checked by AISC code, which achieves acceptable performance through local buckling. The steel tubes were connected doubly by welding the inner and outer tube concentrically. The variables of the practical part included: the percentage of steel fibers in the concrete mixture of about 0.5% and 1.5%, cross-sectional area of the concrete, length of the column, addition of shear ties by welding to the inner tube of the column and the type of concrete. The load was applied axially and concentrated on the column. The results of the work showed that the steel pipes filled with reactive powder concrete gave a high maximum resistance compared with normal concrete if used. Also, it was found the inner tubes of the columns that enhanced with shear connector along its overall length, led to increase the strength of columns filled with reactive powder concrete. The experimental results of the maximum strength were compared with the design strengths of the American Institute of Steel construction (AISC), American Concrete Institute (ACI), and the European Code (EN 2004). The mentioned design criteria

gave a better and more conservative expectation for square steel sections than for circular sections.

CONTENTS

LIST OF FIGURES

LIST OF Plates

LIST OF TABLES

ABBREVIATIONS

Symbol	Description
CFDST	Concrete Filled Double Skin Tube
CFT	Concrete Filled Tube
CFST	Concrete Filled Steel Tube
CHS	Circular Hollow Section
SHS	Square Hollow Section
RHS	Rectangular Hollow Section
RPC	Reactive Powder Concrete
CFTC	Concrete Filled Tube Circular
LVDTs	Linear Voltage Displacement Transducers
CFDSCT	Concrete Filled Double Skin Circular Tube
CFRP	Carbon Fiber Reinforcement Polymer
HDSCF	Hybrid Double Skin Concrete Filled Circular Steel Tube
RuCFDT	Rubberized Concrete Filled Double Skin Steel Tube
UHPFRC	Ultra-High-Performance Fiber-Reinforced Concrete
UHPC	Ultra-High-Performance Concrete
CFDSCT	Concrete Filled Double Skin Circular Tube
CFDSST	Concrete Filled Double Skin Square Tube
NC	Normal Concrete
RC	Reinforced Concrete
RPC	Reactive Powder Concrete
UAE	United Arabian Emirates
UHPC	Ultra-High-Performance Concrete
B.S	British Standard
ASTM	American Society for Testing and Materials
ACI	American Concrete Institute

NOTATION

Symbol	Description
(e / D)	Eccentric Ratio
D	Diameter of Circular Section (mm)
Di / ti	Inner Diameter to Inner Thickness Ratio
Do /to	Outer Diameter to Outer Thickness Ratio
(L/B)	Global Slenderness Ratio
(L / D)	Length to Diameter Ratio of Column
MPa	Mega Pascal (N/mm^2)
Es	Modulus of Elasticity of Steel (Mpa)
L/D	Aspect Ratio of Steel Fiber
Fy	Yields Stress of Steel (Mpa)
Ec	Modules of Elasticity of Concrete (Mpa)
$f'c$	Cylinder Compressive Strength of Concrete (Mpa)
Δmax.	Maximum Deflection (Mm)
Δy	Deflection of The Material Reaches to Yielding
Δu	Deflection of Ultimate Load
μΔ	Ductility Index

CHAPTER ONE

CHAPTER ONE

INTRODUCTION

1.1 General

Concrete filled double skin tube members (CFDST) is a brand-new class of traditional members filled with concrete, which is a double tube place centrally and concrete sandwich between them. It usually possesses the same traditional pipes properties filled with only concrete (CFT). They have lighter weight and a stronger bending rigidity, and as a way to speed up bridge building despite the expense. Concrete filled double skin tube (CFDST) columns are also expected to have higher fire resistance capacities than their (CFT) counterparts because the former interior tubes are effectively protected by sandwiched concrete under fire conditions [1].

Composite steel-concrete architecture is commonly used to design new buildings and bridges, including in high seismic-risk areas. Ideally, the combination structure incorporates the strengths of both steel and concrete. When the steel tube with concrete in the members filled with concrete (CFST) due to the effect of the interaction. The stresses of the concrete cause the local buckle of the steel tubes, in contrast, the tube serves to maintain the concrete constrained. The steel tubes may be a circular part (CHS), square part (SHS) or rectangular part (RHS) as shown in Figure(1.1) [2].

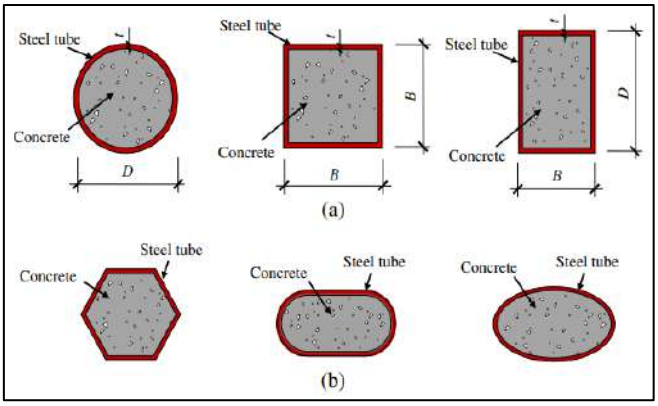

Fig(1.1): Traditional concrete filled steel cross sections [3]

1.2 Applications for Concrete Filled Steel Tubular (CFST)

Throughout the 1980s, concrete-filled steel pipes were used in construction to prevent making a column with extremely wide sizes. Since the 1990s, many different projects have been built in China. Several CFST-column buildings were built in the regions of Beijing and Fujian[4].To offer some insight into how the CFST column actually plays a significant role in civil engineering, some examples are given here. The use of CFST columns in composite steel floor structure is seen in plate (1.1), and in subway stations, steel tubular members are used as support column because they bear high axial pressure loads. The plate (1.2) shows an application of concrete filled tube columns used in a subway station. Guangzhou TV Astronomical and Sightseeing Tower is the third tallest in the world as seen in plate (1.3), it is situated at the corner of the Central Axes of Guangzhou New City and the Pearl River. The height of this tower is 600 (m) , the main body is (450 m) also antenna of (150 m) is included. Twenty-four circular tube members filled with concrete are used as an inclined column. The diameter of this pipe is 2 meters and the thickness is of 5 cm [3]. Also, of a rise building in China is SEG plaza in Shenzhen that uses this type of composite member shown in Plate (1.4).

Plate (1.1) Composite steel storey system [3].

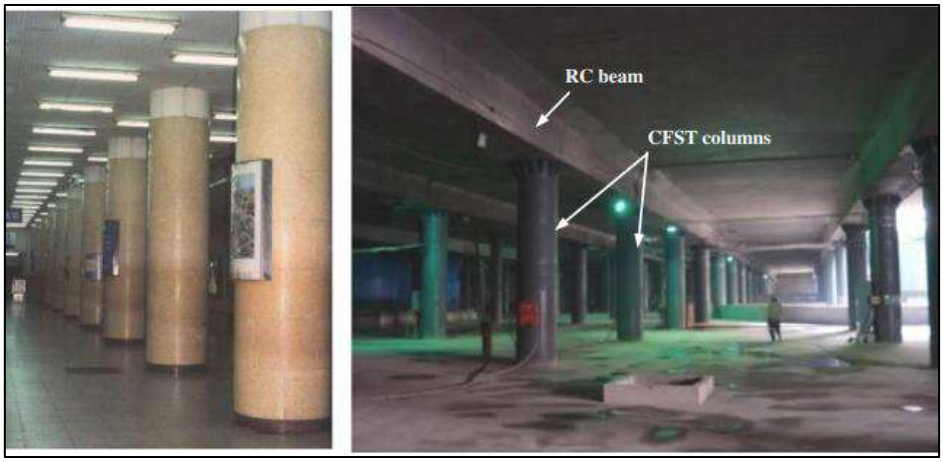

Plate (1.2) CFST columns used in a subway station [3]

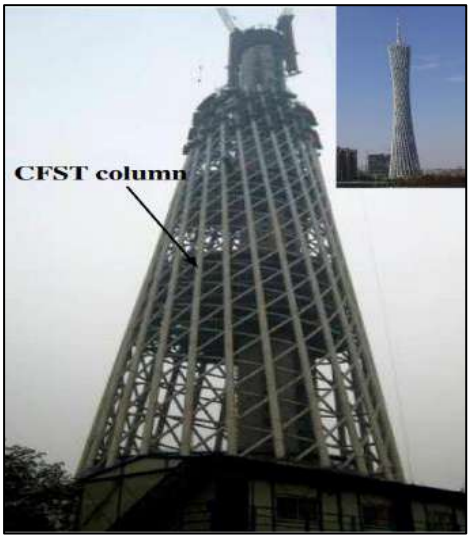

Plate(1.3) GuangzhouTV Astronomical and Sightseeing Tower [3].

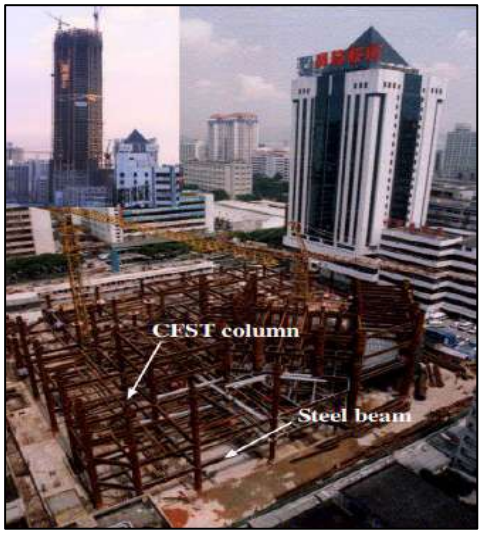

Plate (1.4) SEG plaza in Shenzhen [3].

1.3 Types of CFST Sections

There are three types of composite columns that have been addressed and divided by previous studies, the division appears in below [4]:

- Fully encased columns (FEC)
- Partially encased columns (PEC)
- Concrete filled steel tube (CFST), (circular, rectangular and square)

There are many types of cross-sections of the composite members, which are referred to in the Figure (1.2).That the first type of the composite column was the steel section covered with concrete Figure (1.2a). This column was confined by concrete due to low grade and to resist fire [5].

To reduce the use of temporary formwork while remaining in the use of the universal parts of the composite members, a partial encasement method can be used in which the concrete is poured between the edges of the steel section (Figure (1.2b)). The fire resistance of this steel web is very high due to the reasonable protection provided by the concrete.

From previous studies it was found that it is better to use high strength concrete, which provides good improvement in column durability, in addition, it can be with smaller cross sections. At the present time, due to the inappropriate appearance and the need for molds to pour concrete, pipes filled with concrete are widely used more than steel members covered with concrete (Figure (1.2c)). Moreover, the use of steel tubes as ready-made molds increases construction speed and gives an aesthetic appearance, as well as high fire resistance. Since construction speed is an important advantage, reinforcement is usually not used [6]. But if the insertion of reinforcement is required, a second and third tube is inserted into the main outer tube (Figure (1.2d)).

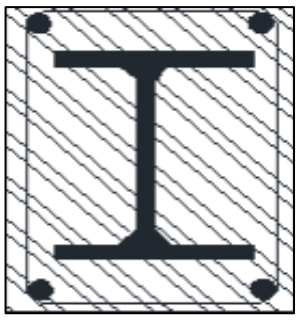

(a) Steel section with full encased concrete

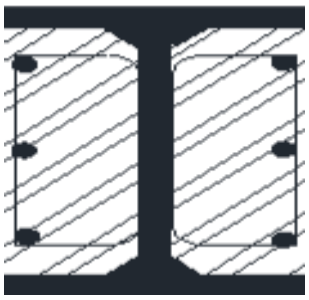

(b) Steel section partially encased concrete

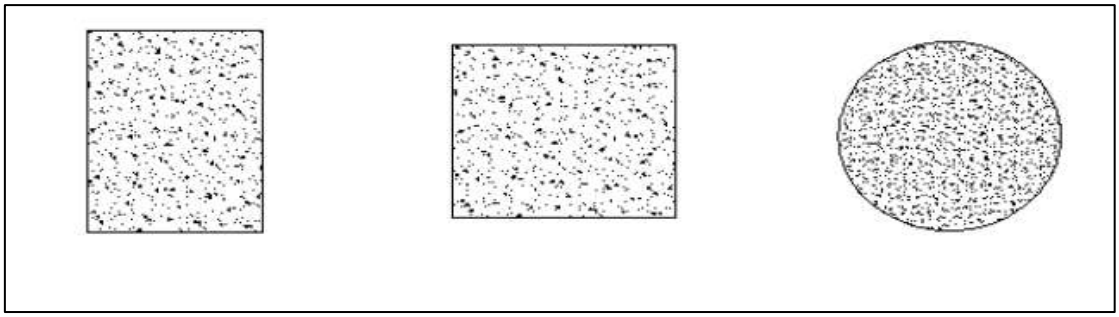

(c) steel part filled with concrete

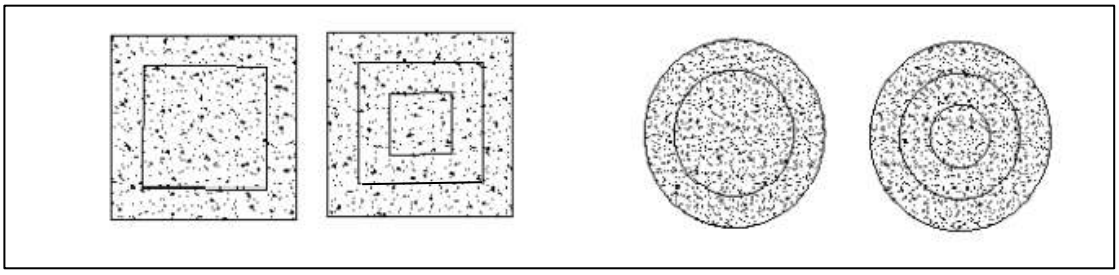

(d) Double part of steel filled with concrete

Figure 1-2 Standard shapes of steel section filled with concrete

1.3.1 Fully Encased Columns (FEC)

The structural section of this type shall be composed of (I- section, T- section, H- section, etc.) of steel coated with reinforced concrete (RC) from all sides. The interaction the constituent materials of this type lies in the improvement of the reinforced concrete (RC) the buckling ability of steel section, while the steel enhances the shear strength and ductility of the column. It is known that the problem of steel in all forms of cross-section is buckling; therefore modifying its ability to unstable is one of the advantages that have been worked on.So the carrying capacity of FEC section is greater than the simple assembly of squash loads of RC and encased steel [7][8][9].

There are several advantages that this kind of sections:

1. It has fire protection from external covering with concrete layers.
2. Its high resistance and good efficiency with a small cross-section compared to other types.
3. The species has anti-corrosion resistance, which is why it is suitable for use in coastal areas [10].

History of its inception in japan four decades ago and its resistance to earthquakes made it widely used in the structures of buildings in the city of Taiwan after the Ji-I earth – quake in 1999 [11]. This does not mean that it is free from disadvantages:

1. It requires necessity of mixing, casting and curing of concrete, all of which it influence the final strength of concrete.
2. The price of the forms used to cast concrete is relatively up.
3. It has less compression to steel where the ratio is about 1:10 depending on material which leads to big sections in columns or beams of multistory buildings. Cracks are developed in concrete due to shrinkage and in the application of live loads.
4. It has precarious behavior when is subjected to tension and is prone to creep and shrink with time [12].

1.3.2 Partially Encased Columns (PEC)

Composite columns are created using different combinations of steel and concrete in an effort to take advantage of the beneficial characteristics of both material in an economical manner. Partially Encased (PEC) column in a type of composite column that generally, its structural frame is made of H-section steel with concrete pouring on its edges. One advantage to this type of column over fully encased columns is that it the formwork is used on only two sides of the column. In the mid - 1990s, the Canam group Inc. (Canam) develop a new design for PED columns intended to make it more economical, particularly for mid – and high – rice steel structure. Since then, Canam and several North American Universities, led primarily by Ecole Polytechnique de Montreal, have been involved in an aggressive research program to better understand PEC column behavior and establish design rules. This program has led to the inclusion of PEC columns in the Canadian standard for design of steel structures, CSA S16-01 (CSA2001). These design provisions permit the use of PEC columns only when loaded concentrically and they contain limitations on the permissible concrete strength (must be less than 40 MPa).

The new PEC columns utilize bare steel sections to carry a portion of the dead load and the construction live loads, so that the speed of erection of all-steel construction is maintained. The columns are then cast with the floors and once the concrete has cured, the columns then rely on composite action to support the full dead load and occupancy live load of the building [13].

1.3.3 Concrete Filled Steel Tube(CFST),(Circular, Rectangular and Square)

The third type of composite columns is a steel tube filled with concrete, which is characterized by high efficiency, high performance and speed in construction compared to other types. The efficiency is due to the good synergy between concrete and steel, as the steel tube keeps the concrete filler from cracking and

expanding, which provides the steel hollow section with higher bending resistance [14].

Concrete- filled with double skin composite columns CFDST were recently invented. The structural section of this consists of two layers of steel tubes, which are filled between them with concrete arrangement. This type proved higher resistance against the global buckling under the influence of loads than in CFST due to the increase in steel area Ast. Available in several forms of hollow cross-sections filled with concrete or grout (round, square and rectangular section) [15].

1.4 Advantages of Concrete-filled Steel Tube

The members that concrete-filled steel tubes (CFST) were used in numerous structural and infrastructure projects, such as columns in height building, industrial infrastructure, towers for the transmission of electricity and bridges. The advantages of using this technique are summarized as follows [16]:

- The steel pipe offers permanent formwork for concrete during building .
- The steel tube may carry large building loads before pouring wet concrete through the parts.
- Strength and ductility improved. The steel tube provides concrete containment that enhances the concrete's capacity. The concrete further strength hens the steel frame, minimizing or removing local steel segment buckling resulting in improved ability to support load, carrying capacity absorption in the event of an earthquake.
- The steel tube's fire resistance is improved by concrete thermal characteristics.

recently was utilizing two steel tubes and fill the concrete between the gap of the tubes, known it concrete-filled double skin tubes (CFDST) technique and offer the following properties [17]:

- Very light weight.

- High bending rigidity.
- Good performance with cyclic loads.
- Good acceptance to fire safety.
- Energy absorption is high due concrete infill and internal tube.
- Concrete core tube supports the steel local buckling.
- High global stability, due to an increased section module.

1.5 Concrete Filled Tube Connection

In the last few decades a large number of CFT connections (beam-to- column) has been investigated. Some kind of connections transfer the force from the beams directly to the steel wall, while others transfer the force to both the steel tube and the concrete core as shown in Figure (1-3).

Figure (1.3) Type of connections of CFST with beams

The kinds of CFT connection (steel beams-to-column) in the case of having beams welded to the steel wall, are mostly appropriate for the simple connections. For the moment connections, these forms of connections impose high deformation demands for the steel wall and perhaps lead to stress fracture of the steel wall. This causes a degradation of stiffness and strength. therefore, in some of the connection systems, it is regular to distribute the beam force around the steel wall by the use of external and internal diaphragm plates which have been welded to the steel wall. For the circular CFT connections [18], Schneider and Alostaz (1998) [19], observed

that the types of connection having twisted stiffening bars or extended plates in the concrete which made better both stiffness and strength. For the rectangular CFT structures connections, Ricles et al (2004) [20], observed that using split tee connections along with post-tensioned bolts or through-bolts provided with great hysteretic efficiency.

1.6 Types of Reinforced Concrete Columns

Concrete columns are usually reinforced with longitudinal and transverse rebars, and it can be basically classified into three types [21]:

1. Columns reinforced with longitudinal bars and lateral ties (tied columns), as shown in Figure (1-4a).
2. Columns reinforced with longitudinal bars and closely spaced spirals (spiral columns), as shown in Figure (1-4b).
3.
4. Columns reinforced longitudinally with structural steel shapes, pipes or tubes with or without longitudinal bars (composite columns), as shown in Figure (1-4c). The first and second types are more commonly used.

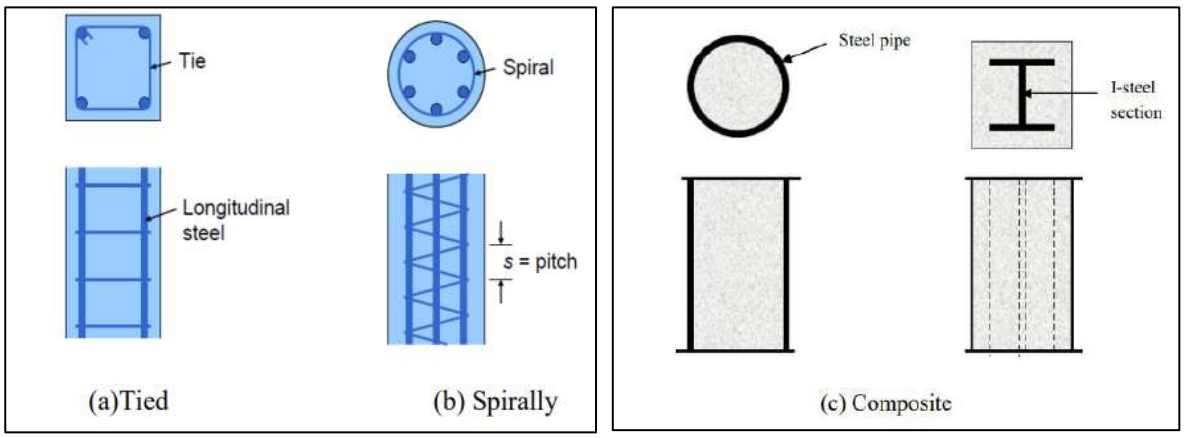

Figure (1.4) Types of concrete reinforced columns

1.7 Slenderness Ratio and Column Failure Mode

Based on the slenderness ratio of the columns, it is classified into short and long columns, where the slenderness ratio is known kL/r, in which kL denotes the column's effective length, while r the radius gyration of column according to ACI [22].Based on [23], when ratio of the effective length to its least lateral dimension is less than or equal to 12 it is called as short column, and when the ratio of the effective length to its least lateral dimension exceeds 12 it is called as long column. The failure patterns differ in concrete columns with reinforcement and divided into three modes depending on the ratio of the height to the minimum lateral distance of the column [24] as shown in Figure (1-5):

1- Concrete or steel reinforcing failures are both possible.

2- Buckle and compression failures combined to cause failure.

3- Failed to buckle.

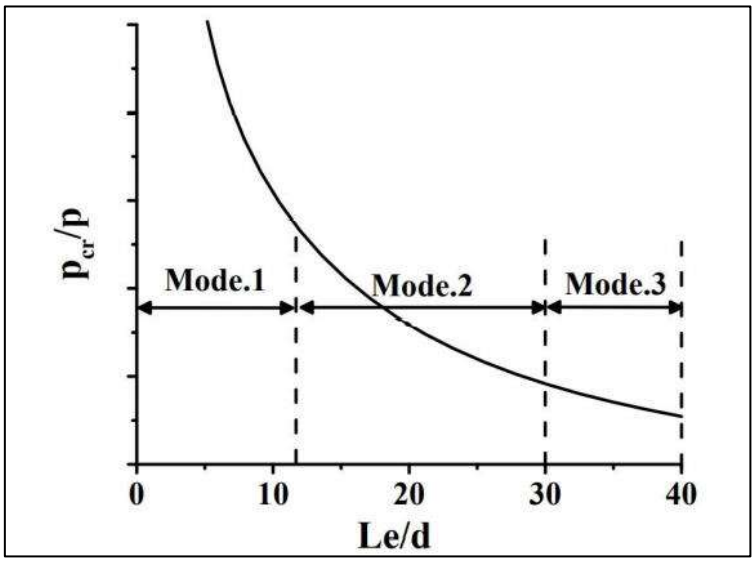

Figure (1-5): Pattern Failure of samples of column to wide various (Le/d) value presented in [24].

It is possible that the failure mechanism of the columns differs in the short column (stocky) from the long column (slender), where the compression failure with the column material, followed by the concrete crushed concrete that characterizes the short columns, while the long column fails to bend as shown in Figure (1-6).

Compared to a shorter column, A longer columns of the same substance and cross - sections would bear less pressure.

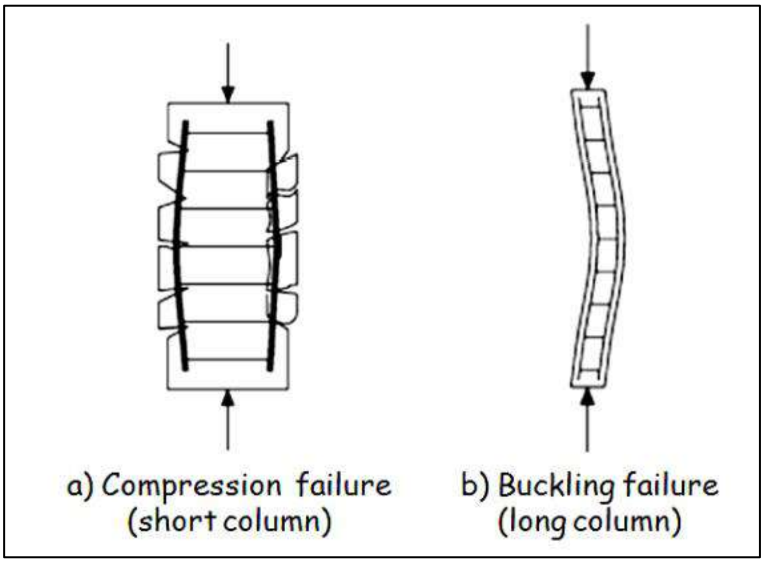

Figure (1-6): failure modes of columns for (a) Short column (b) Long column.

1.8 Slenderness ratio of Column According to ACI Code and AISC Code

Ratio of Slenderness is the product of dividing the effective column length to its minimum radius of gyration with respect to the cross section, as defined by ACI Code and AISC Code (360-10). Slenderness ratio is defined as [ACI code][102] [AISC Page 429 (2017)][103]:

$$Slenderness\ ratio = \frac{Le}{R} \quad \ldots\ldots\ldots\ldots\ldots\ldots\ldots\ldots\ldots \quad (1.1)$$

where:

Le =is the column's effective length = K.L

K=is the effective length factor.

R=is the smallest gyration radius where $R = \sqrt{\frac{I}{A}}$.

A=is the area of steel and concrete in the cross-section of composite column.

I =is the second moment of area for cross section.

1.9 Mechanism of Concrete Column Strengthening by Confinement

Steel plates or other confining devices (CFRP jackets, transverse reinforced steel) are added to the concrete column, at low stress levels in the concrete, no stresses are generated into the confining device; thus, the concrete is unconfined. But due to the lateral concrete expansion and gradual internal cracking, the transverse strains become very strong when the stresses reach highest level of the compressive strength (uniaxial stresses).Therefore, the concrete in the last loading stages and confinement method becomes too against the cracking of concrete, become it in a triaxial stress state. The triaxial compressive stress state improves significantly strength and ductility of concrete. This confinement way is passive method and there are recent cases where there is an initial confinement active pressure, as is the case between the column and an exterior jacket where an enormous grout is injected. Compared to the passive pressure generated by concrete dilation, the containment in this case is usually very limited [25].

By way of an axial load history, passive confining forces can be constant or variable. Constant confining strain, as the confinement given by conventional mild lateral steel reinforcement, is created by an elasto-plastic constraining substance after yielding. Variable confining pressures are created where the confining material maintains a substantial stiffness throughout the axial load background, as the confining given by FRP.

The experiments showed the confinement given for a circular, square and rectangular cross section of a composite column is different. Where the

confinement of circular section is more active than the square and rectangular sections, the explanation for that is the gap in effectiveness shown in Figure (1-7), which shows that a circular segment would keep the confinement system in hoop tension due to its shape and make it has a continuous confining pre-containment. In the other side, the containment system applies constraining action near the corners and the central region of the square or rectangular part, keeping the sides uncontained, leading to the column being partly enclosed [26].

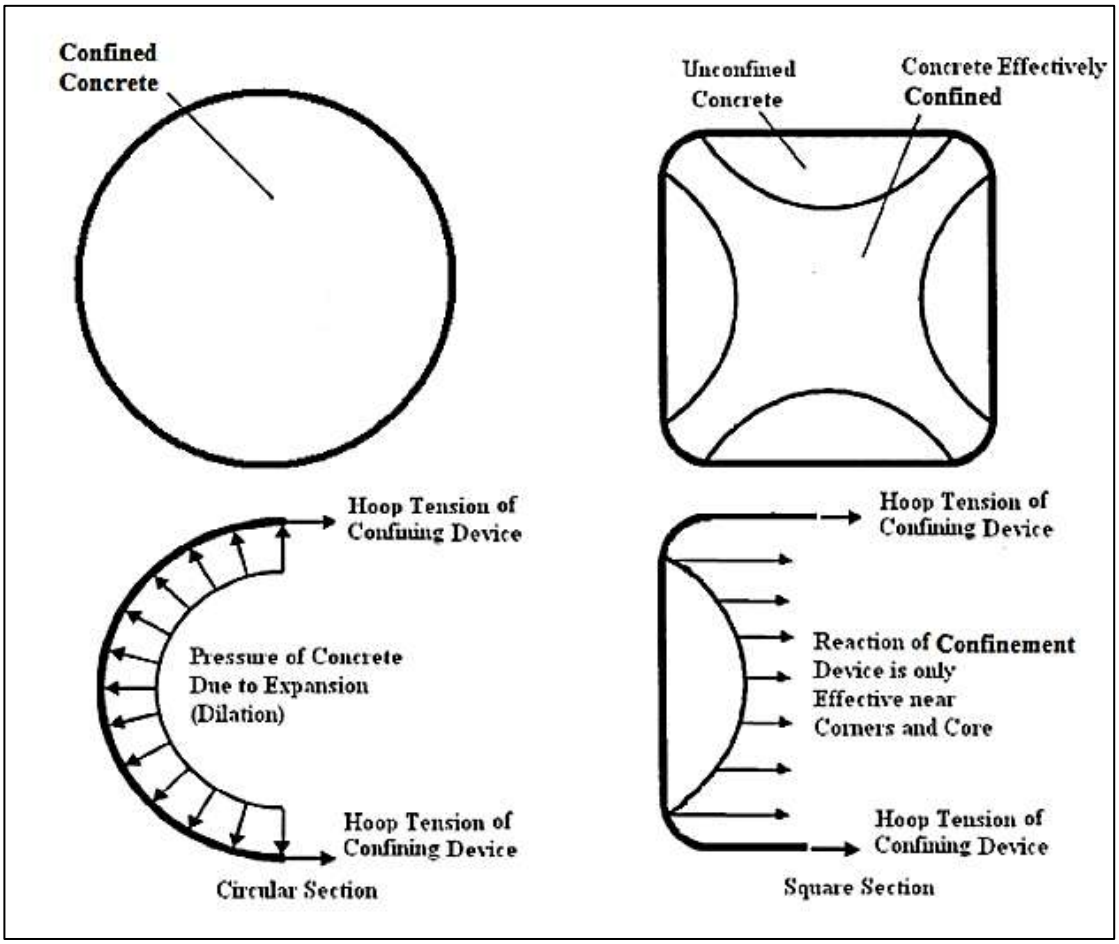

Figure (1-7) the influence of confinement on circular and square section [26].

1.10 Shear Connectors

Shear connectors are placed between concrete and steel in several cases, including linking concrete with steel or when there are high shear forces between the two materials. This connection prevents vertical separation and movement between steel and concrete elements during the transfer of shear force from concrete to steel or vice versa, as in mechanical connections. Before casted, these connections are installed on the steel beam top flange. These connections make both components work as one material [27].

The stud connector is one of the most popular types of connectors used by users, and it is the most common among them, as shown in the Figure (1-8). This connector consists of a head as an upper part and a shank as a lower part which is connected by welding to the steel components[28]. Failure is in the stud connector, either by the crushing of the surrounding concrete, and this condition occurs in the large diameters of studs, or by the end of the stud grooving when the connector is slender [29]. The shape of failure and the failure load can also be visualized by the strength of the concrete [30].

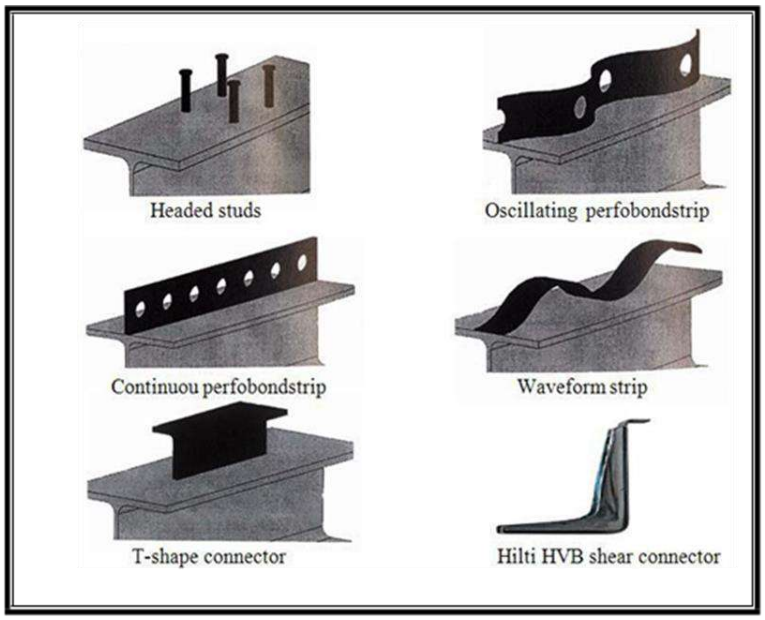

Figure (1-8) Types of Shear Connectors [30]

1.11 Reactive Powder Concrete (RPC)

In the recent years, there has been research works on concrete technology which led to the use of a new type of high-strength concrete, Reactive Powder Concrete (RPC). It was developed in France in 1990, and Sherbrooke footbridge, shown in plate (1.5), was the first RPC structure in the world in 1997.

It is a material with a very fine composition, with high strength and ductility. In addition to the ideal mechanical properties. It consists of steel materials in the form of fibers and plasticizers to reduce the proportion of water and silica fume. The water percentage is very low in relation to the weight of cement, and the sand used is very fine compared to the normal sand, as it is characterized by particles with diameters of 0.5-0.6 mm. The content of cement material in this type also reaches about 900-1000 kg/cubic meter [31].The properties of fine sand give high tensile strength and hardness to this type of concrete.

Reactive powder concrete plays a major role in many applications, such as long bridge spans, high-pressure pipes and is also suitable for waterproofing hazardous fluids or nuclear waste. In addition, it is used in anything that requires extra protection, such as blast resistant or any other dynamic loads. It is also used in structures requiring light weight and thin materials, such as the Stadiums roofs [32].

Plate (1.5) Sherbrooke footbridge [from google website]

The concept of RPC is based on the principle that material with a minimum defect, such as micro cracks and interval voids, will have higher capacity-carrying loads and greater durability. This can be done according to the following concepts [33]:

1- Elimination of the coarse aggregate: improving the homogeneity of the concrete material by removing all coarse aggregates, dried ingredients materials of the same particle size as much as possible. All dry components maximum 600 μm used in RPC.
2- The grain size distribution is changed to maximize the density of the mixture.
3- Heat treatment to enhance the microstructure.
4- Adding of steel fibers: they are used in order to increase the concrete ductility and improve its tension, splitting and rupture strength.
5- Using superplasticizer to decrease the water cement ratio and improve the workability. Some reactive powder concrete application occurs in Plate (1.6).

Plate (1.6) Applications of reactive powder concrete [from Google website]

1.12 Objectives of the Present Study

The primary objective of the research program is to study the behavior of different types of concrete filled double skin tubular column under repeated loading. The general goals of this study could be focused on the following points :

1 .Studying experimentally the behavior under two types of concrete, a dual tube column is filled with concretes which is normal concrete and reactive powder concrete.

2. Studying the effect of steel fiber volumetric ratios (Vf) used by reactive powder concrete (RPC), and making a comparison with normal concrete (NC).
3. Studying the effect of welding high strength bolt (shear connector) on the capacity of column when filling with reactive powder concrete.
4. Assessing the performance of column when filled with reactive powder concrete and using different cross section of sandwich concrete area.
5.Studying the effect of global slenderness ratio (length to width) of column on the capacity of column.
6. Checking the strength of the steel tube when it is not filled with concrete.

1.13 Thesis Layout

The research program of the thesis was presented through five chapters, as follows:

Chapter one: presents the fundamental information and general introduction regarding concrete filled tube, connection of CFT, and Reactive powder concrete.

Chapter two: presents a background on the applications, researches and the documents that are related with concrete filled steel tube. Also, a literature review refers to the researches and experimental studies about RPC and are presented .

Chapter three : the materials used in the present study and the test results of these materials, details of concrete mixing and casting procedures used in concrete column, installation procedure of steel tube, instrumentation and testing setup were briefly displayed in this chapter.

Chapter four: represents the experimental results of the study and the effect of the parameters which have been used in this study on the ultimate load, deflection and failure mode. The experimental results of the maximum strength were compared with the design strengths of the American Institute of Steel construction (AISC), American Concrete Institute (ACI), and the European Code (EN 2004).Then discussion concerning the effect of these parameters is given .

Chapter five: summarizes the overall findings and the main conclusions of the research program. Recommendations for future studies are also presented.

CHAPTER TWO

CHAPTER TWO

LITERATURE REVIEW

2.1 Introduction

The characteristics of adding high performance concrete to steel hollow columns have several properties such as, compression strength, stiffness and ductility. These properties make it particularly favorable for high structural buildings and large structures that are exposed to earthquakes. The larger internal capacity in the cross-section of the column makes little occupied space for the floor, through the thin column. The ductility property improves behavior of buildings and bridges in seismic areas [34]. The concrete-filled hollow columns in many areas of the building not only have high bearing capacity but also economy and rapid construction, thus saving additional costs [35].

This chapter presents a review of the available information and researches related with the concrete filled steel tube column subjected to axial loading. The review also involves past studies concerning the reactive powder concrete (RPC) used in composite column. The literature review also summarizes previous studies for favorable different ways to design concrete filled double skin and repeated loading mechanism.

2.2 Present Development of CFST Columns

In engineering systems, Columns composed of steel tubes filled with concrete (CFST) were widely used. In the past, the different criteria were studied in the experimental and numerical studies, namely: form of section, diameter of section, steel tube thickness, steel and core concrete strengths, column length, eccentricity of load, and so on [3].

The use of CFST columns is widely accepted use when compared to steel and reinforced concrete columns, as it has high load bearing capacity, ductility due to

the compression effect, ease in production and construction due to the steel tube serving as permanent shaping [36]. Several design guidelines in various areas were produced for the design of CFST columns, such as Eurocode 4 (2004) in Europe [37], DBJ/T 13- 51-2010 (2010) in China [38], AIJ (2008) in Japan [39], ANSI/AISC 360-10 (2010) in U.S.A [40]. and AS 5100.6-2004 (2004) in Australia [41].

Some recent research has focused on the development of various types of CFST columns in order to further improve structural performance and satisfy various design specifications. In order to enhance the structural strength of composite columns, one solution is aimed at using modern alloys or modifying the structure of traditional CFST columns. Columns were developed on two concentric steel tubes with an annulus between them filled with concrete known is concrete-filled double-skin steel tubular columns CFDST. These had nearly all the same benefits as traditional CFST columns, but with a lighter weight and improved cyclic efficiency [42,43].

One of the advanced column have been investigated the stiffened columns of CFST for the enhancement of thin-walled steel tubes.To reduce the impact of local buckling on the thin-wall steel tubes, welded stiffeners were used for economical purpose [44].

Recently, a series of experiments on bent, tapered and straight-tapered-straight CFST columns was performed in order to theoretically implement these constructs that can satisfy the criteria of architecture [45]. In addition, experiments were performed on the tapered CFDST columns documented in[46]. Demonstrating that this kind of new revolutionary composite column could be used as transmission towers.

Another technique for the modern production of CFST columns is to implement high-performance steel. High quality steel with a yield strength of up to 700 MPa has been used in CFST column steel tubes and numerous experimental works have been performed in recent years [47,48].

Another high-performance steel that possesses high strength, as well as greater corrosion resistance and hardness was stainless steel, which has been studied by researchers for nearly a decade as an exterior content for CFST columns [49,50]. On the other hand, as concrete still plays an essential role in CFST columns, different engineers and researchers have sought to build composite columns using alternative forms of concrete other than standard concrete for example, the load carrying ability of CFST columns may be greatly increased by high-strength concrete (compressive strength greater than 100 MPa) or even ultra-high-strength concrete (compressive strength close to 200 MPa) [51-53].

To preserve natural resources and decrease landfill requirements, CFST columns built with recycled aggregate concrete were developed [54].The use of lightweight aggregate concrete in CFST columns was suggested to greatly minimize the structural weight [55,56].

2.3 Placing of Concrete in Steel Tube

In order to pour the concrete in high quality inside the hollow steel tubes, there must be a method forming the tube as high as possible. Although it is difficult to check the pressure of the concrete filled inside the empty tube, the filled concrete should be well compacted in addition to a good mixing method. Several different methods were used in China to pour concrete inside the pipe. Two traditional methods were developed for steel pipes to be filled with concrete as shown in the Figure (2-1). The first method was to fill the steel tube from the base of the tube through an opening near to the pumping hole as seen in the Figure (2-1a). The second method is to pour concrete from the top by the action of gravity as shown in the Figure (2-1b). When the tube is opened from the bottom, there must be a test of the strength of the pipe wall near it. Depending on the progress of construction methods and the pumping of concrete, the concrete can be pumped to high heights of the structural construction. These methods are preferred to use self-consolidating concrete (SCC) and well blended concrete [3].

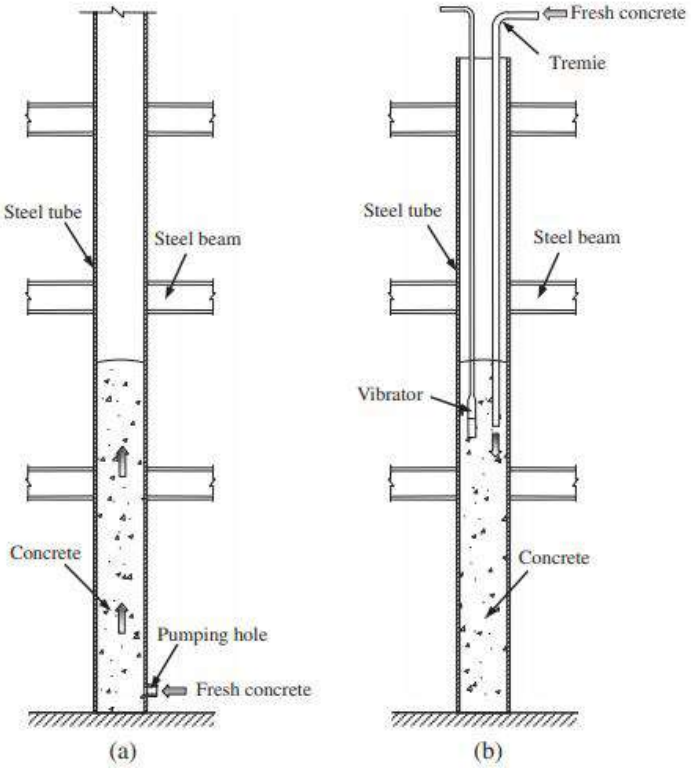

Figure (2.1) filling of concrete in steel tubing

2.4 Historical Researches Related to Study of Concrete Filled Steel Tube

Several studies have been applied to steel pipes filled with concrete, and some of them will be addressed in this study:

Uy et al. (2011) [57] had covered out a series of tests on non-slender and long of type CFST stainless steel tube to identify their conduct placed under the axial loading as well as the results of the joint test of axial strength and bending moment. Non-slender hollow sections as well used to identification by examination. Nine specimens, six round and three square, stub concrete-filled tube columns were studied for the verify of the conduct of CFSST for various loading cases. Data of the examination explain that behavior of specimens is very efficient, so this type of columns can be used widely as structural members.

CFSST made of stainless steel has high flexible performance and very high reside resistance compared to those made of traditional carbon steel. It is also compared with hollow tubes and has been found to have higher resistance even while loading the steel tubes only. The use of stainless steel tubes in place of conventional carbon steel, improves the flexible disposition of the column in non-slender samples. The use of stainless steel in slender samples had no changing in the strength of samples, at the stage of observing test and failure patterns. In the future of long CFSST columns. The experimental results were compared with several methods from the current design of the conventional carbon steel composite columns and from these methods are: Australian standard AS 5100(2004), American code AISC (2005), Chinese code DBJ/T 13-51-2010(2010) (2010), and Eurocode 4 (2004). All of these indicators showed a reservation in predicting and measuring the load carrying capacity of all types of CFST slender and non –slender columns.

Portolés (2013) [58], experimental work included several samples of slender circular tube columns filled with different types of concrete including normal, high-strength and very high-strength concrete. Reinforcement bar was used once with concrete and once steel fibers were used as shown in Plate (2-1). It was subjected to a central and non-central axial load with eccentricity e (0, 20 and 50 mm) respectively. 24 samples of tubes filled with concrete (CFST) were examined. From the results, it was concluded that adding steel fibers to normal concrete can compensate for the reinforcement, but this effect was not noticeable when adding the fibers to high-strength and very high-strength concrete. It was also concluded that slender columns that were subjected to eccentric load gave better ductility regardless of the type of concrete filled. Where the addition of high-strength concrete gives better behavior under concentric load and also the use of steel reinforcement was better than steel fibers. The loads were predicted

by the European code and gave better results for concentric load, but the eccentric load needs additional studies.

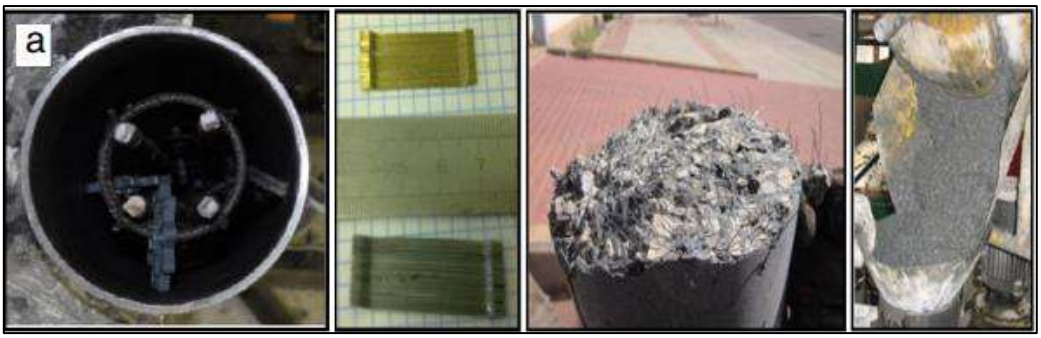

Plate (2-1) Reinforcement bar and steel fibers were used

Essopjee, and Dundu (2015) [59], 32 samples of CFDSCT columns were loaded in axial compression until failure as shown Figure (2.2). The research variables consisted of an external dimeter, thickness of the outside pipe, the column's height and strength of the outer tube. The lengths of the column ranged from 1 to 2.5 m, in increments of 0.5 m and the diameters of the outer steel tube were 139, 152, 165 and 193 mm. All the steel tubes had a thickness of 3 mm, except for one tube, which had a diameter of 193 mm and a thickness of 3.5 mm. The ratio of change diameter to thickness of the outer tube ranged from 46 to 55, while the maximum strength of the tube was from 392 to 552 MPa. The inner tube was of the same metal as the outer tube and had a diameter of 76 mm while its maximum strength reached 324 MPa. The concrete cubes had an overall strength of 30.7MPa. All these variables were selected to know the appropriate variable to be used in the practical applications. The results showed that there were two types of failure patterns that occur in these columns. The columns failed with a length of 1 meter by crushing the concrete after which a local buckling occurred in the outer tube, while the columns were of 1.5, 2 and 2.5 length meters failed to fully bend due to the high thinness of these columns. The columns also showed less bearing for higher height of the composite column.

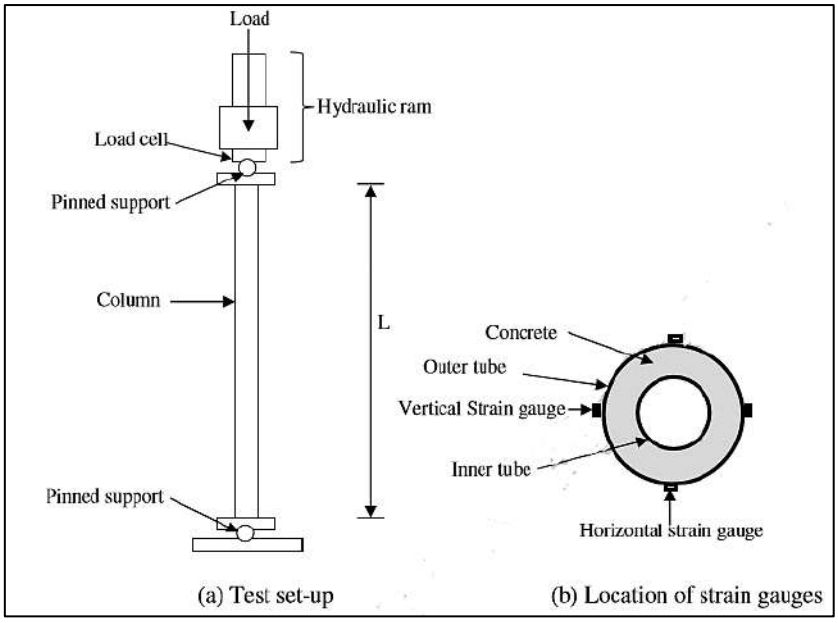

Figure (2.2) Schematic test set-up and location of strain gauges

Also, it was observed that increasing the diameters increased the bearing of the column. The axial pressure of the columns CFDSCT was predicted by the establishment of new formulas because these columns were not protected by SANS 10162-1 and EC4 design standards duplicated on CFTs. By SANS10162-1 and EC4, the average variations between the study results and the current formulae are conservatively 1 % and 6 %, so the strengths predicted were safe.

For (SANS 10162-1) [60] the axially capacity of CFDSCTs in compression state can already be estimated by :

$$N_p = (\tau A_{so} f_{yo} + A_{si} f_{yi} + \tau' A_c f_{cu})(1 + \lambda^n)^{\frac{-1}{n}} \quad \text{..... (2-1)}$$

In EC4 [37], the compressive strength of concrete-filled tubes is given by:

$$N_{pl,Rd} = \chi(A_{so} f_{yo} + A_{si} f_{yi} + A_c f_{cu}') \quad \text{.....(2-2)}$$

Mahgub et al. (2017) [61], this paper provides an experimental study of the axial compressive behavior of elliptical steel tube columns packed with self-compacting concrete. In total, ten specimens of varying heights, section sizes and concrete strengths, including two empty columns, were tested for failure. The experimental findings showed that the global buckling controlled the failure

modes of the self-compacting concrete filled columns of elliptical steel tubes with a large slenderness ratio. In addition, because of the composite interaction, the concrete filled steel columns had greater crucial axially compressive capabilities compression to their hollow segment companions. However, the change in the compressive strength of the concrete core did not show a significant effect on the critical axial compressive capacity of the concrete filled columns due to the large slenderness ratio of the test specimens, although the axial compressive capacity increased with an increase in the concrete grade. There was a reasonable agreement between the contrast between the axial compressive load capacities obtained from the experimental analysis and the forecast using the simple methods given in Eurocode 4 for concrete filled steel circular tube columns. The experimental findings, study and contrast presented in this paper explicitly support the use in the practice of construction engineering of self-compacting concrete-filled elliptical steel tube columns.

Elchalakani, M., et al (2018) [62] the rubber concrete technique was used, which was filled inside circular steel tubes with double skin. Fifteen of the composite columns were examined, in which three concrete mixtures were produced with a rubber ratio of 0% (control), 15% and 30% by weight of sand and gravel respectively. Rubber sizes ranged from 2 mm to 7 mm. The delivery consisted of two sets of rubber sizes, 2-5 mm, and 5-10 mm. The 5-10 mm particles were put through a 6.75 mm sieve to attain a maximum aggregate size of 7 mm. A visual representation of the crumb rubber particles sizes is shown in Plate (2.2).

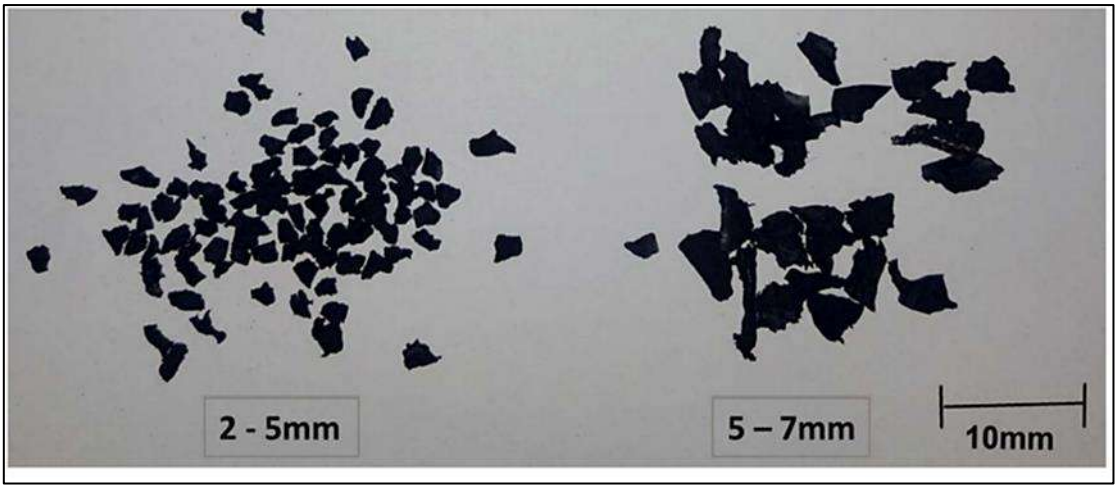

Plate (2.2) rubber particles sizes

The results of the practical examination showed RuC mixes have a lower compressive strength than normal concrete. Concrete strength decreased by 50% and 79% for 15% and 30% rubber replacement by aggregate respectively. Also, 15% rubber replacement with 25Mpa strength was a viable alternative for applications such as footpaths and footings. As well as NaOH rubber pre-treatment improved the concrete rubber bonding and reduced concrete segregation due to the inclusion of rubber particles. Rubberised concrete significantly improved ductility and energy absorption of CFST and CFDST by up to 2.5 times. The research results supplemented existing methods and design codes' projections for design ultimate axial capacity as details in Table (2.1).

Table (2.1) Comparison between experimental strengths with different design model strengths

Specimen	$P_{ul,Exp}$ [kN]	$P_{ul,Zh}$ [kN]	$P_{ul,Tao}$ [kN]	$P_{ul,Has}$ [kN]	$P_{ul,EC4}$ [kN]	$\frac{P_{ul,Zh}}{P_{ul,Exp}}$	$\frac{P_{ul,Tao}}{P_{ul,Exp}}$	$\frac{P_{ul,Has}}{P_{ul,Exp}}$	$\frac{P_{ul,EC4}}{P_{ul,Exp}}$
CHS-O165-0	1876	1541	1603	1574	1582	0.82	0.85	0.84	0.84
CHS-O165-15	1291	1118	1189	1241	1215	0.87	0.92	0.96	0.94
CHS-O165-30	1130	942	1016	1101	1063	0.83	0.90	0.97	0.94
CHS-O114-3.2-I42-00	1073	960	1019	1007	1101	0.89	0.95	0.94	1.03
CHS-O114-3.2-I42-15	824	793	851	876	956	0.96	1.03	1.06	1.16
CHS-O114-3.2-I42-30	742	724	781	821	897	0.98	1.05	1.11	1.21
CHS-O114-3.6-I42-00	1255	1048	1131	1120	1240	0.83	0.90	0.89	0.99
CHS-O114-3.6-I42-15	968	884	964	991	1096	0.91	1.00	1.02	1.13
CHS-O114-3.6-I42-30	900	816	894	937	1039	0.91	0.99	1.04	1.15
CHS-O165-I42-00	1888	1646	1704	1677	1658	0.87	0.90	0.89	0.88
CHS-O165-I42-15	1428	1254	1319	1368	1325	0.88	0.92	0.96	0.93
CHS-O165-I42-30	1245	1090	1159	1239	1187	0.88	0.93	1.00	0.95
CHS-O165-I89-00	1855	1698	1740	1720	1610	0.92	0.94	0.93	0.87
CHS-O165-I89-15	1561	1409	1457	1492	1374	0.90	0.93	0.96	0.88
CHS-O165-I89-30	1441	1288	1339	1397	1278	0.89	0.93	0.97	0.89
Average						**0.89**	**0.94**	**0.97**	**0.99**
Standard deviation (SD)						**0.04**	**0.05**	**0.07**	**0.12**

Talha and Hussein, (2019) [63] presented in this paper is a study on the role of the inner tube and its effect on mechanical response to the CFDST column subject to the axial loads. Sixteen samples of CFDST columns were used in the practical program, with two variables proportion from diameter to thickness D/t, to inside and outside steel layers forming the column. Two different compressive strengths are used for concrete. In order to reach the desired results, the axial loads curves were analyzed against axial displacement curves, collapse patterns, the contribution ratio of materials forming the column (steel and concrete) and the ability index. The results obtained indicate that the CFDST columns have higher efficiency and better performance compared to CFST, due to the effective impact of inside tube in improving the performance and conduction of the column. Also, one of the advantages it provides is the presence of the inner diameter to reduce the failure condition of the column and it works in harmony with the concrete core, providing good confinement ability even with high-strength concrete. SI ratios indicate that increased thickness wall of inside tube improves confinement capacity. In addition, a theoretical study was presented in this paper to calculate the usability of CFDST columns design method. Five design formulas were proposed and calibrated based on the results of the practical examination to determine the exact formulation of the CFDST columns.

Eom, S.-S., et al. (2019) [64], four separate specimens were produced in this experiment. Two tests were made with and without the joint with each type of shear connectors (M16 and plate studs). The specimens included interior and exterior steel tubes as well as concrete filling the space between tubes. To cause a composite action, two different shear connectors from the M16 studs and steel plate studs were used. Sixteen studs were welded between the inner and outer steel tubes on the cross-section of the tubes, while the longitudinal section of the tubes was welded. To meet the specifications of the steel structure design criteria, the studs were placed at a spacing of 250 mm. They study investigate the behavior of the double skin composite column under the influence of bending condition

and found that M16 studs gave better bending behavior than steel plate studs. Models were tested by the FE programmed, so there was harmony between the findings of the experience and the FEA. The pattern can be used on pipes of various sizes.

(Yuan, et al. 2019) [65], an experimental study was conducted under eccentric compression with different slenderness ratios on rigid square concrete-filled steel columns. The significant findings of this analysis are that the local buckling in the stiffened columns was different from the unstiffened columns. When the longitudinal stiffeners were used, local buckling of the tube was slower and less pronounced, the longitudinal stiffeners increased the composite column's overall strength, the exterior deformation of steel tubes was reduced, the confinement of the steel tube on the central concrete was improved and the overall axial stress of concrete was increased. Finite element research was subsequently performed, in order to investigate the impact of welding stiffeners using the (CFST) column operating mechanism.

Xi-Feng and Yan, (2020) [66] proposed a simple and accurate formula that predicts the resistance of non-slender round CFDST columns under axial load by providing a set of parameters. The paper was completed using 24 CFDST samples consisting of an inner and outer steel tube in round cross-section of axially loaded. At the same time, results were collected from 35 samples of short columns composed of conventional round carbon steel tubes from previous studies. A new formula has been proposed to calculate the confinement factor in a way that shows the impact of the confinement on the scalability of columns according to the work data in a current research and the data of previous studied. The results showed that the estimated confinement coefficient gave a reasonable estimate of the nature of the interaction between concrete and steel. This parameter decreases with increasing fc, while increasing fsyo increase it. Therefore, when the high

strength of concrete is combined with the high resistance of steel tubes in the installation of the column, it does not achieve an increase or improvement in the efficiency of confining. The confinement coefficient also helped to predict a new formula to estimate the compressive resistance of axially loaded non-slender circular CFDST. This formula proved more accurate predictions of the maximum column resistance from the available design formulas. The effect of the hollow ratio and the steel yield strength was also calculated and found to have an effective effect on the maximum ductility of the column. The same in the case of improving compressive resistance of concrete and the thickness of outside steel pipe wall also has a positive impact on strength of round CFDST columns.

Vipulkumar et al., (2020)[67] studied the technique of non-slender double-skinned composite columns in a round section A computational model was accomplished to verify structural conduct of non –slender round CFDST columns tested under the influence of the eccentric loads, with the calculation of the effect of confining resulting from steel layers and the extreme hardening of stainless steel layers. This computational model was validated and accuracy by comparing results with available practical data, and after comparison is available to speculate the effect of engineering variables on the structural efficiency of the round CFDST columns. An important point affecting the strength of short round cross-section CFDST columns is the concrete compression, as it has a positive impact on maximum capacity and elementary stiffness to these columns. This leads to making the contribution of stainless steel and its ductility a secondary factor in improving the maximum column capacity. The effect of Di/ D0 on the column strength is negative, as the higher the Di/ D0 ratio the final column strength decreases and at the same time the ductility and contribution of stainless-steel increases. The same effect is to increase Di/ti ratio, as increasing this ratio leads to a decrease in the maximum strength of the column and an increase in the contribution of stainless steel.

2.5 Reactive Powder Concrete (RPC)

In recent decades, a new type of concrete known as reactive powder concrete (RPC) or ultra-high-performance concrete (UHPC) has appeared to have high properties and performance. This type of concrete was suitable for applications on infrastructure and other special buildings. Given the high cost of producing this form of concrete, there are some benefits of using engineering projects of this kind, and the thickness of unreinforced concrete slabs supported on all sides can be minimized because of high mechanical properties [68].

RPC is a high strength, ductile, and durable construction material developed by mixing Portland cement, silica fume, fine sand, superplasticizer, water and steel fibers. This is developed on the premise that a material with a minimum of flaws or defects such as microcracks and pore spaces is capable of achieving a higher quality of the total ultimate capacity for carrying the load [69,70].

2.5.1 Past studies for mechanical properties of Reactive Powder Concrete

RPC's first success was the return in 1994 of Richard and Cheyrezy [71]. Two forms of RPCs were produced with 200 MPa and 800 MPa compressive strength. Consecutively, in Tables (2.2) and (2.3), Richard and Cheyrezy, worked to develop an ultra-high strength ductile concrete known RPC (Reactive Powder Concrete). There were two types; RPC200 and RPC800. Four groups of the mixture were conducted with fiber and without fiber. Where every two groups of mixtures, with fiber and without fiber, are varied by added crushed quartz and post-heat curing. The optimum fraction of the silica fume content was 25% of the cement content. Envelop figures for optimum compression strength values obtained for different relative density values of RPC concretes, with or without fibers, for both surrounded and heat treated (90ºC) specimens are given in Figure (2.3). Also, in this study discovered that the compressive strength is highly

dependent on the relative compacted density at demolding. Addition of small size (φ = 0.15 mm L = 13 mm) steel fibers at a ratio of 2-2.5% per volume gives to RPC a ductile behavior.

Table (2.2) Typical RPC compositions (by weight) [71]

	RPC 200				RPC 800	
	Non fibered		Fibered		Silica aggregates	Steel aggregates
Portland Cement	1	1	1	1	1	1
Silica fume	0.25	0.23	0.25	0.23	0.23	0.23
Sand 150 - 600 µm	1.1	1.1	1.1	1.1	0.5	-
Crushed quartz d_{50}=10µm	-	0.39	-	0.39	0.39	0.39
Superplasticizer (Polyacrylate)	0.016	0.019	0.016	0.019	0.019	0.019
Steel fiber L=12 mm	-	-	0.175	0.175	-	-
Steel fiber L=3 mm	-	-	-	-	0.63	0.63
Steel aggregates <800 µm	-	-	-	-	-	1.49
Water	0.15	0.17	0.17	0.19	0.19	0.19
Compacting pressure	-	-	-	-	50 MPa	50 MPa
Heat treatment temperature	20°C	90°C	20°C	90°C	250-400°C	250-400°C

Table (2.3) Mechanical properties of RPC 200Mpa & 800 Mpa [71]

Mechanical properties	RPC 200	RPC 800
Compressive strength of cylinders	170-230 Mpa	490-680 Mpa 650-810 Mpa
Flexural strength	30-60 Mpa	45-141 Mpa
Fracture energy	20000-40000 J/m2	1200-2000 J/m2
Young's modulus	50-60 Gpa	65-75 Gpa

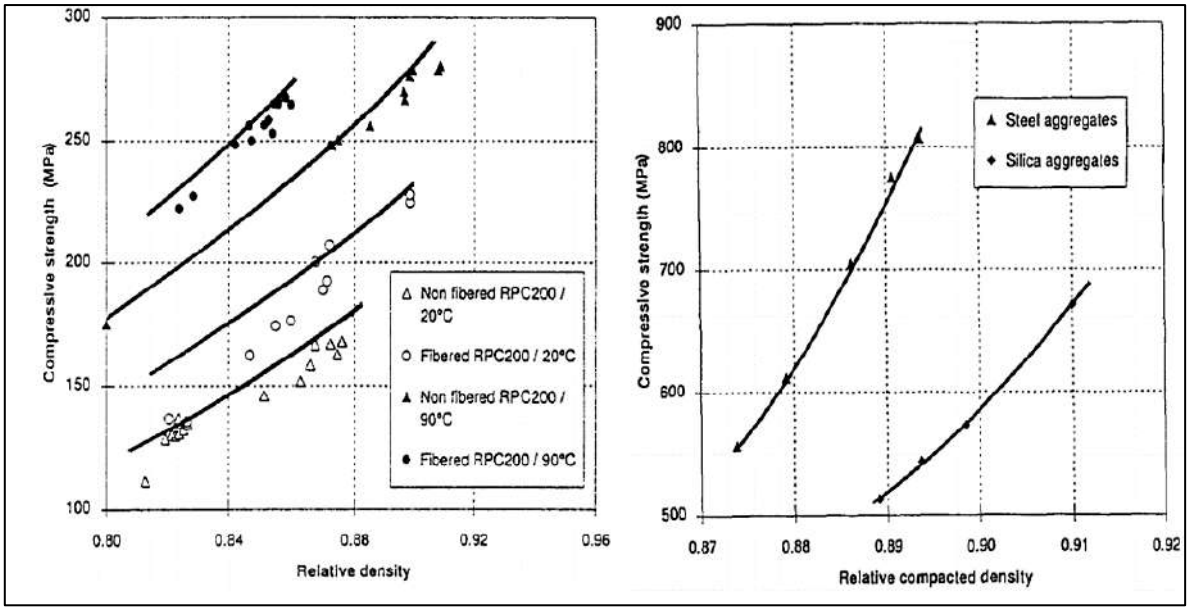

Figure (2.3) Variation in strength with relative density

In 2012, Hassan [72] The punching shear behavior of slabs made of ordinary, modified reactive powder concrete was studied. Twenty specimens with measurements (1000*1000*50 or 70 mm) were casted and examined on the experimental side. These specimens contained four variables that are ratio of steel fibers, steel reinforcement ratio, slab thickness and concrete type to assess variables upon on punching shear strength with solely assisted Reactive powder concrete and MRPC slabs under point load at the slab sandwich. The experimental component also included the effect of the ratio of steel fibers and the lack of coarse aggregates on certain mechanical properties such as compressive strength. Splitting tensile strength, elasticity module, and rupture module. The laboratory tests showed that the increased quality of the fibers strengthened RPC's mechanical properties. It also demonstrated that the punching shear failure occurs unexpectedly in slabs not containing steel fibers, where there is no notice until failure except for the rapid movement of the dial gage, Generally, improve ultimate load by increasing slab thickness, steel reinforcement ratio and steel fiber material.

Properties of reactive powder concrete reinforced with random distribution of fibers were studied in (2013) by AL-Amery [73]. The experimental program included the effect of steel fiber shape (straight or crimped) and volumetric ratio of steel fibers on the mechanical properties of RPC. The mechanical properties tested in this study included: compressive strength, splitting tensile strength, modulus of elasticity, density, modulus of rupture, and impact resistance. The results showed that increasing steel fiber volumetric ratio from (0%) to (2%) led to increasing all the mechanical properties of RPC. It was also found that using crimped fibers achieved high mechanical properties than straight fibers.

Hoang et al., 2016 [74] presented a new approach for mix design of the UHPC. This approach depended on stepwise optimization of particle packing density and strength by finding out corresponding affordable materials such as; cement, silica fume, quartz powder, and superplasticizer. The investigation showed the effect of using the four-grain size of coarse aggregate of 1mm, 2.5mm, 4mm, and 8mm without any special treatment on the compressive strength. Fine aggregates are classified in accordance with its finesse of partial size, so trail mix between types of fine aggregate to get optimum packing density. An experimental trial mix was conducted to find optimum water cementitious ratio. That result was equal to 25% of cementitious.

In 2017, Abdulrahman et al [75] studied mechanical properties under different curing of reactive powder concrete. This research was done to find out the benefits of different treatments for the mechanical properties of reactive powder concrete such as compression, tension splitting and fracture modulus. It was treated in three different methods, immersion with water at a temperature of 35 °C that was chosen as a reference for treatments and immersion in water at 90 °C for 5 hours per day, as well as the method of steaming the same period per day until 28 days of treatment are completed. The proportion of silica fume was taken as a factor to know its effect on the mechanical properties as a percentage of the

weight of the cement where the proportions (5,10,15) %. The results showed that the method of immersion with a temperature of 90 °C was the best for all types of treatments with different silica ratios. The test results are listed in Table (2.4).

Table (2.4) Compressive strength, splitting tensile strength and modules of rupture at 28 day of different curing condition

Curing method	Silica fume %	Compressive Strength for cubes fcu (Mpa)	Splitting tensile strength for cylinders ft(Mpa)	Modulus of rupture fr(Mpa)
Immersion water 35°C	0	53.55	3.2	10.22
	5	55.78	5.77	12.95
	10	58.77	7.6	13.9
	15	55.1	3.66	9.4
Immersion In hot water 90°C	0	59.79	7.55	15.2
	5	80.45	9.45	18.7
	10	83.9	10.32	27.3
	15	44	4.92	19.9
steam	0	63	2.55	10.3
	5	68.5	8.01	11.6
	10	71.9	8.76	15.6
	15	41	3.2	12.3

2.6 Repeated Loading Mechanism

To represent the hysterical properties of building materials, it is very important to study and analyze the dynamic or repeated loading. This type of loading is considered a complex load because it consists of compressive and tensile loads. Several experiments were conducted to find out the behavior of normal concrete subjected to a repeated load, whether the load was in in tension or compressive phase. Results showed unloading damage and reloading damage lead to decrease concrete hardness upon exposure to repeated loads. Figure (2.4) Demonstrates exposure of plain concrete to repeated regular compression, unloading, reloading and periodic loading.

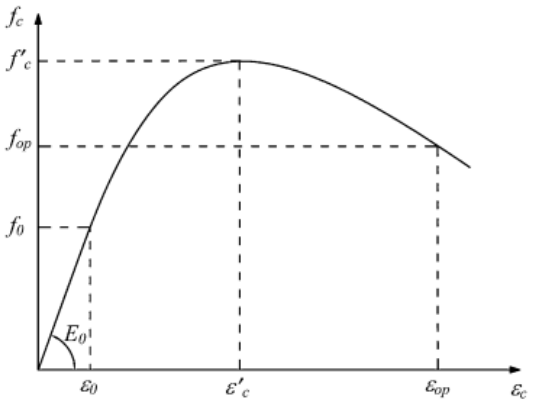

(a) Complete repeated in compression

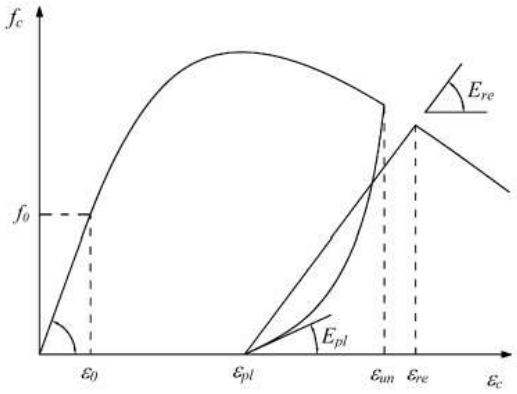

(b) complete unloading and reloading repeated in compression

Figure (2.4) exposure of plain concrete to repeated regular compression, unloading, reloading and periodic loading

It is very important to obtain the unloading and reloading cycles for any repeated load because they are related to the accumulated damage that contributes to the deterioration of the hardness and strength of plain concrete, through which the amount of energy dissipation can be determined [76].

2.7 Summery

Table (2.5) shows the summary of past literatures on axially loaded concrete-filled steel tubular columns are presented below:

Table (2.5) Experimental studies on axially loaded CFST column test.

Reference	Experimental Synopsis	Main Parameters
Zeghiche and Chaoui (2005)	eccentric loading of columns (CHS)	• **L/D** • **e** • **fc′**

De Nardin (2007)	CFST columns subjected to axial compression.	• **Type of tubing**
Han (2008) and Liu	Short CFST columns subjected to axial local compression.	• **Type of tubing** • **Local compression area** • **thickness of loading plate**
Lama and Gardner (2008)	CFST columns subjected to axial compression for stainless steel sections	• **fc′** • **Type of tubing**
de Oliveira (2009)	CFST columns subjected to axial compression	• **L/D** • **fc′**
Uenaka (2010)	Concrete filled double skin tubular (CFDST) stub columns columns subjected to axial compression	• **D/t**
Park and hong (2011)	CFT column system reinforced by CFRP subjected to axial loading	• **(D/t)** • **number of carbon FRP sheet layers**
Ganesh Prabhu, and Sundar raja (2011)	The compressive behavior of the circular columns filled with concrete (CFST) reinforced by (CFRP)	• **The distance between the CFRP layers and the number of strips**
Yang and Han (2012)	The behavior of composite columns (CFST) thin-walled, sujected to partial and concentrated load	• **Type of tubing** • **Localcompresion area thickness of loading plate** • **L/D**
Portolés (2013)	slender circular tubular column (CFST) subjected to concentric	• **fc′** • **type of reinforcement**

	and eccentric axial load	
Khodaie (2013)	Investigated the concrete-steel bond strength of CFST	• **D** • **fc**
Essopjee, and Dundu(2015)	CFDSCT columns loaded in axial compression	• **D** • **t** • **Length**
Mahgub (2017)	the axial compressive behavior of elliptical steel tube columns packed with self-compacting concrete	• **D** • **fc′** • **Length**
Elchalakani (2018)	Axial compression for CFST and CFDST	• **Rubber ratio for rubberised concrete.**
Zhou (2019)	Axial compression for oval hollow section (OHS) tubes	• **D/t** • **fc′**
Naseem Baig (2006)	Axial compression for non-slender composite columns CFST	• **Type of tubing** • **D/t**
Gupta (2007)	Axial compression for circular columns filled (CFST)	• **D/t** • **fc′** • **fly ash ratio**
Uy (2011)	non-slender and long of type CFST stainless steel tube under the axial loading as well as test of axial strength and bending moment	• **Type of tubing**

Li (2018)	eccentric loading of high strength concrete filled high strength square steel tube (HCFHSST)	• **B/t** • **E**
Mi, (2020)	impact loading of of ultra-high-performance fiber-reinforced concrete (UHPFRC) steel tube	• **the ratio of steel** • **the ratio of axial load** • **Axial load ratio**
Huang (2002)	CFST columns subjected to axial compression.	• **B / t** • **D/t** • **Type of tubing**
Tao et al (2005)	Short CFST columns subjected to axial compression	• **welded longitudinal stiffeners** • **Length/thickness**
Eom, (2019)	behavior of the double skin composite column under the influence of bending loading	• **Type of stiffeners**
Yuan, (2019)	The behavior of (CFST) column under eccentric compression	• **L/B**
Vipulkumar et al., (2020)[	Non slender circular tubular column (CFST) subjected to eccentric axial load	• **Di/Do**

According to the researches that were discussed in this chapter, it concluded that there is littele previous studied or investigation to predicted the influence of the repeated loading for CFDST columns. That led to going on to adopted this study.

An experimental study with various parameters such as; type of concrete filled, type of section of steel tube was adopted to the repeated loading case.

CHAPTER THREE

CHAPTER THREE

EXPERIMENTAL WORK

3.1 General

The major objectives of this research work is to study to the performance and strength of double skin tubular columns filled with concrete, and subjected to axially compressive repeated load test. In this research, there are many main parameters which have been studied and analyzed, such as concrete cross section area, L/B, and L/(D) ratio, steel fiber ratio, shear connectors and type of concrete filled .This chapter explains the concrete filled double skin portion, the properties of the materials used, different types of concrete mixtures, the material characteristics of concrete samples and the concrete filled double skin specimen testing procedure. All the tests had been carried out in the laboratories of Collage of Engineering of the University of Kerbala.

3.2 Test Specimens Details

The present experimental program consisted of all the units tested in this study, such as samples of cube, cylinders, and fourteen of concrete filled double skin tabular column specimens, which have been examined to represent all variables of the research plan. The CFDST was made up of inner and outer tubes, as well as sandwiched concrete between them as illustrated in Figure (3-1). Two of these specimens were reference columns casted with normal concrete while other specimens ten columns were filled with reactive powder concrete and two specimens were only not filled. All specimens have a total length of (800 mm), except two specimens have 700 mm. The cross-section dimension of the outer and inner square tube is equal to (100 mm*100mm) and (50mm*50mm) respectively. While the external and internal diameter of the cross section of circular tube is

100mm and 50 mm respectively. The thickness of the steel used for square and circular sections is 2.2 mm.

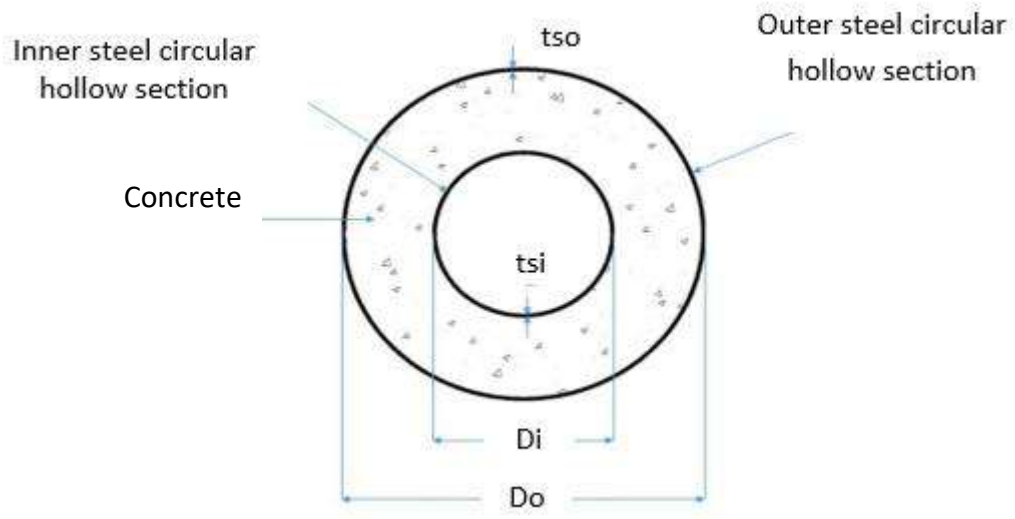

Figure (3.1) cross section of CFDST

All the samples divided into seven groups to clarify the details of the samples as below:

First group: this group consists of two samples; the first one composed of two tubes of steel with a circular outer and inner sections,while the other sample was consisted of a square outer and inner tube as shown in Plate (3.1).These samples were filled with reactive powder concrete with a percentage of steel fibers 0.5%, and length of 800 mm for both samples.

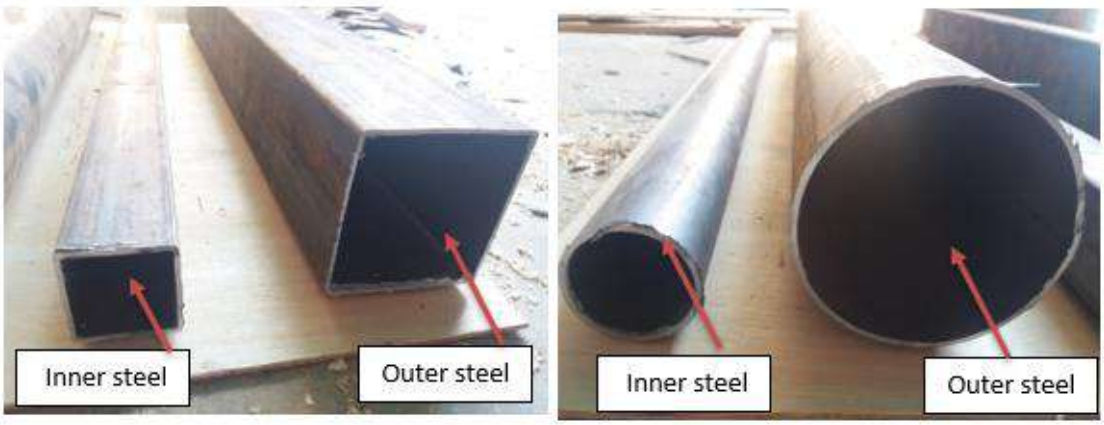

Plate (3.1) inner and outer steel section

Second group: this group consists of two samples, the first one was composed of two tubes of steel with a circular outer and inner sections, and the other sample was with a square outer and inner tube. These samples were filled with reactive powder concrete with a percentage of steel fibers 1.5%, and length of 800 mm for both samples.

Third group: This group was made up of two steel samples, one of them have a circular section as an exterior tube and the other with a square section as an inner tube, and conversely for the other sample. These samples were filled with reactive powder concrete with a percentage of steel fibers 1.5% and length of 800 mm for both samples as shown in the Plate (3.2).

Plate (3.2) describe of inner and outer skin

Fourth group: this group consists of two samples the first one composed of two tubes of steel with a circular outer and inner sections, and the other sample was with a square outer and inner tube. These samples were filled with reactive powder concrete with a percentage of steel fibers 1.5%, and length of 700 mm for both samples.

Fifth group: the fifth group consists of two samples first one composed of two tubes of steel with a circular outer and inner sections, and the other sample have a square outer and inner tube. These samples were filled with reactive powder

concrete with 1.5% steel fibers and have lengths of 800 mm for both samples and they contain bolts (studs) welded to the inner tube for these specimens only as shown in Figure (3.2).

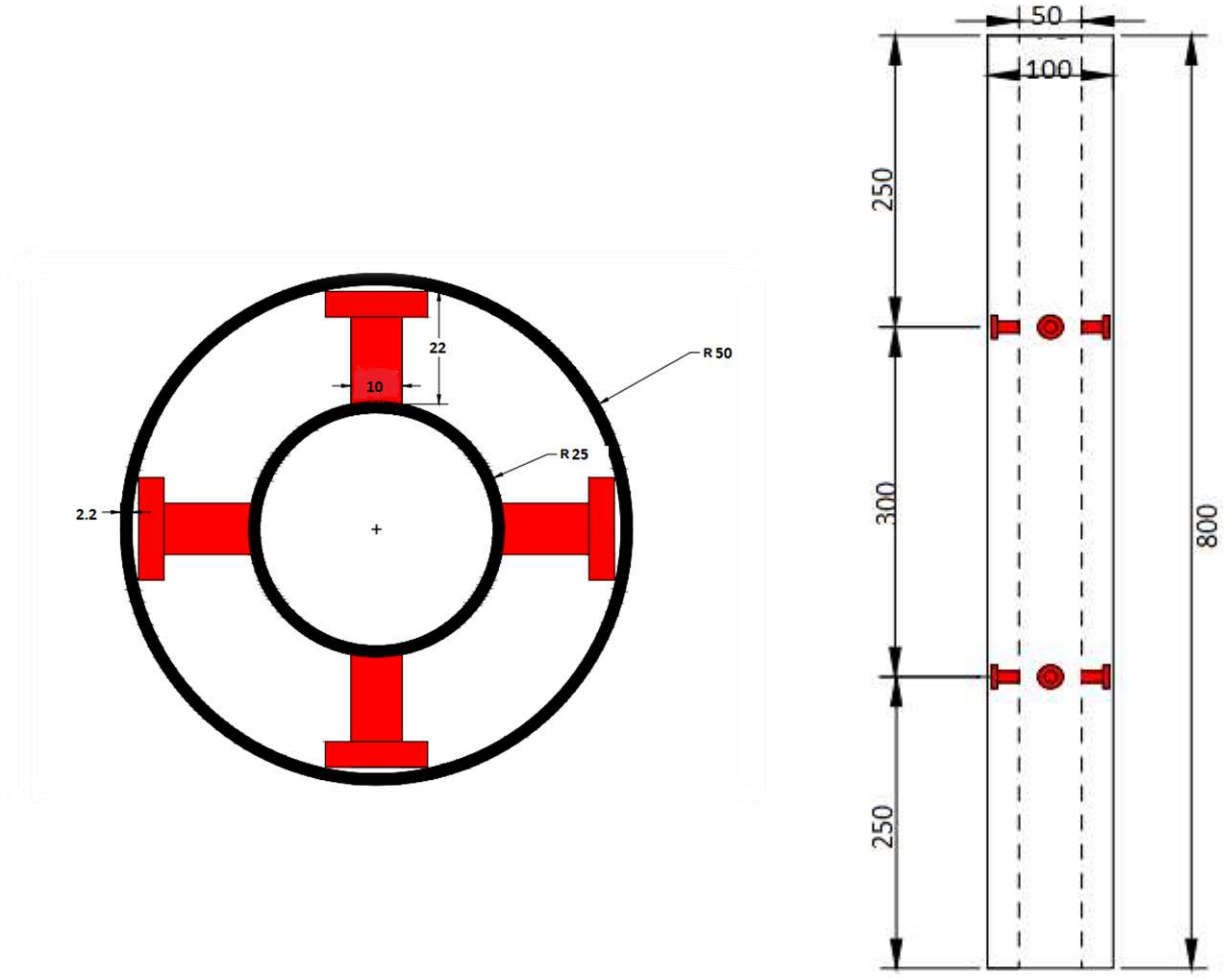

Figure (3.2) welded bolts for inner tube of column(all dimension in milimeter)

Sixth group: this group consists of two samples first one composed of two tubes of steel with a circular outer and inner sections, and the other sample have a square outer and inner tube. These samples were filled with normal concrete and have length of 800 mm for both.

Seventh group: this group consists of two samples first one composed of two tubes of steel with a circular outer and inner sections, and the other sample was with a square outer and inner tube. These samples were not filled with concrete and have

a length of 800 mm for both samples. Tables (3.1) and (3.2) below shows the details of the samples used in this research.

Table (3.1): Details of concrete filled circular double skin column (CFCDS)

Type of concrete used in specimen	Name of specimen	Length of specimen	Parameter of specimen
Reactive Powder Concrete	CHS (1)	800	0.5% steel fiber
	CHS (2)	800	1.5% steel fiber
	CHS (3)	800	1.5% steel fiber Square inner tube
	CHS (4)	700	1.5%steel fiber Global Slenderness (L/B) =7
	CHS (5)	800	1.5% steel fiber Shear connector(bolt)
Normal concrete	CHS (6)	800	Normal concrete
Steel only	CHS (7)	800	Empty tubing

Table (3.2): Details of concrete square filled double skin column (CFSDS)

Type of concrete used in specimen	Name of specimen	Length of specimen	Parameter of specimen
Reactive Powder Concrete	SHS (1)	800	0.5% steel fiber
	SHS (2)	800	1.5% steel fiber
	SHS (3)	800	1.5% steel fiber Circular inner tube
	SHS (4)	700	1.5%steel fiber Global Slenderness =7
	SHS (5)	800	1.5% steel fiber Shear connector(bolt)
Normal concrete	SHS (6)	800	Normal concrete
Steel only	SHS (7)	800	Empty tubing

3.3 Preparation of Specimens

The tube of the steel was provided in length of 6000 mm, the structural steel tubing was produced by fulad Mehr Company of Iran. The total length of tubes was cut in order to provide the laboratory length of the samples (required). The inner tubes were carefully placed at the middle of the outer tubes in the preparation of the test specimens, to conform the center of the inner tube with the center of the outer tube. A plate was welded to the base of the steel tube with a thickness of 3 mm, while the upper part of the tube was left open to allow the concrete to pour. To create uniform load transfer around the cross-section during processing of test, the welding points were smoothed. In double tube columns CFDST, the gap was equal between the outer and inner tubes by welding steel strips at depth 10 mm located at the tip of the samples as seen in plate (3.3). In CFDST, the upper inner tube opening was kept closed during the casting process to avoid fresh concrete entering, which is not desirable for the study. After the completion of the casting, it can be opened to prepare the sample for examination. After that, the specimens were coated to prevent them from corrosion during the curing to become ready for pouring the concrete into the tube.

Plate (3.3) Sample preparation steps

3.4 Material

Several building materials will be dealt with in this research to complete its requirements as listed below:

3.4.1 Cement

There are several commercial cement products in the local market. The conventional cement form KARASTA as Portland-limestone cement type CEM II/A-L, which is manufactured by LAFARGEHOLCIM, Karbala Cement Manufacturing Limited, KCML, has been chosen for this research as seen in Plate (3.4). This type of cement has been used for both NC and RPC mixture in the experimental work. It was stored in dry region to avoid exposure to moisture. Tables (3.3) and (3.4) show the cement's physical properties and chemical composition respectively. The test results show that the cement meets the specifications of Iraqi Specification No.5/1984 [77]. These experiments were carried out in the College of Engineering / Kerbala University's Materials Laboratory.

Plate (3.4) Cement Used in this study

Table (3.3) Chemical Composition Of Cement *

Compound Composition	Chemical Composition	Weigh t (%)	Iraqi specification No.5/1984 %
Lime	CaO	51	-
Silica	SiO2	18.7	-
Alumina	Al2O3	4.97	-
Iron oxide	Fe2O3	5.22	-
Magnesia	MgO	2.24	5 % max
Sulfate	SO3	1.89	2.5 % max
Loss on ignition	L.O.I	3.94	4% max
Insoluble residue	I.R	0.7	1.5% max
Lime saturation Factor	L.S.F	0.83	0.66-1.02
Tricalcium Aluminates	C3A	4.34	-
Tricalcium Silicate	C3S	24.66	-
Diacalcium Silicate	C2S	33	-
Tetracalcium alumina ferrite	C4AF	15.88	-

Table (3.4) Physical Properties of The Cement

Physical Properties	Test Result	Iraqi specification No.5/1984
Initial setting (min)	190	More than 45 min
Final setting (hr)	4.55	Less than 10 hr
Compressive strength for cement paste at		
3 days age	17.28	Not less than 15
at 7 days age	25.97	Not less than 23

3.4.2 Fine Aggregate (Sand)

Property	Test result	Specification limits % Iraqi specification No.45/1984
Material Passing 75 µm Sieve	3.1 %	< 5 %
Sulfate content (SO3)	0.097 %	≤ 0.5 %

There were two types of fine aggregate employed in this study:

1) 1) Al-Akhaidher normal sand with the optimum particle size (4.75 mm) was used for a traditional concrete mixture. The graded and chemical properties of this form of sand are shown in Tables (3.5) and (3.6) respectively. This form of sand was appropriate under Iraqi Specification No. 45/1984 [78].

2) Quite fine sand with the largest granule size (0.6 mm) was used on only RPC mixtures. It was removed from the natural sand by sieve analysis (600 µm), as seen in Plate (3.5). Table (3.7) presents the findings of the very fine sand sieve analysis which complied with the No.45/1984 Iraqi specifications. These testing carried out in the Materials Laboratory of the College of Engineering/ University of Kerbala.

Table (3.5): Natural sand grading

Sieve size (mm)	Passing accumulative %	Specification limits % Iraqi specification No.45/1984
10	100	100
4.75	97	100-90
2.36	87	100-85
1.18	76	100-75
0.6	67	79-60
0.3	32	40-12
0.15	4	10-0

Table (3.6): Sand's Chemical Composition *

Table (3.7) Quite fine sand grading

Sieve size (mm)	Accumulative passing %	Specification limits % Iraqi specification No.45/1984
1.18	100	90-100
0.6	100	80-100
0.3	40	15-50
0.15	9	0-15

Plate (3.5) quite fine sand separation

by sieve 600 µm

3.4.3 Coarse Aggregate (Gravel)

Only standard concrete was made from crushed river gravel obtained from Al-Akhaidher with a maximum particle size of (9.5) mm. For cleaning it from dirt, the gravel was washed by spray, and left to dry in the air before using. The coarse aggregate test results including the Iraqi specification limits are given in Table (3.8).Test results of the coarse aggregate showed that this type has been acceptable according to the Iraqi specification No.45/1984 [79]

Table (3.8): Coarse Aggregate Grading Results

Sieve size (mm)	Passing %	Specification limits % Iraqi specification No.45/1984
12.5	100	100
9.5	100	85-100
4.75	10	10-30
2.36	2	0-10
1.18	0	0

Table (3.9): Chemical Property Of Coarse Aggregate Chemical Property

Property	Test result	Specification limits % Iraqi specification No.45/1984
Material Passing 75 µm Sieve	0.3 %	≤ 3 %
Sulfate content (SO3)	0.062 %	≤ 0.1 %

3.4.4 Mixing Water

All concrete mixture type of the sample was mixed and cured with tap water.

3.4.5 Silica Fume

The type of silica fume which was used in the RPC mixtures of the experimental program was commercially known as (Megaadd MS (D)) UAE [80] as explained in Appendix (A). This type was a very fine pozzolanic material consisted typically of non-crystalline silica produced by electric furnaces as a secondary production as describe in Plate (3.6). The physical and chemical properties of this type of silica fume are shown in Table (3.10). The results show that there was conformable with standard specification of (ASTM C 1240-05) [81]. In this study, the content of silica used in RPC mixtures was 22 % of the additive weight of cement can be used As recommended in the datasheet.

Plate (3.6) Silica Fume powder

Table (3.10): Properties of Silica Fume [80]*

Property	Test result	Limit of specification requirements ASTM C-1240
Color	Grey powder	---
Density (kg/m^3)	600	(500-700)
Specific gravity	2.26	(2.1-2.4)
Chemical properties		
Sio_2 %	85.6	85.0 (minimum)
Moisture content %	0.5	3.0 (maximum)
Loss of ignition %	4.2	6.0 (maximum)
Physical properties		
Specific surface (m^2/gm)	19	15 (minimum)
Percent retained on 45 µm NO (325) %	8	10 (maximum)

3.4.6 Superplasticizer

A high range water reducing admixture was used in this research work for RPC mixture only as explained in Appendix (A). It was supplied by Sika company under the name of (Sika ViscoCrete®-5930)[82].It was a third-generation superplasticizer for concrete and mortar, this type is suitable for producing many types of concrete and it can be used in both cold and hot weather conditions. Sika ViscoCrete®5930 was high water reducing up to 30 % and it has several advantages besides reducing water content in the mixture such as; improved shrinkage and creep behavior, increased high early strength, and density as shown in Plate (3.7).The characteristics of this type of superplasticizer are shown in Table (3.11), where it was conform to the requirements of superplasticizer according to ASTM-C- 494-99 types G and F[83].In this study, the content of superplasticizer in RPC mixtures was 5 % of the of cement.

Plate (3.7) Sika ViscoCrete -5930

Table (3.11) Sika ViscoCrete ® -5930 Scientific Details[82]

Property	Description or Value
Basis	Aqueous solution of modified polycarboxylate
Appearance	Turbid liquid
Density (kg /lt)	1.095
Boiling	100 º C
PH	7-9
Recommended Dosage	0.2-0.8 % litter by weight of cement for NC 0.8-2 % litter by weight of cement for flowing and self- compacting concrete.

3-4-7 Steel Fibers:

Straight micro steel fibers made by Ganzhou Daye Metallic Fibers Co. Ltd., China were used in this research, the key parameter for the manufacture of ductile concrete, which also raises the compressive strength and improves the mechanical properties of the UHPCs [84]. The aspect ratio (fiber length to fiber diameter) of the steel fiber was nearly 59 as explained in Appendix (A). The tensile strength of the metal fibers and density were around 2850Mpa,7850kg/m3 respectively. The micro steel fiber is shown in Plate (3.8). In this research, two fraction volumes of 0.5 %, and 1.5 % were adopted.

Plate (3-8) Steel Fibers Material

3-4-8: Steel Tube

To determine the material properties, a tensile stress coupon test was done on steel tubing. The curved tensile coupon specimens were extracted from tubes that were manufactured similarly by the same process. The typical tensile test is performed as seen in Plate (3.9).It has been taken three pieces of tensile coupon to measure the average of tensile strength, and to measure yield stress (fy),the ultimate strength (fu) and the elastic modules (Es) of steel were lists in Table (3.12).The sample preparation, dimensions of the geometric properties of the steel coupon and test speed were complied with ASTM-A370 requirements. Figure (3.3) suggests the descriptions of the coupon as per ASTM-A370[85]. All samples were examined at the Iraqi Ministry of Construction and Housing's National Center for Laboratories and Structural Research.

Plate (3.9) typical tensile test of coupons

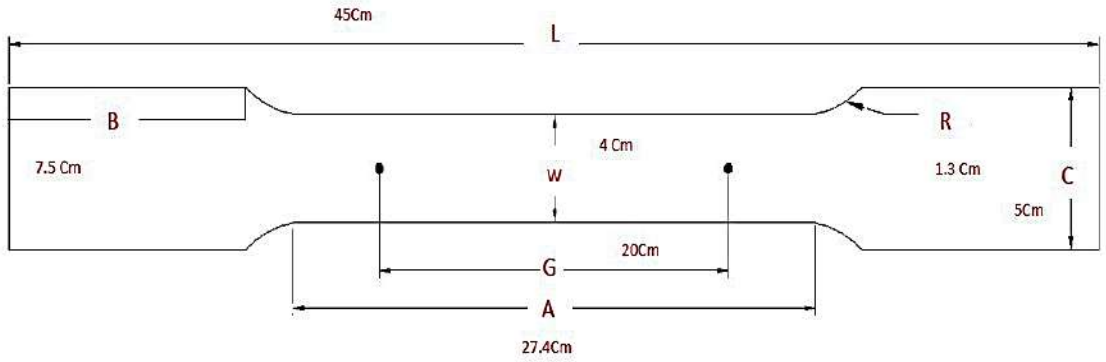

Figure (3.3) descriptions of dimension coupon as per ASTM-A370

Table (3.12) properties of the steel coupon

No.of coupon	Yielding stress (Fy) Mpa	Ultimate stress(Fu) Mpa	Elongation at fracture %	Modulus of elasticity(Es) (Mpa)	Thickness (t)
1	337	393	23.7	200695	2.2
2	364	416	20	201350	2.2
3	333	385	10.9	201150	2.2
Mean	344.6	398	18.2	201065	2.2

3-4-9: Shear Studs

In two tests of specimens, stud shear connectors with head marking (8.8),also 10 mm diameter and a 55 mm overall length were employed, which after cutting became of a maximum height of 22 mm, in order to prevent the vertical contrast between the concrete and steel surfaces. Welding was used to attach the shear connectors to the inner steel tube. Plate (3-10) reveals images of the studs used prior to and after cutting. For the determination of the shear connector's mechanical properties, three specimens were randomly selected and examined at extreme stress. Plate (3-11) shows the results of the research conducted in the mechanical laboratory according to ASTM-F606 at the College of Engineering, University of Kerbela. The results of tensile tests are provided in Table (3-2).

(A)before cutting **(B) after cutting**

Plate (3-10) The head Studs

Plate (3-11) Tensile Testing Machine

Table (3.13) Mechanical Properties of Shear Connector

Steel Sample	Sample No.	Yield Stress (F_y) (MPa)	Ultimate tensile strength (F_u) (MPa)	Elongation %
Steel Bolt (stud)	1	661.8	783.5	13.3
	2	632.7	791.2	13.8
	3	625.1	785.4	13.6
Average		639.8	786.03	13.5

3.5 Concrete Mixes

3.5.1 Normal Concrete (NC)

This kind of concrete mixture basically consists of cement, sand, gravel and water. In this type of mix the compressive strength value ranged between 25-35 MPa. To achieve the best designed mix, many mixes created there in the lab to get final quantities being ((1) cement: (1.2) sand:(1.4) gravel) and water to cement ratio is 0.4. Table (3.14) shows product quantities by weight per cubic meter. mixing was done using rotary mixer of 0.1 m3 as shown in Plate (3.12). The mixing process was done by incorporating the dry materials like cement, Sand, gravel, then combined for two minutes respectively. After that, water was applied and mixed to obtain homogeneous mixture for two minutes, this form of concrete was cured in water at 25 ^{0}C.

Plate (3.12) Rotating Machine Used for Making Normal Concrete (NC)

Table (3.14): Quantities of the Materials by (kg) for One Cubic Meter of Normal Concrete (NC) Mix

Cement	Natural sand	Gravel	Water
563	680	787	225.2

3.5.2 Reactive Powder Concrete

Reactive powder concrete (RPC) was obtained by reacting cement, very fine sand, silica fume, fiber metal, superplasticizer and little (W / C) ratio, while removing the coarse aggregate. The important factor affecting this type of concrete is the low ratio of W/C by taking into account the workability of concrete. This form of concrete was used for many composite columns. Plate (3.13) shows the mixer used for this purpose. Several trail of blending were carried out to find the right proportion of ingredients to create the RPC blend. Finally, the best proportion of ingredients that have been gotten in the present study are listed in Table (3.15). Two fraction volumes of 0.5 %, and 1.5 % were adopted, which were used to produce RPC for many double skins**.**

Plate (3.13) Mixer Used to Produce Reactive Powder Concrete

Table (3.15) Final Proportion of the Ingredients kg /m3

Mix	Cement	Silica Fume	Very Fine Aggregate	W/(cm)	Superplasticizer	Steel Fiber ratio of volume mix
RPC-0.5	900	200	1100	0.23	45	0.5%
RPC-1.5	900	200	1100	0.23	45	1.5%

Cm=Cement materail

3.6 Mixing Procedure

There are some previous studies that dealt with how to produce reactive powder concrete such as (Al-Amery, and Kindeel) [86, 87]. The method of mixing was illustrated by adding the very fine sand to the silica fume and mixing in dry state for 5 minutes to ensure homogeneity between powder particles and silica fume, after that cement was added and also mix for about 5 minutes. Then quantity of water added and mixing for other five minutes. After that, superplasticizer was added gradually and mixed well for about 3 minutes until the materials seem properly mixed. Finally, steel fibers were added gradually to ensure uniformly distribution and mix for 2-3 minutes. These stages are described in Plate (3-14). The total time of mixing was about 20 minutes for each mix. This procedure was carried out according to (Will et al.) [88]. To give reactive powder concrete a high compressive strength of approximately 100 MPa after the completion of the casting process, the samples were left for a period ranging between 36-48 hours to harden. Then they were treated with hot water that reaches 60 °C for a period of three days only. Then complete the treatment by the age of 28 with normal water at 25 °C to obtain high material properties.

Plate (3.14) Summary of Blends

3.7 Mixture Casting in Tube and Curing Procedure

The tubes were well cleaned of the inner surfaces before inserting concrete in the molds to ensure stronger bonding of the hardened concrete between concrete and steel tube. In a vertical location, the tubes were filled and the concrete was poured in two equal layers into the mold. Compaction was accomplished for a few minutes by using electric vibrating and compaction rods to eliminate air voids for obtain well compacted concrete. Then, by using a steel trowel, the excess concrete at the top edge of the tube was cut and finely milled to making the upper surface of the steel tube appeared at the same level as the surface of the concrete. For each stage of casting, three standard cubes by dimensions (100*100*100) mm had been taken for compression strength test, and six cylinders with dimension (100*200) mm had been also taken for splitting tensile strength test and modules of elasticity tests. It was levelled by means of a steel trowel, and compacted into two layers at the same time as seen in Plate (3-15). Specimens were protected using nylon coverings to prevent water evaporation from fresh concrete. An important action to generate RPC is the curing of concrete. There are many treatment processes, such as steam curing, hot bath healing, or ambient temperature, that are used. In the current analysis, the samples were de-molded after 36-48 hours of casting and submerged

in a hot water bath with 60 ºC for 3 days and then 25 ºC until the age of 28 days [89], as seen in Plate (3.16).

Plate (3.15) Mixing, placing and compacting of concrete.

A-Before curing concrete

B-After curing concrete in water at 60 ºC

Plate (3.16) curing of specimen

3.8 Levelling Concrete and Coating of Columns

The concrete mixture passes through various variables after pouring concrete into steel tubing, contributing to a reduction in its size. The cement hydration temperature, evaporation, micro-gaps, and other factors that affecting the completion of the concrete mixture reactions. In the current research, a very small decrease in the concrete at the top of steel molds was found, this is not logical in terms of load distribution, so Flo-Grout BP800 was used for this state as seen in Plate (3.17).

Plate (3.17) Flo-grout

Flo-Grout BP800 is a grey powder consists of a pre-mixed, pre-packed, high strength. It is free of chloride and hydrogen elements,compound of cement as well as other carefully selected additives, well-rated fillers and non-reactive aggregates designed to impart a flow characteristic and reduce shrinkage and high pressure strength according to ASTMC1107,Grade C [90] and appendex (A).

3.8.1 Uses of Flo-Grout

1. For grouting areas under bridge bearing pads.
2. Pile caps treatment.
3. Suitable for requirements of bulky pile bases and plate bases at high strength.

3.8.2 Advantages

1. It has less shrinkage ability.

2. Suitable for hot weather conditions.

3. Impermeability and high density.

4. It is quick to harden and has high strength, which allows for high installation.

5. The flow can be pumped into variable thicknesses of up to 10 mm.

6. It is easy to apply because it is made of one compound and only requires an addition of water.

7. It does not contain the elements of hydrogen and chloride.

3.8.3 Mixing of flo-grout and placing

The cement powder mixing process is carried out using a mechanical mixer device. A quantity of 3.75 liters of clean water is placed in a container depending on the required consistency of the paste. After that, The 25 kg powder is then added slowly to the water while mixing continuously with low speed mixer (400 - 600 rpm) as shown in Plate (3-18). Mixing time can continue for 4 to 5 minutes. The mixture would be rigid for the first 2 minutes of mixing. The mixed grout shall be poured immediately to the top of tubing after mixing ,and at the same time levelling the thickness of these grouting.The grouting operation must be carried out contiuously.

Plate (3.18)Placing of groute-flo

Afterthat,all specimens were marked with distinct colors to differetiatebetween criteria and names for comparative purposes and to be ready for testing, as illustrated in the Plate (3.19).

Plate (3.19)Coating of columns

3.9 Installation Of Strain Gauge On Steel Tube

The present study focuses on the behavior of the external tube for column and failure mode.Therefore, in such case it needs to monitor the longitudinal strain for each checked column's steel tube of each load stage. One type for strains gauge sensors was used to measure the longitudinal tensile strain of steel

tube,which is made through TML Tokyo Sokki Kenkyujo Co., Ltd [91]. Plate (3-20) shows an example of such strain gauges.

Plate(3.20) Strain gauge instrument

Four peices of strain gauges' sensors gluded based on their manufacturing instructions on the steel surface for each column.Two of the strain pecies were installed in a distance equal to 25mm from the top of column in pependicular faces. and the others were installed in the mid height of the column in perpendicular state also as shown in plate (3-21). After determination the suitable location of strain gauge on steel, the strain gauges were installed according to the following procedure as shown in Plate (3-22):

1-Set exact points and locations for strain gauge fixation.

2-Smoothing and removing impurities of the steel surface in the specified locations by special tools for smoothing.

3-Use acetone to clean the sites and place a tape in the contact area between the wire elctrical and the steel surface to avoid electrical contact.

4- Spread the CN-Y adhesive thoroughly and properly on the strain gauges, then place them on the steel surface and push for a minute to ensure that they are totally glued.

6- Finally strain gauge were numbered to designate their locations.

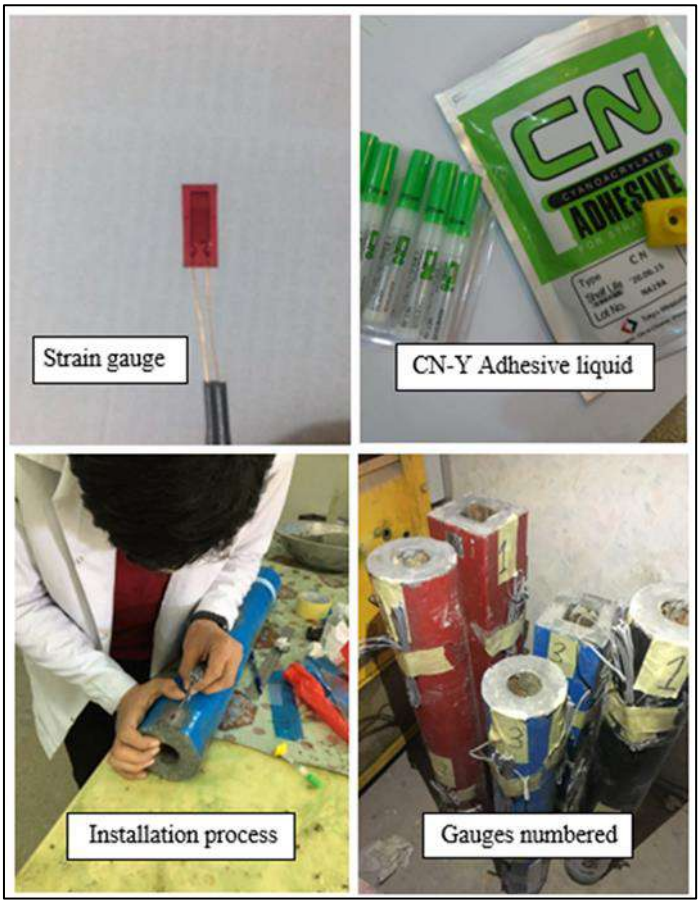

Plate (3.21) Processing of installing strain gauge

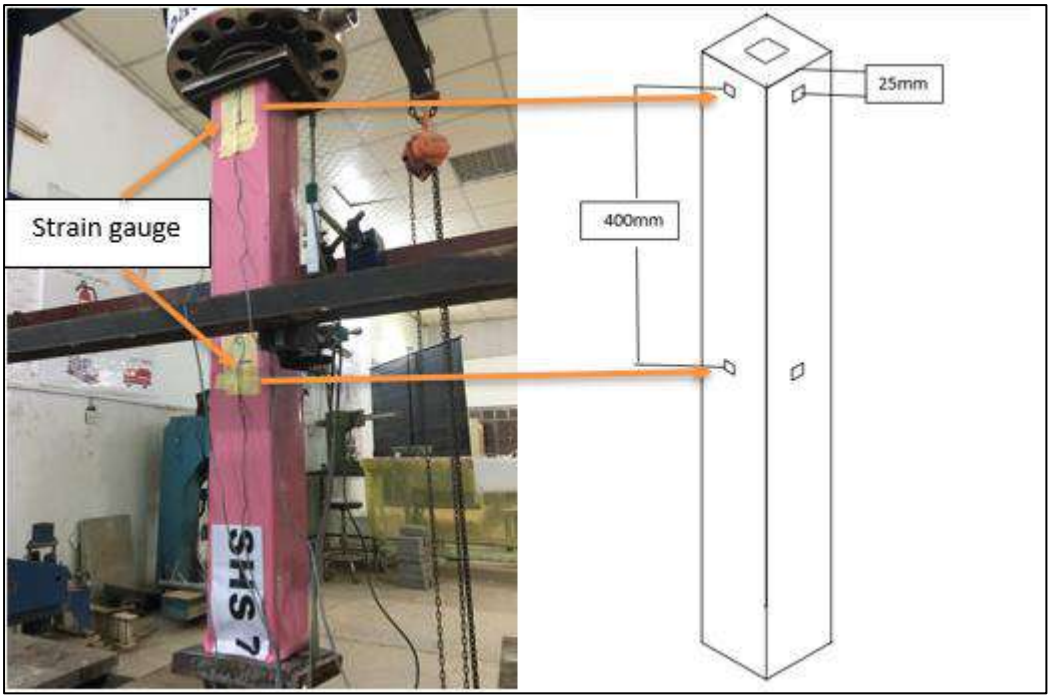

Plate (3.22) places of strain gauges

During the test, all of the strain gauges were connected in the channels given in the data logger that was used throughout the test, according to the channel numbers.

3.10 Tests of Fresh Concrete.

3.10.1 Slump Test

One of the important tests for the consistency and success of concrete as a practical mixture is the slump test. This test was carried out according to (ASTMC143,05a) [92]. The test consists of a truncated cone with height 30 cm. The diameter at the top and the bottom 10 and 20 cm respectively. The test had carried out the fresh concrete in the 3-layer compacted by tamping rod. Each layer was 25 stroked in a uniform and homogeneous manner by the rod. After the cone was filled with concrete, it was slowly lifted, then the difference was measured by the height from the top of the cone to the concrete surface. According to the American code, the permissible precipitation in the case of the column ranges between 25-100 mm according to (ACI 211.1-91) [93], as shown Plate (3-23)

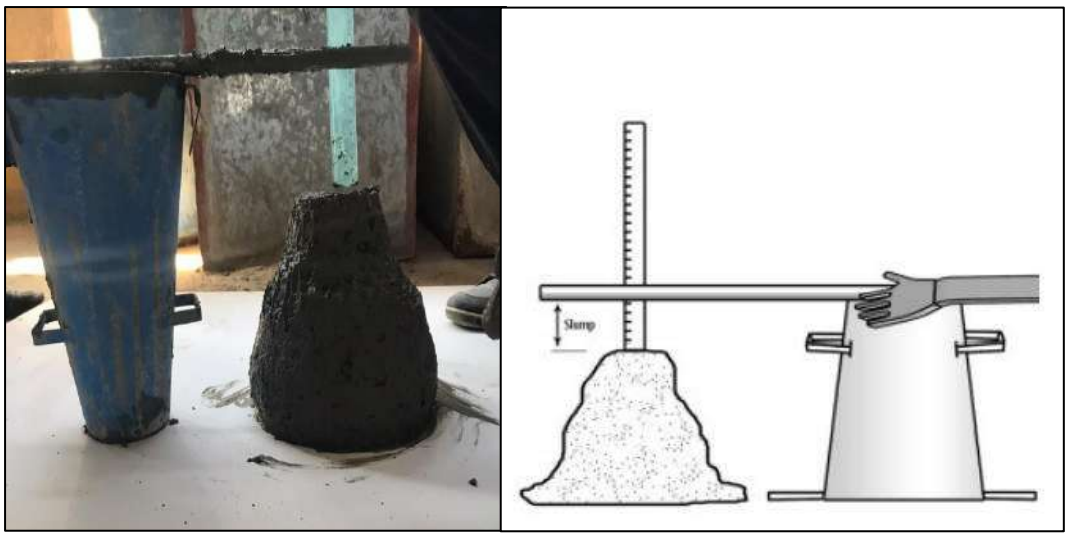

Plate (3.23) slump test

3.11 Mechanical Properties of Hardened Concrete

Several properties for concrete mix were consider important to determine the performance, and they are as describe below:

3.11.1Compressive Strength

The compressive strength test was carried out on (100 * 100 * 100) mm cubes according to B.S: 1881: section 116[94] using digital compressive machine of 2000 kN capacity as shown in Plate (3.24). A charge rate of 0.6 MPa / sec was applied with static load. The cubes were tested after 28 days of cured water for each NC and RPC. The average of three values for specimens was taken to represent the compressive strength.

Plate (3.24) Compressive strength machine

3.11.2Splitting Tensile Strength

The splitting tensile strength was tested using cylinders of (100*200) mm according to the ASTM C 496 M-2004 [95]. The testing machine of 2000 kN ultimate capacity was used to determine this test as shown in Plate (3.25). The test had been carried out on the cylinders after 28 day of water curing. The average value of three samples was used to represent the tensile strength for each of NC and RPC. The Splitting tensile strength can be calculated from the equation (3.1) as below

$$fs = \frac{2p}{\pi DL} \qquad \ldots\ldots\ldots\ldots\ldots\ldots\ldots\ldots\ldots\ldots (3.1)$$

Where

fs: Split tensile stress (MPa), P: Peak apply load (N)

L: Cylinder length (mm), and D: Cylinder diameter (mm)

Plate (3.25) splitting tensile test

3.11.3 Elasticity Modulus

The modulus of elasticity in compression test was conducted to provide a stress to strain ratio value for hardened concrete. This test was achieved according to ASTM C469-2002[96].The apparatus to measure the modulus of elasticity contained a two-yoke attached to the specimen at two diametrically opposite points. Hinge the yoke at the pivot point to pemit rotation of the two segments of the yoke in the horizontal plane, as shown in Figure (3.26). Each mix also included cylinders in three number with 200 mm of heights and 100 mm of diameters. The deformation of concrete was measured by Laser LVDT, which fixed at opposite direction of the hinge rotation pivot. The modulus of elasticity test for each cylinder specimens can be calculated using equation (3.2).

Ec = (S2- S1)/ (Є2-0.00005) **……. (3.2)**

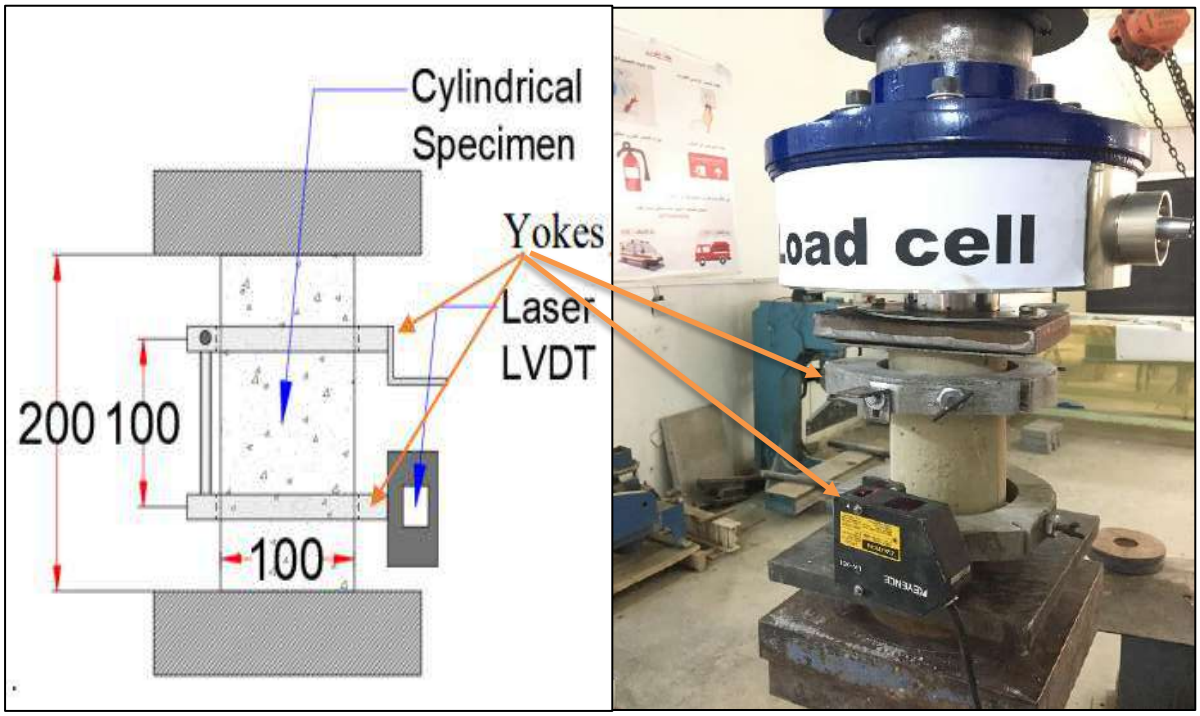

Plate (3.26) modulus of elasticity test

Where:

Ec: modulus of elasticity in (MPa)

S2= stress corresponding to 40% of ultimate load, in (MPa).

S1= stress corresponding to a longitudinal strain, Є1, of (0.000050), in (MPa),

and Є2= longitudinal strain at stress S2.

3.12 Support industry

For the purpose of making the pin support, an upper support was made for the column and a lower anther one. The upper support consists of three plates , the first plates with a thickness of 25 mm and two plate with a thickness of 3 mm is attached to it from the top and bottom of plate had 25 mm. A circular groove is made on the top plate had 3 mm thickness for the purpose of fixing the bearing tooth from the top. Also, the bottom plate grooves are made on it in a circular or square shape that is fixed by bolts before loading and the grooves are compatible with the shape of the cross section of the column for the purpose of fixing it as shown in Plate (3-27).But the lower support be in the form of three parts which are the top and, bottom plate and the ball. The top and the bottom plate made on its circular grooves for stability ball of support as shown in plate (3-28).

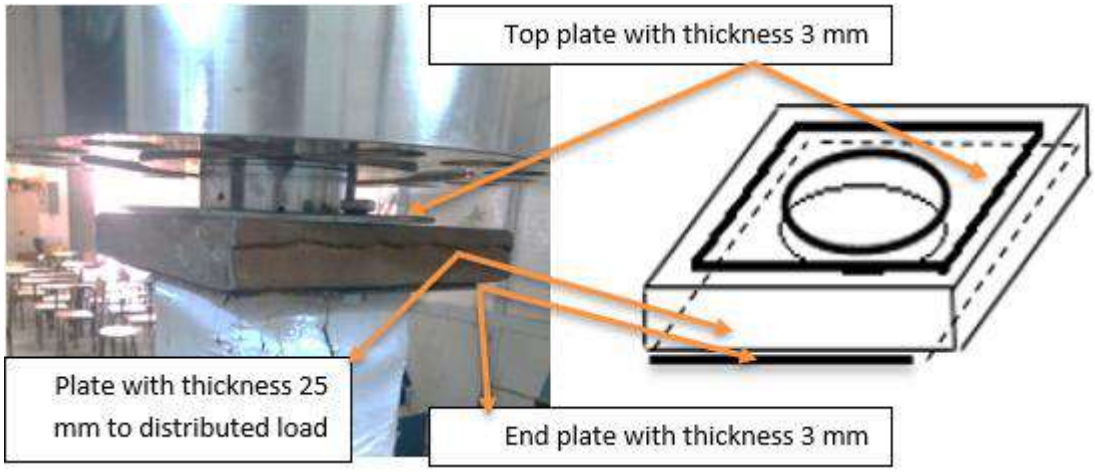

Plate (3-27) Top support of sample

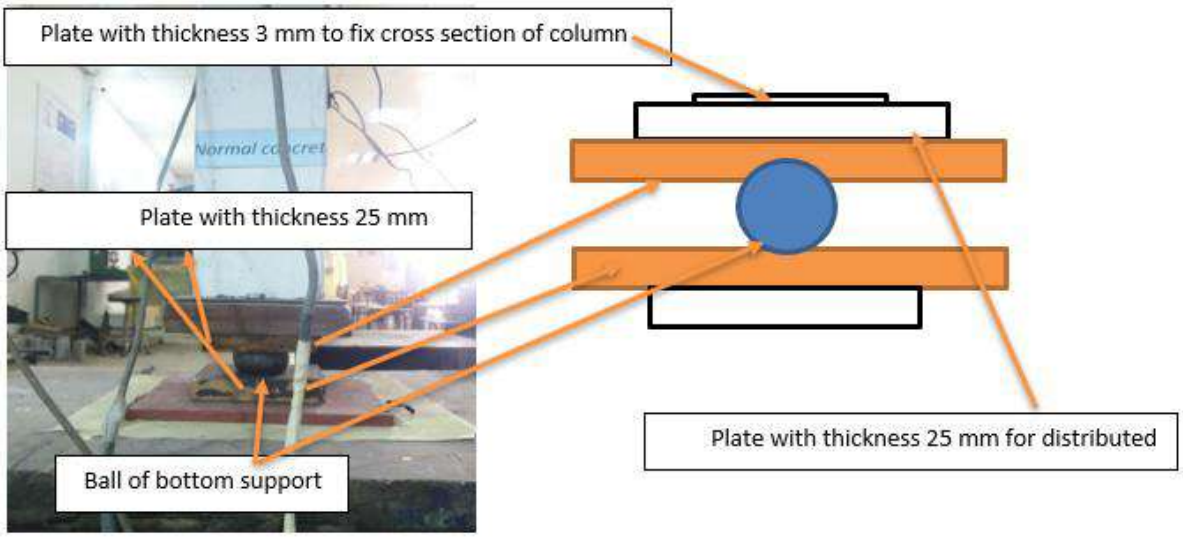

Plate (3-28) Lower support of sample

3.13 Instrument and Installation Procedure of Specimen

The general view of test setup and panorama used in the experiment are shown in Plate (3.29). After the curing of samples has been completed (after 28 days of casting the composite column), the column specimens were removed from water basins. Then it was cleaned and colored in order to clarify the variables and show patterns of failure. During the testing, iron caps 25 mm thick were set above the column for load distribution and fixation purposes, while the column 's lower support was pinned. The longitudinal tensile of steel was measured by using four strain gauges. Two strain gauges were placed 2.5 cm from the top of the tube in perpendicular faces,and the other two strain were placed in the mid height of column. To find out the change in vertical and lateral movement of the column during the inspection process, three Linear Variation Displacement Transducers (LVDT) were installed where the minimum readings for the division were about 0.01 mm with a slight effect of electrical noises. The horizontal deflection was measured in the middle of column through Two LVDT's. Another sensor was used to measure the deformation at the top of the column. The machine of test has a capacity of approximately 2000kN. The test was performed on the columns up to

failure. The load was recorded by load cell with capacity 2000 kN linked to computer as shown in Plate (3.30). Throughout the loading of the test specimens, a loading control rate of 0.6 kN/S was applied.

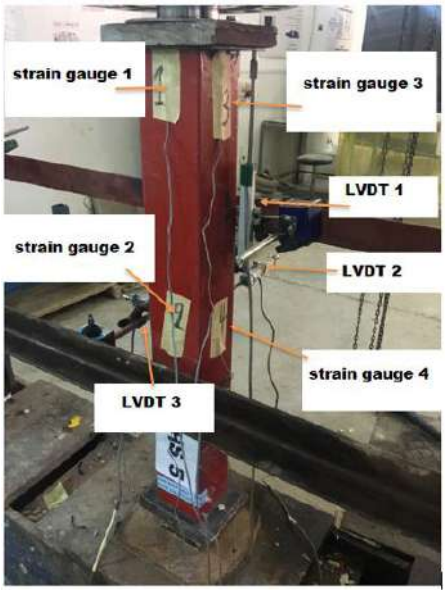

Plate (3.29) Specimen Installation

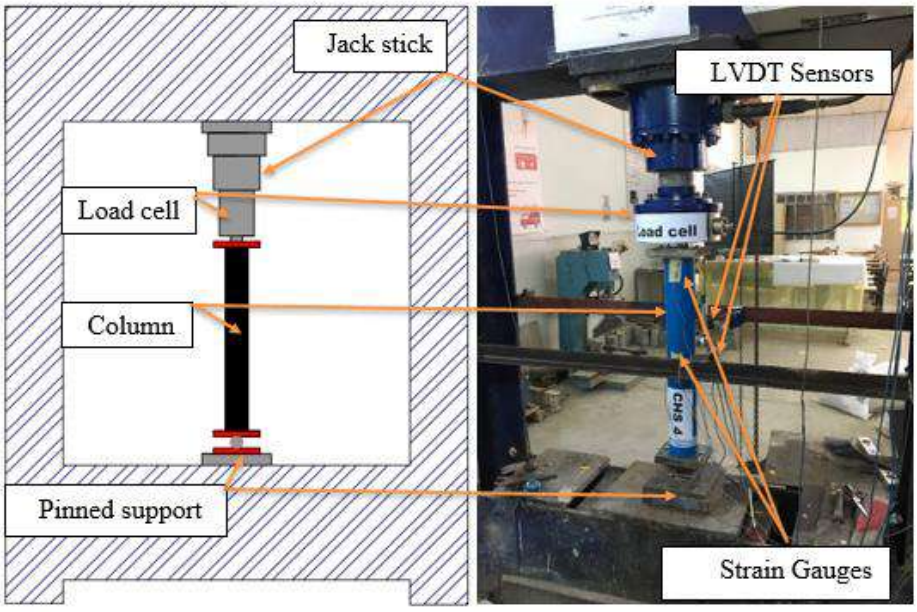

Plate (3.30) Testing machine

3-14 Method of Repeated Loading

Repeated axial loading was applied to the specimen. The testing process was divided into two methods variable repeated loading and static loading (last cycle of loading). The repeated test included seven cycles of one direction repeated loads with different intensity, where the specimen loaded gradually each 10 kN up to the maximum load level in that particular cycle and then unloaded by lifting the load cell of testing machine mechanically until reaching zero value, the maximum load in these cycles was 25% of the (the maximum estimated load reached about 929KN but taken approximately 900 in this study). Then, the same process was applied with 50% and 75% of the maximum load(900KN).Each ratio of cycle one ,two ,and three apply two twice and back to zero After that, loading the specimen until failure (static loading).

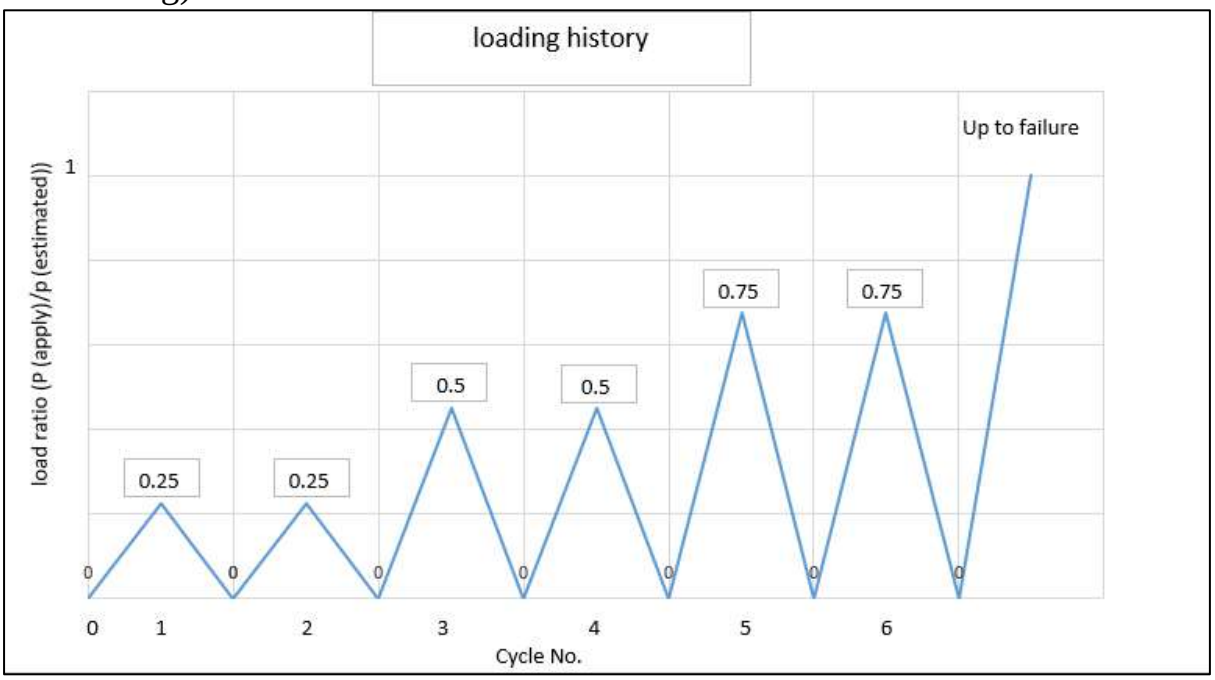

Figure (3.4) process of loading

CHAPTER FOUR

CHAPTER FOUR

EXPERIMENTAL RESULTS AND DISCUSSION

4.1 Introduction

The aim of this study is to investigate the behavior of concrete filled double skin column subjected to axial concentric load under repeated loading experimentally. The mechanical properties of normal concrete (NC) and reactive powder concrete (RPC) have been presented firstly in this chapter including the effect of volumetric ratio of steel fibers (Vf) on the mechanical properties of RPC samples. This chapter also presents the result of experimental test of the behavior of fourteen concrete filled double skin column including two columns (non-filled with concrete). The tested composite columns were divided according to the type of mixture into three groups: column filled with reactive powder concrete, normal concrete and without filling. The experimental variables included the presence of RPC in the composite column by two volumetric ratio 0.5%, and 1.5%, Slenderness ratio, shear connector place and cross section. The effect of these variables was studied and discussed in term of load-deflection behavior, ultimate load capacity, axial strain and failure modes of the columns.

4.2 Mechanical Properties

Includes the mechanical properties of concrete samples that have been tested in this study included compressive strength, tensile strength, and modulus of elasticity. The average values of three samples was recorded to represent each item of the mechanical properties.

4.2.1 Compressive Strength Results

The compressive strength is one of the most important parameters of the hardened concrete. To describe the effect of this property on the behavior of composite column, two types of concrete have been adopted in this research work; NC and RPC with 0.5% and 1.5% volumetric ratio of steel fibers. The compressive test results of the two mixtures are shown in Table (4-1). The average value of three samples had been taken to represent the compressive strength.

Table 4.1: Compressive Strength of Concrete Mixes

No. of specimen	RPC1 (0.5% steel fiber)		RPC2 (1.5%steel fiber)		Normal concrete	
	100*200 Cylinder (Mpa)	100 Cubic (Mpa)	100*200 Cylinder (Mpa)	100 Cubic (Mpa)	100*200 Cylinder (Mpa)	100 Cubic (Mpa)
1	61.1	73	78.6	80.15	26.2	27.40
2	53.6	75.14	75.1	95.7	23.3	31.11
3	52	71.76	67	95.11	25.5	34
Average	55.5	73.3	73.5	90.32	25	30.83

The results indicated that increasing steel fiber from 0.5% to 1.5% increases the compressive strength for cube and cylinder by 23.2% and 32.4% respectively. Plate (4.1) shows the failure modes of cubes for each mixture and the effect of changing the volumetric ratio of steel fiber.

Plate (4.1): Failure Modes of Different Mixtures in Compression, a): NC, b): RPC-0.5% steel fibers, c): RPC-1.5% steel fibers.

4.2.2 Splitting Strength

The indirect test method is represented by splitting tensile strength. Three samples of (100*200) mm cylinders were used for each mix and the average value was taken to represent the tensile strength of concrete. Table (4-2) shows these values for NC and RPC mixes.

Table (4-2) Splitting Tensile Strength Results for Concrete Mixes

No. of specimen	RPC1 (0.5% steel fiber) (Mpa)	RPC2 (1.5% steel fiber) (Mpa)	Normal concrete (Mpa)
1	8.98	9.61	2.22
2	8.06	11.3	2.21
3	8.96	12.35	2.94
Average	8.66	11.08	2.45

It was observed from this table that the tensile strength of RPC was much higher than that of NC. It was also noticed that increasing the volumetric ratio of RPC mixture from 0.5% to 1.5% causes an increase in tensile strength by about 27.9%. Plate (4.2) shows different failure types of cylinder specimens for NC and RPC mixtures. It was indicated that the presence of steel fibers in concrete increases the tensile strength as well as reducing the width and number of cracks.

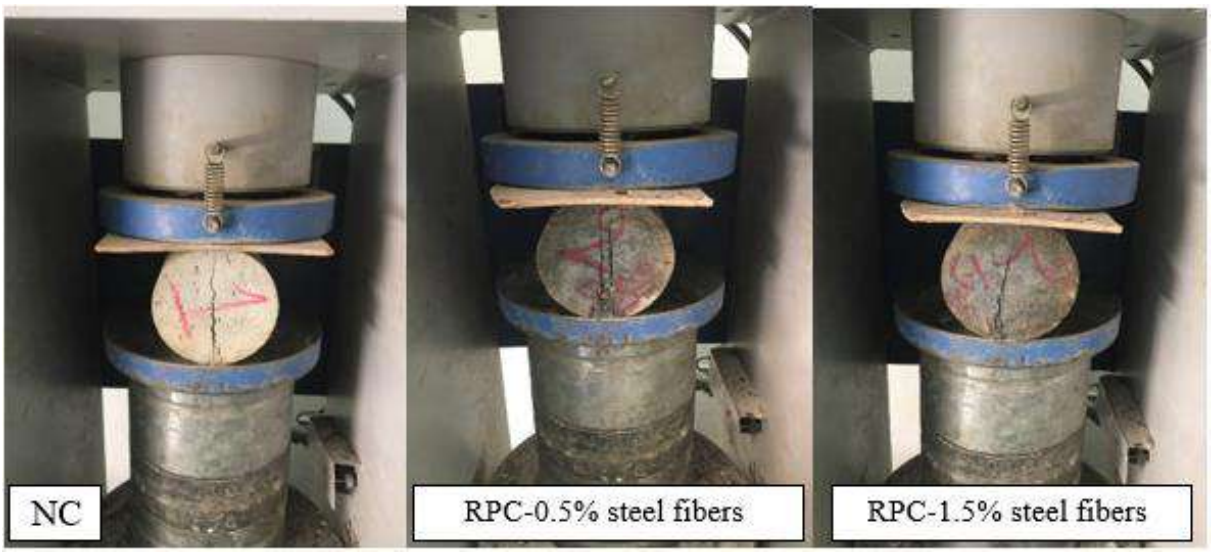

Plate (4.2): Failure Modes of Different Mixtures in Splitting, a): NC, b): RPC-0.5% steel fibers, c): RPC-1.5% steel fibers

4.2.3 Modulus of Elasticity

The modulus of elasticity was tested for each mix of NC and RPC using the average value of three samples of cylinders with dimension (100*200) mm. The vertical displacement was measured when the load applied by compressive state. Table (4.3) shows the value of modulus of elasticity for each mixture. For NSC, the elastic modulus was compared with ACI-318 [97] formula:

$$Ec = 4700\sqrt{fc} \quad \text{.....(4-1)}$$

In this study the formula which was found by Graybeal [98] was used to compare the results of the modulus of elasticity of RPC.

$$Ec = 3840\sqrt{fc} \quad \text{..... .... (4-2)}$$

Table 4.3: Average Modulus of elasticity Results

No. of specimen	Modulus of elasticity (Ec) for RPC1 (0.5% steel fiber) (Mpa)	Modulus of elasticity (Ec) for RPC2 (1.5% steel fiber (Mpa)	Modulus of elasticity (Ec) for Normal concrete (Mpa)
1	30015	34044	24057
2	28113	33255	22686
3	27690	31431	23733
Average	28606	32910	23492

Through the calculations of the modulus of elasticity for powder-reactive concrete mixtures, it was found an increase in the percentages of steel fiber in the mixture, lead to increases modulus of elasticity. Where the value of elasticity modulus in the mixture that contains a percentage of fibers 1.5% was 32910,

while its value at the percentage of fibers 0.5% was 28606 as shown in Figure (4.1). In ordinary mixtures, the modulus of elasticity was much lower than previously mentioned in reactive concrete, where its value reached about 23492. In general, the modulus of elasticity is improved by increasing the proportions of steel fibers relative to the reactive mixtures. Plate (4.3) shows the modulus of elasticity curve for the three used mixtures, which are the reactive with a ratio of steel 0.5 % ,1.5 % and normal concrete. The modulus of elasticity was calculated using equation (3.2) and the results as follows when compared with the previous equations, the value of modules for normal concrete was 14000, and for the mixture containing fibers ratios of 0.5 %, and 1.5 % were 23368 and 32941 respectively.

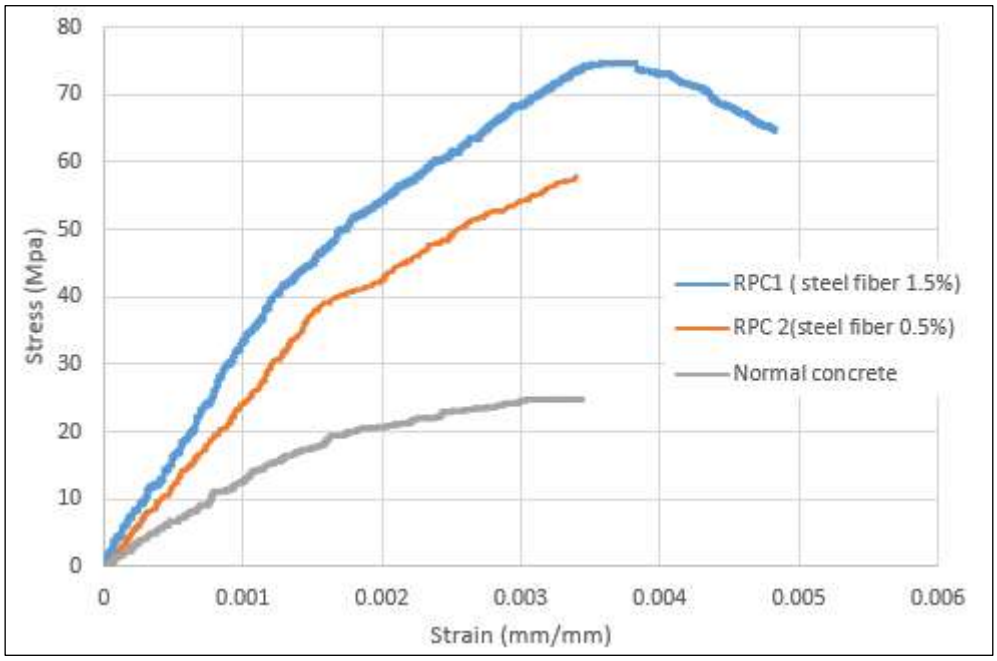

Figure 4.1: Stress-Strain Curves for three mixes

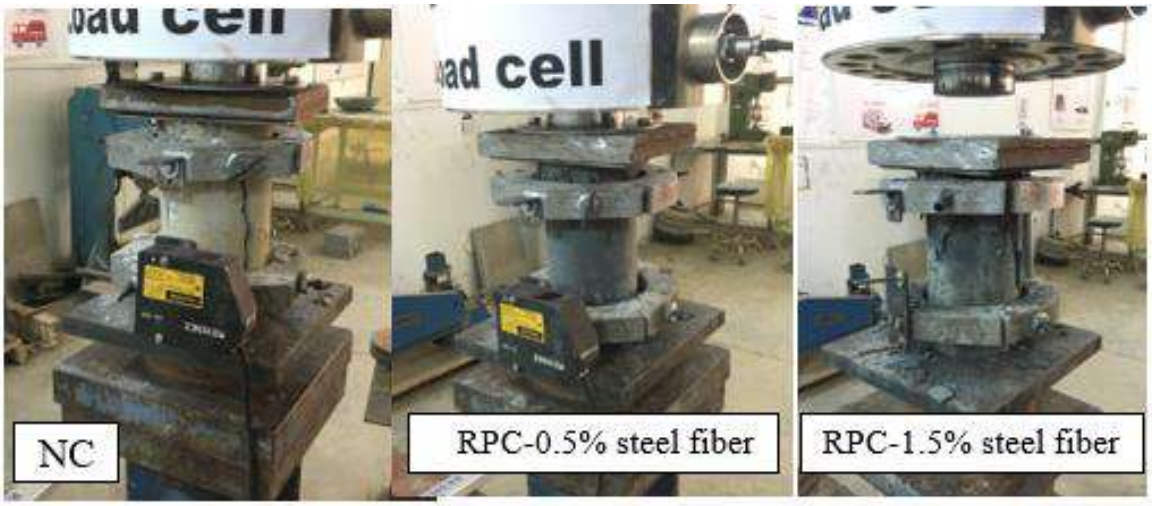

Plate (4.3): Failure Modes of Different Mixtures in the Compression a): NC, b): RPC-0.5% steel fiber, c): RPC-1.5% steel fiber

4.3 Failure Modes

In general, the slenderness ratio (length to width), the capacity of the filled concrete, shear connections and the composite column's cross-sectional structure are all important factors that influence and provide an important indicator of the form of the column's failure. The failure modes of the CFDST circular and square column are shown in Plate (4.4),to (4.15).

During the test of columns, nothing is evident during the initial stages of repeated load. When the load near its ultimate load, the sounds of cracks is audile. After that the buckled of tubes is appeared. Bends on the tube occur in the event of an increased load, through the examination process for the types of failure occurring for each column. One of the expected failure situations for short columns is the occurrence of a fracture in the concrete after that the steel reaches the stage of maximum stress under the conditions of axial loading However, the failure patterns of the columns changed with the change in the characteristics of the outer and inner tubes, and when the inner tube was removed, the following was obtained:

1- All square sections showed internal and external buckle on the steel due to the presence of crushing concrete between the two tubes. Most of the columns failed in the region near the load except in cases where the bend appeared in the middle and the lower. The failure was obvious, because the form of the buckle was larger than in the circular so the square's confining effect was smaller than that of the round after that the concrete was crushed.
2- As for the circular sections (CHS1, CHS2, CHS3, CHS4), it failed in the local external bending preceded by the cracking of the concrete. The failure occurred to a lesser degree than the square section. This was due to the concrete being confined to a high degree by the outer tube.

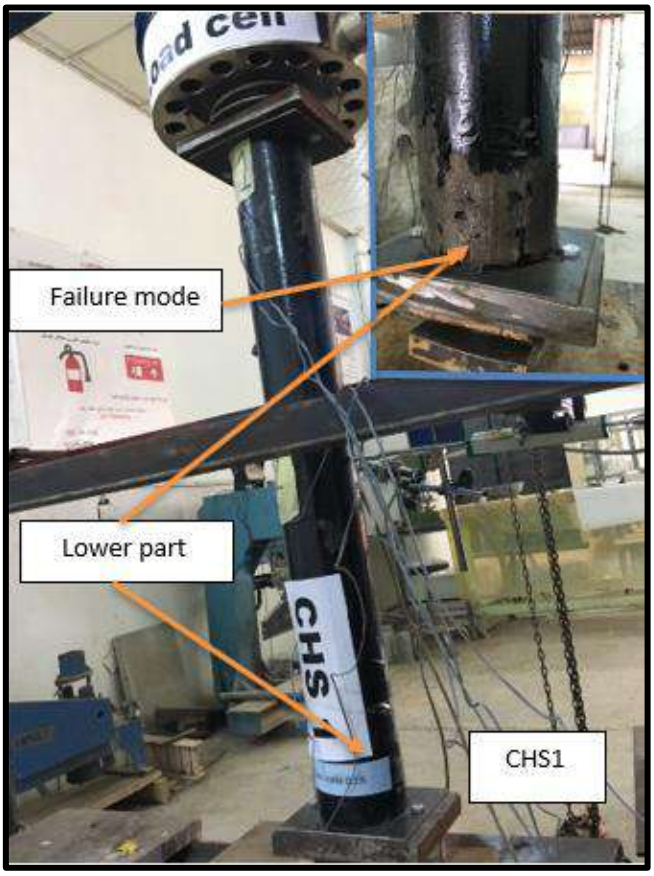

Plate (4-4) failure mode of (CHS1) sample

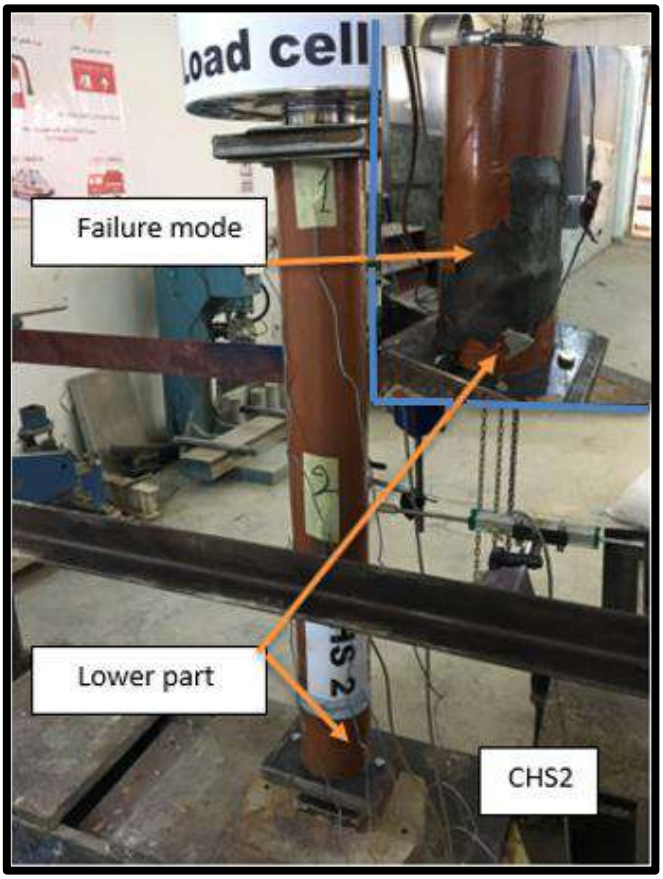

Plate (4-5) failure mode of (CHS2) sample

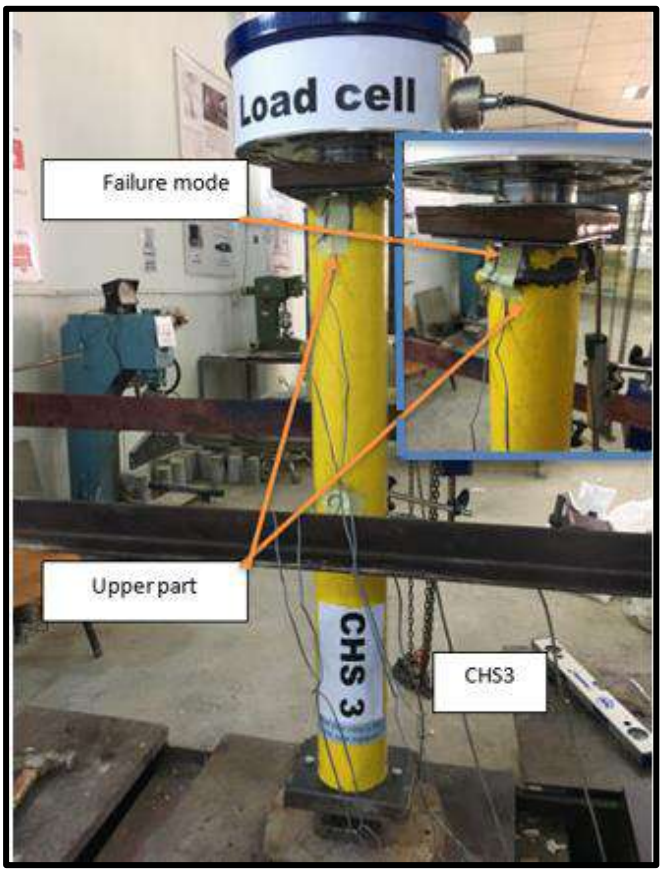

Plate (4-6) Failure mode of (CHS3) sample

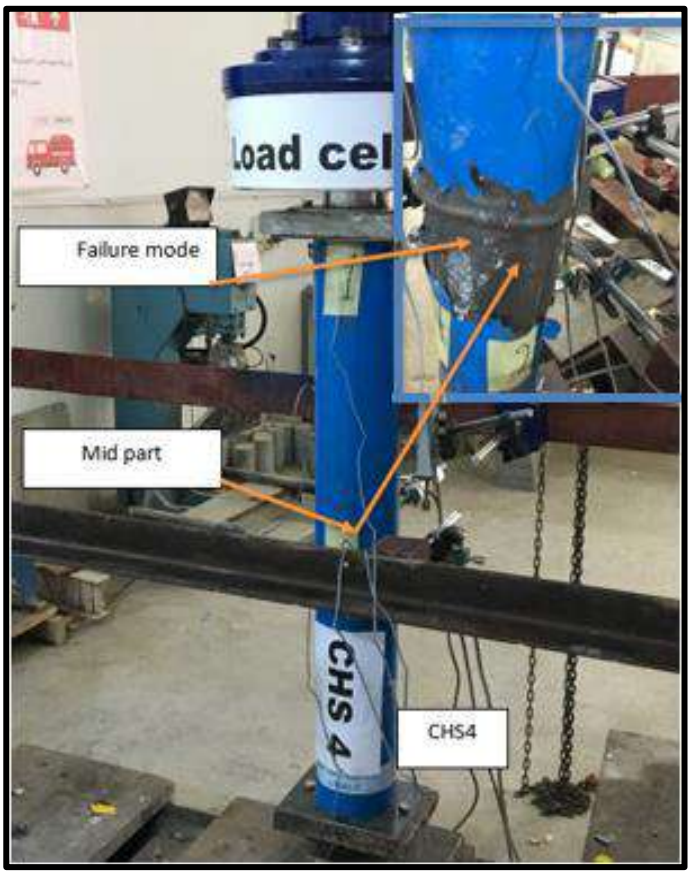

Plate (4-7) Failure mode of (CHS4) sample

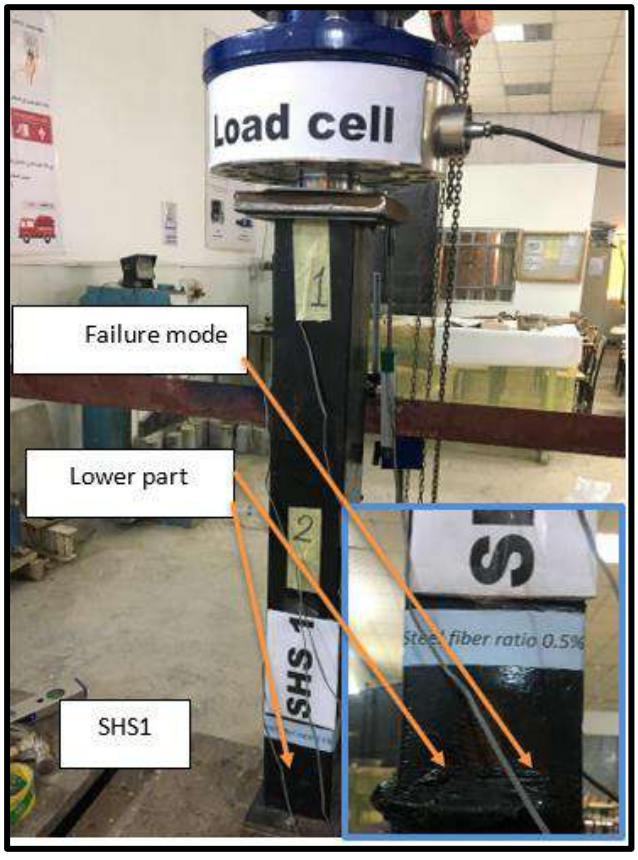

Plate (4-8) Failure mode of (SHS1) sample

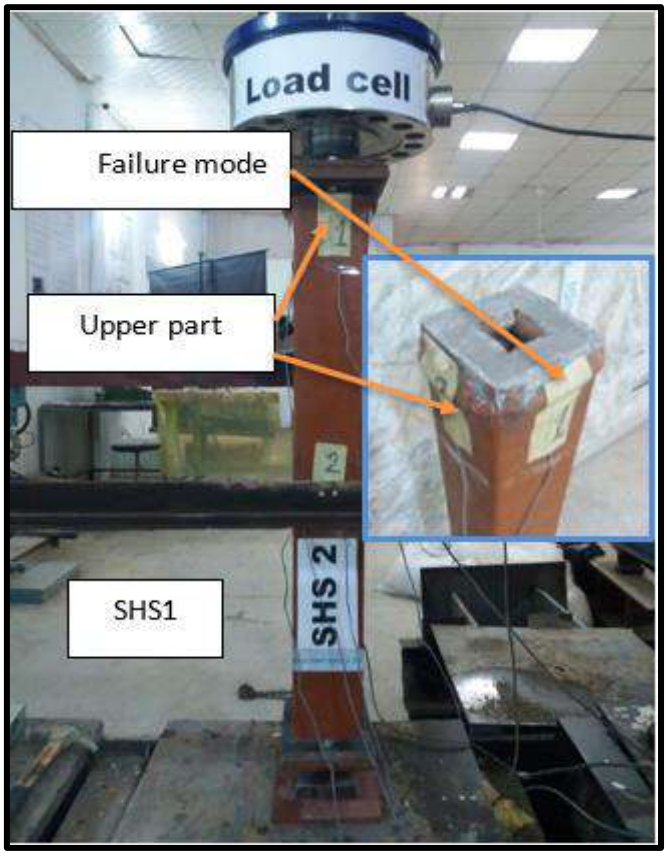

Plate (4-9) Failure mode of (SHS2) sample

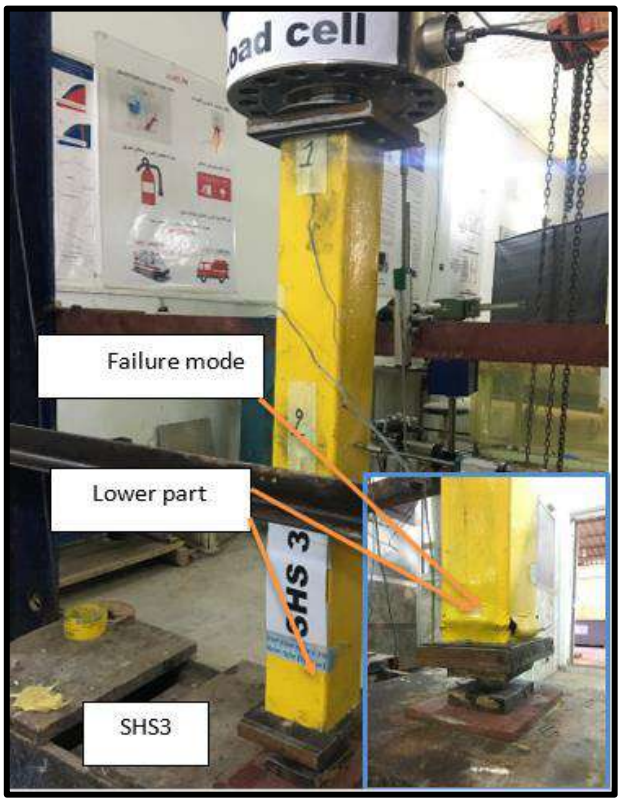

Plate (4-10) Failure mode of (SHS3) sample

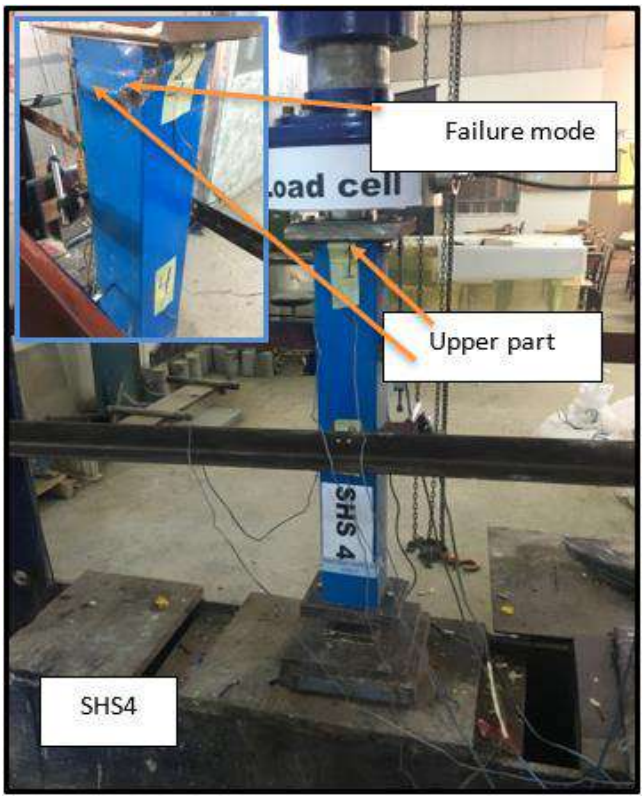

Plate (4-11) Failure mode of (SHS4) sample

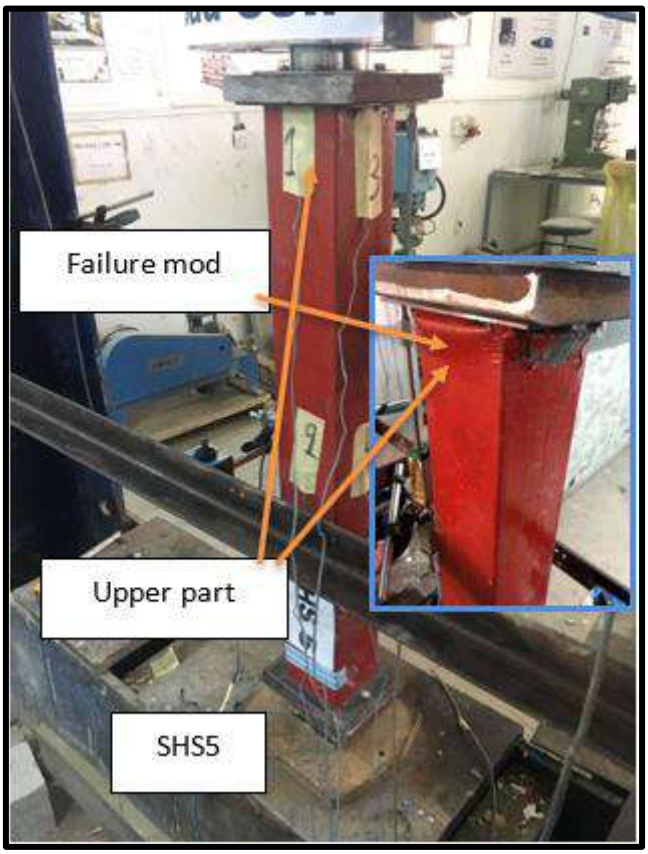

Plate (4-12) Failure mode of (SHS1) sample

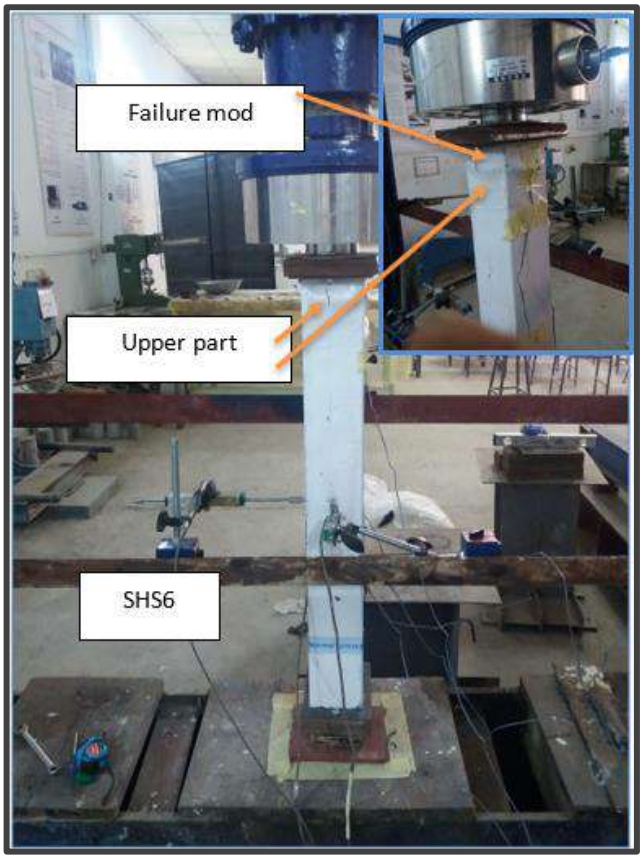

Plate (4-13) Failure mode of (SHS2) sample

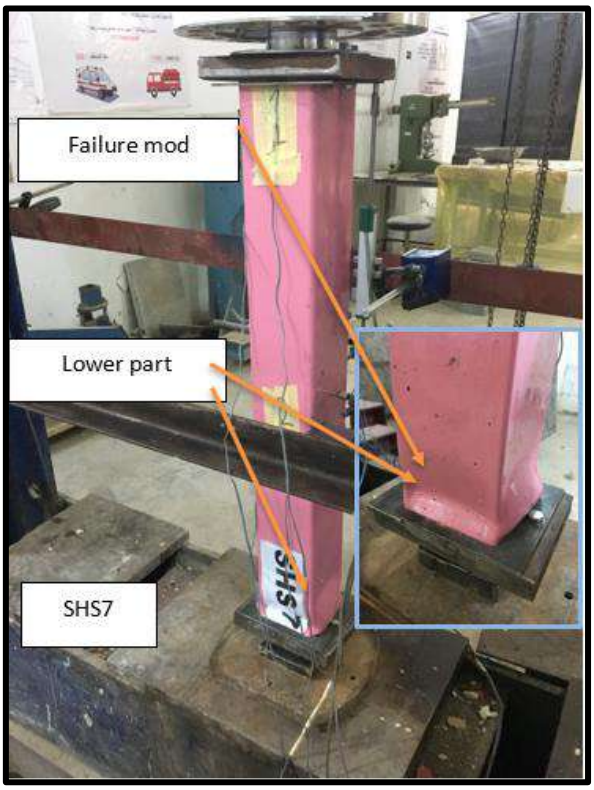

Plate (4-14) Failure mode of (SHS7) sample

3- For the column (CHS5) in which shear connections were used longitudinally, the concrete failure was initiated at a certain angle and the upper part slipped over the lower part in the mid length of the column. This type of failure is called shear failure as shown in Plate (4.15).

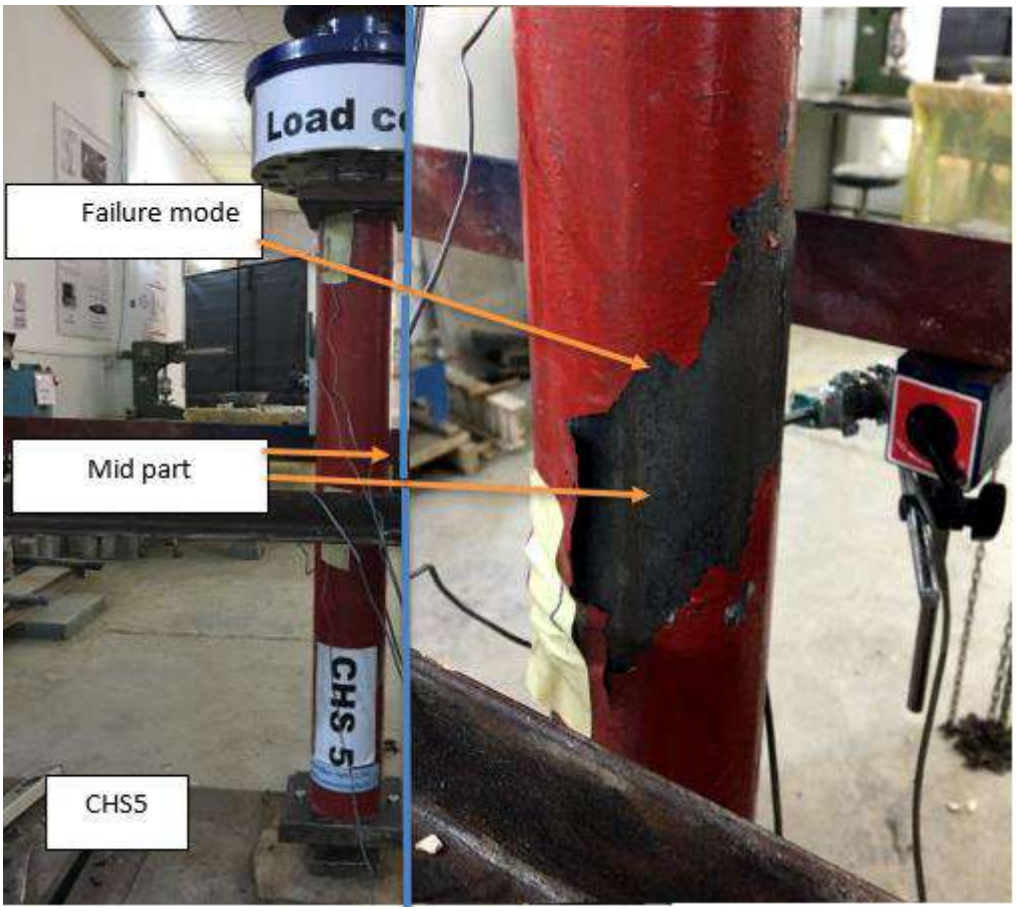

Plate (4-15) Failure mode of (CHS5) sample

4-For columns (CHS6, CHS7) with L/B(D) ratio =8, failure was initiated by global buckling. This failure may be attributed to the weak properties of ordinary concrete (NSC) and empty tube when compared to RPC in mid height of column and because of greater flexibility which resulted in larger lateral mid height displacement [99] as shown in Plate (4.16).

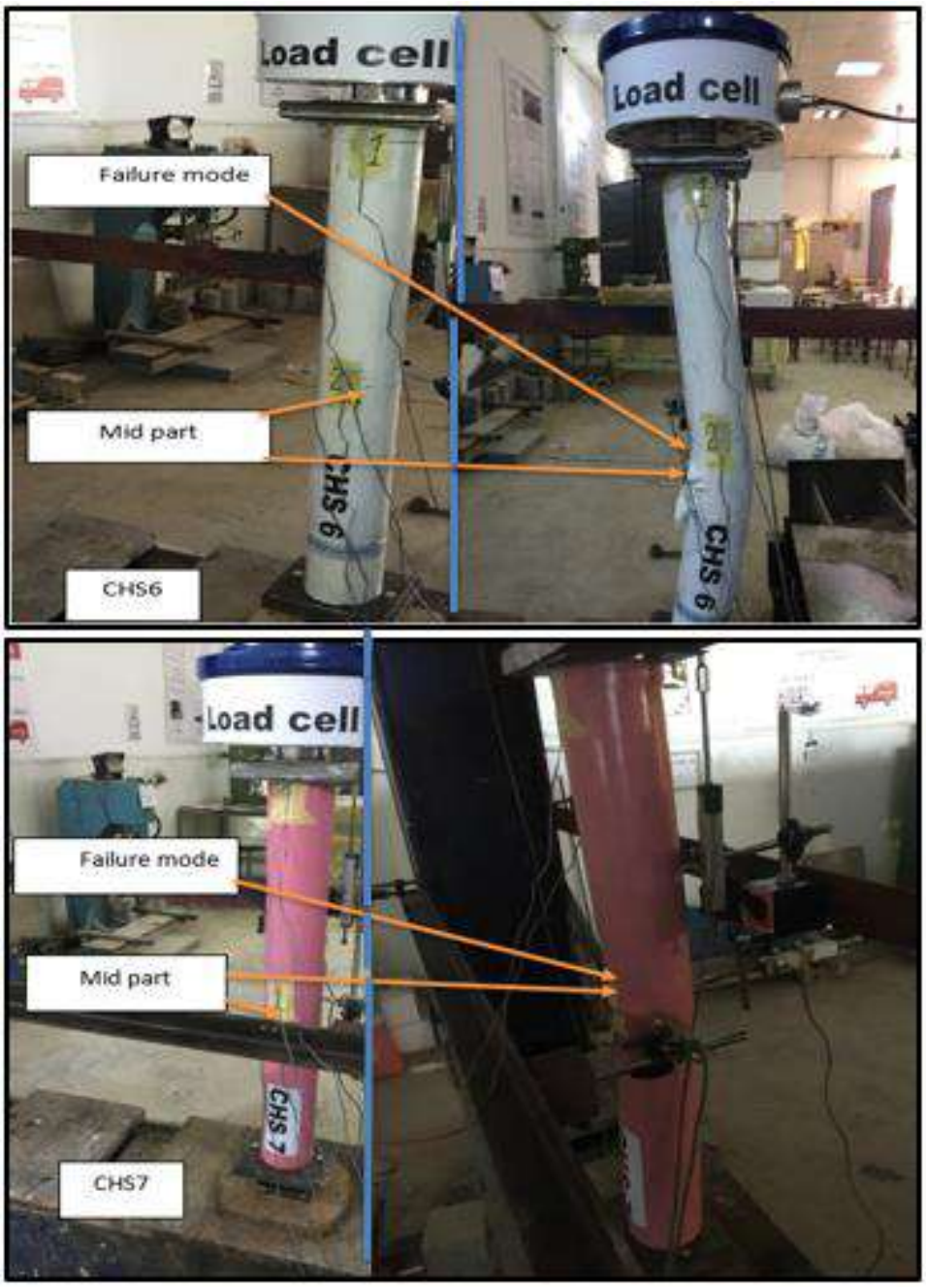

plate (4.16) Failure mode of (CHS6, CHS7) sample

Table 4.4 The failure modes of the CFDST column

Specimen	Concrete compressive strength fc′ (Mpa)	Overall slenderness (L/B)	Pu (exp)	Pattern for Failure
CHS1	73.3	8	800	Outward local buckling
CHS2	90.32	8	835	Outward local buckling
CHS3	90.32	8	775	Outward local buckling
CHS4	90.32	7	900	Outward local buckling
CHS5	90.32	8	910	Shear failure
CHS6	30.83	8	580	Global buckling
CHS7	Not fill	8	300	Global Buckling
SHS1	73.3	8	750	Outward local buckling
SHS2	90.32	8	775	Outward local buckling
SHS3	90.32	8	815	Outward local buckling
SHS4	90.32	7	850	Outward local buckling
SHS5	90.32	8	888	Outward local buckling
SHS6	30.83	8	540	Outward local buckling
SHS7	Not fill	8	340	Outward local buckling

4.4 Load-Displacement Behavior

The effect of the added steel-fiber ratio in the concrete mixture and the length-to-width (diameter) ratio in the cross-section of the sample can be known, as well as the effect of the strength of high strength concrete and shear connector from this relationship. Three LVDTs installed to recorded the action of each column, and four strain gauge update in the mid and top of column to find out that the tube has reached the yield stress or not. The yield stress of steel was determined by the tension coupon tested. During the testing, it was observed that the steel started to bend approximately 80 percent of the final column endurance. The load-deflection and the deflected shape all of these columns are illustrated in Figures (4-2) to (4-13)

4.4.1 Circular Section

4.4.1.1Influence of steel fiber

High-strength concrete mixtures (RPC) were designed with two different percentages of steel fibers. Figures (4.2.a) and (4.2.b) show the load-displacement values of the first and second specimens which have 0.5 % and 1.5 % respectively, from volume of mix. This rise in the percentage led increase in the compressive strength and thus increase in section's stiffness. It was noted that the volumetric expansion of the concrete was reduced by the increase in the compressive strength. Which in turn delayed the crushing of concrete in the tube and local buckling. The rapid rise in the section's compressive strength was from 73.3 Mpa for sample (CHS1) to 90.32 Mpa for sample (CHS2) reached to 4.43 % increase in the section's strength. Where the ultimate load of (CHS1) is 800kN while the (CHS2) is 835kN.In the first, second and third loading cycle for (CHS1) and (CHS2) sample, the deformation was approximately 2,4,6 and 3,5,7 (mm) respectively ,but in the failure (last cycle of loading) was 12mm for the sample (CHS1) and 13 mm for (CHS2). The greater compressive strength, lead to the sudden failure curve. The value of deflections at ultimate load in the samples (CHS1,and CHS2) reached about 8,and11mm respectively.

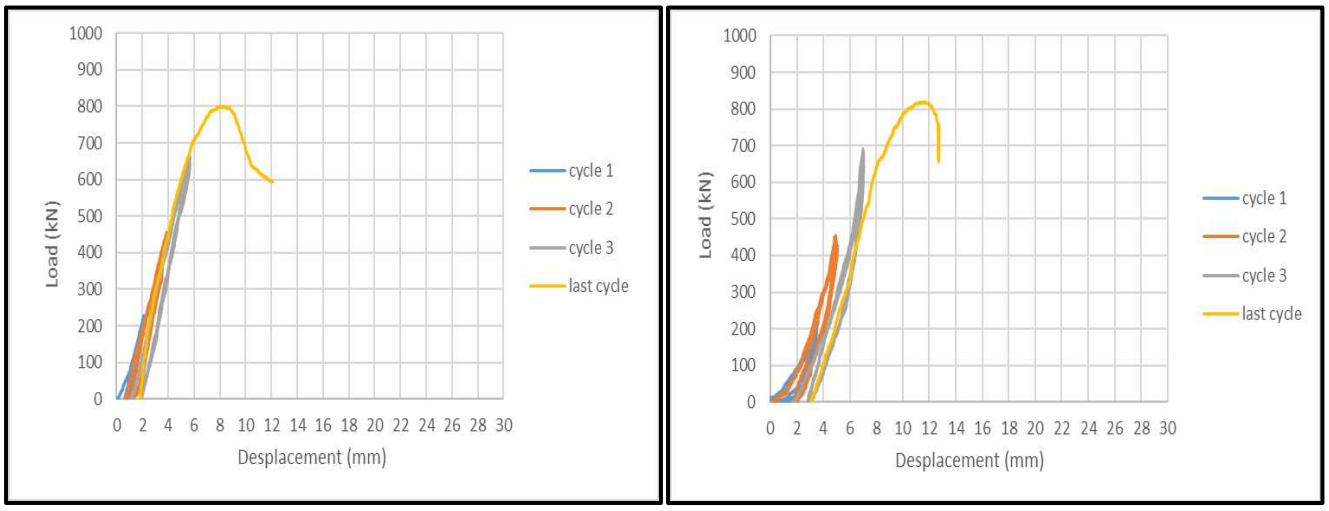

(a) **(b)**

Figure (4-2) (a) Load-deformation curve for CHS1 0.5 specimen, (b) Load-deformation curve for CHS2 1.5 specimen

The contribution of steel fiber in inhibition of both plastic shrinkage cracks. As excessive forces are applied to a member and cracks begin to develop, the even distribution of fibers throughout ensures they will be present at the side of fatigue. At the moment that cracks start forming, the tensile forces applied transfer to the fibers, which can have tensile strengths in excess of 2850MPa. The fibers bridging the cracks lend their strength to the member, allowing it to remain ductile, with stand increasing stresses, and impede crack propagation.

4.4.1.2 The effect of shape of the inner tube

In the following Figures (4-3.a), (4-3.b), the effect of the inner concrete area of the circular section was studied by placing the inner tube of the sample of a square section, where the area of concrete was reduced from 5211 mm to 4675 mm. The amount of the sandwiched concrete determines the hollow ratio in the column and compressive behavior of CFDST columns. It is worth that the hollow ratio in this investigation is controlled by the inner tube diameter reveals that increasing the hollow ratio by replaced circular to square inner tube significantly affects the behavior and the strength of the CFDST short column. This reduction led to a decrease in the bearing capacity by 7.74% of the final capacity when compare with (CHS2). The failure strength of column (SHS3) was 775 kN which was less than the capacity of sample (SHS2). Sample (SHS3) showed deformation during the first, second and third loading cycles of 2.2 mm,2.4 and 4.3 mm, respectively. While the sample (SHS2) deformation during the first three cycles was 3, 5 and 7, but in the ultimate load were 6 and 11mm respectively. Hence, using columns with very greater hollow ratios would decrease the weight of the column without significant strength decrease, so they should be used in practice.

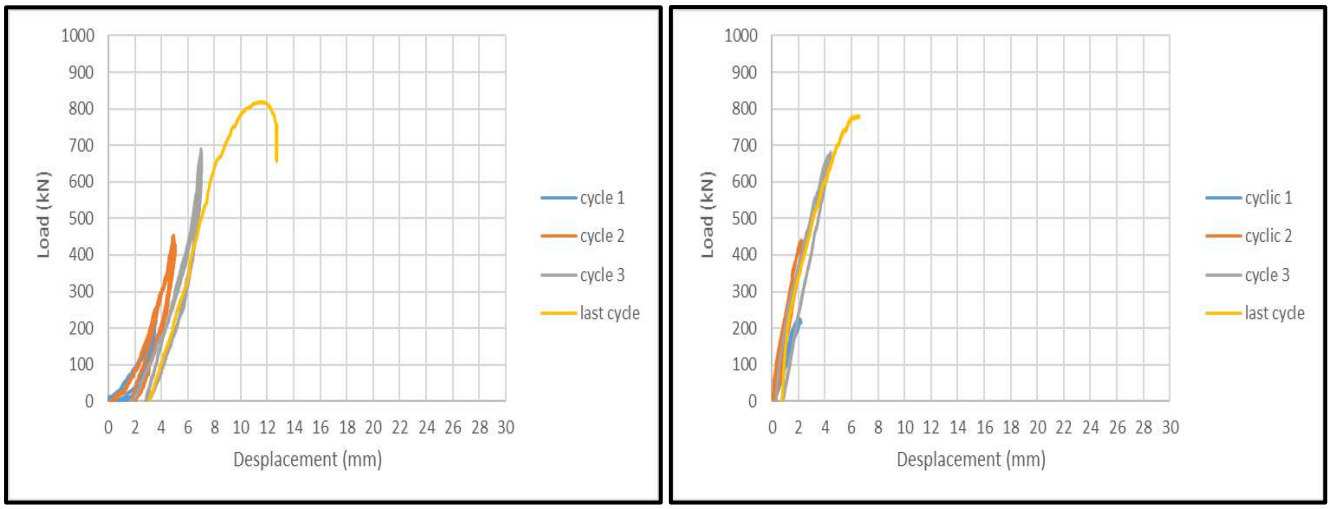

(a) **(b)**

Figure (4-3) (a) Load-deformation curve for CHS2 1.5 specimen with circular inner tube,(b) Load-deformation curve for CHS3 1.5 specimen with square inner tube

4.4.1.3 The effect of aspect ratio L/B(D)

The effect of the L/B ratio on the bearing capacity of the column was studied for the same concrete mixture used in samples (CHS2, CHS4) with steel fibers 1.5 %. It was noticed from Figures (4-4.a), (4-4.b) that the ultimate load of (CHS4) was 900 kN which was higher than the ultimate load for columns with the ratio of L /B(D) of 8 that reached ultimate load 835 KN.

Also, the (SHS4) appeared increases from (SHS2) about 7.78%. The magnitude of displacement through the first, second and last cycle were approximately equal, but the third cycle had 8mm and 7mm for (SHS4) and (SHS2) respectively. It can be also concluded that greater length to width ratio, gives lower bearing capacity of the composite column. The ultimate load increase when the slenderness was started less and, the confinement of steel is high due to increase capacity of column. It was also observed that the load-deformation curve changed after reach the specimens to yielding strain of the steel tube ($\varepsilon = n\ 1713\ \mu\varepsilon$). All strain gauges placing to measure longitudinal strain recorded values higher than 1713 με (yield strain) at the ultimate load. This seems to indicate the beginning of the local buckling process for the short columns (L/D = 7) and the global instability for the

columns with L/D = 8. The specimens with L/D = 8 exhibited insufficient radial strain for mobilizing the confinement effect. This was verified by the four strain gauges placed outside around the column. This may due to that in the early stages of loading, Poisson's ratio for concrete is lower than that for steel, and the steel tube has no restraining effect on the concrete core. As the longitudinal strain increases, Poisson's ratio of concrete which is (0.15-0.2) in the elastic range increases to 0.5 in the inelastic range. Therefore, the lateral expansion of sample (CHS4) gradually becomes greater than that of (CHS2).

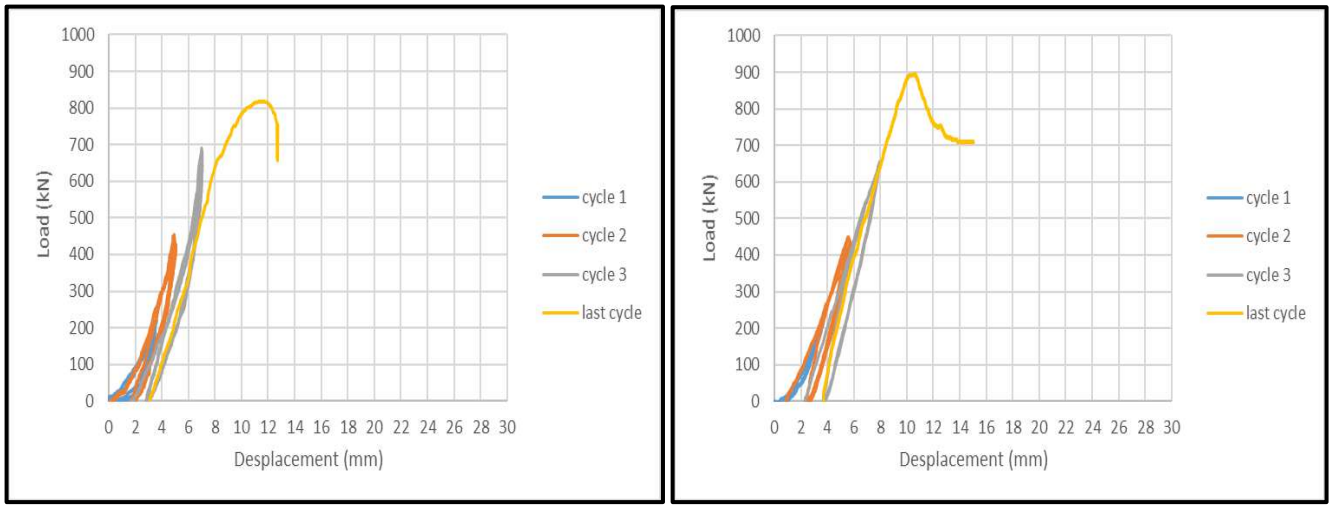

(a) **(b)**

Figure (4-4) (a) Load-deformation curve for CHS2 1.5 specimen with (L/B)=8, (b) Load-deformation curve for CHS4 1.5 with (L/B) =7

4.4.1.4 Effect of shear connector

According to designed the spacing according to the European code (2004) for the distribute of shear stud for the composite column, where the columns with connector showed a very high endurance compared to the sample with no shear stud. The results of strengthening inner steel columns with shear connectors showed an increase in the final capacity of the double-skin composite columns. In fact, this increase was due to the existence of shear conductors, which distribution the load to the elements of column while increasing its strength. The percentage of the increase in this type was strengthing was 8.98%.as shown in Figures (4-5.a), (4-5.b). In practice, the welded shear conductors were operated to spread the stresses on the two parts of the column in such a way that the two components contribute to the load and so delay the fracture of the filled concrete when loading. When comparing the specimen (CHS2) with (CHS5), it was found the ultimate load of (CHS5) is 910 kN at deformation 11 mm. On the other hand, Sample (CHS2) exhibited same deformation at a maximum load. The failure of this column appeared in an angle shape and this failure is called shear failure. Hence eight of stiffener bolt had significant effect in increasing load capacity of

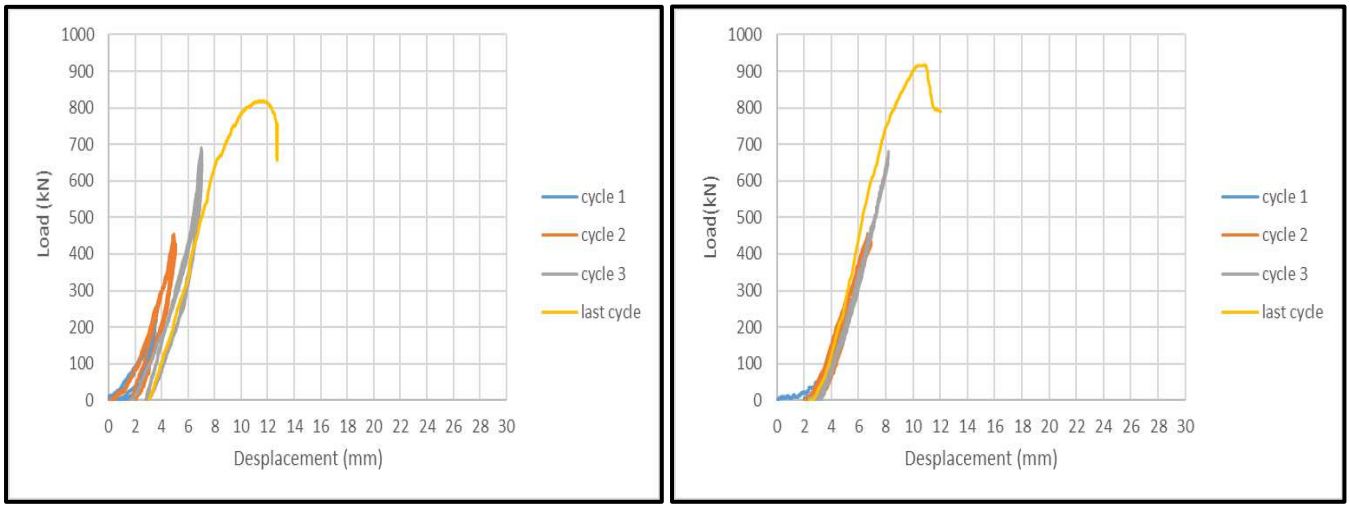

(a) **(b)**

Figures (4-5) (a) Load-deformation curve for CHS2 1.5 without shear connector ,(b) Load-deformation curve for CHS5 1.5, and with shear connector

the column and providing more contact pressure between steel tube and concrete surfaces.

4.4.1.5 Effect of Type Filled Concrete

When compared (CHS2 1.5) sample with the section filled with ordinary concrete (CHS6), the rates of increase in the final capacity of the column by 1.5 % for the column was 42.24%. The greater compressive strength, lead to the sudden failure curve. On opposite in which (CHS6) appeared a curved high ductility of the column as shown in figures (4-6. a), (4-6. b). The value for deflection at ultimate load in the sample (CHS2, and CHS6) reached about11, and 24 mm respectively

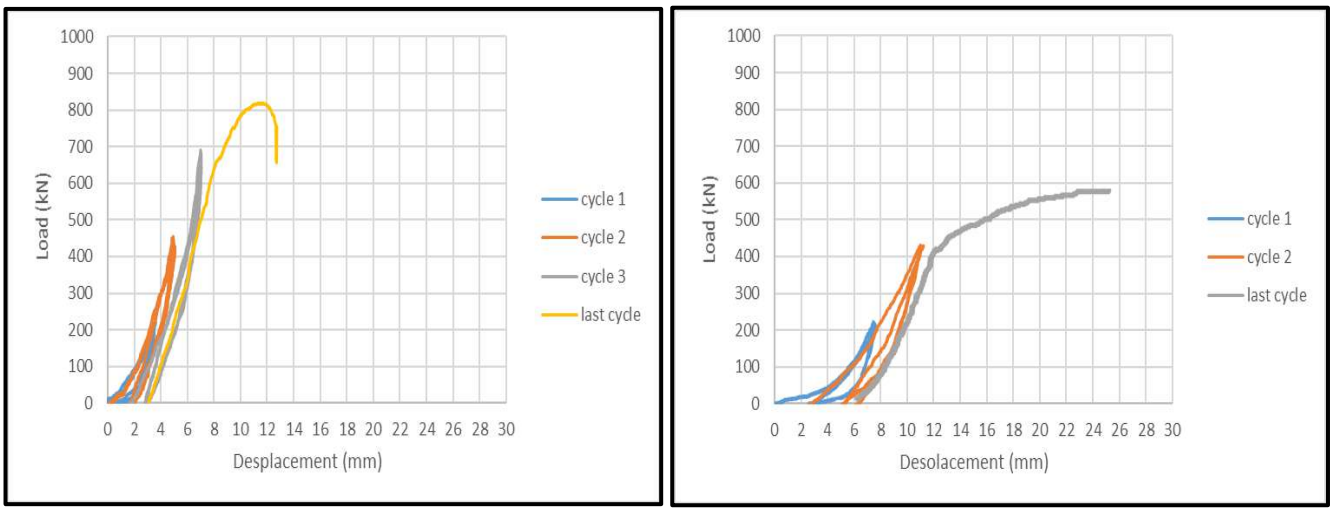

(a) **(b)**

Figure (4-6) (a) Load-deformation curve for CHS2 1.5 specimen, (b) Load-deformation curve for CHS6N specimen

4.4.1.6 Effect of removed filled concrete

The results showed that the added concrete gives more strength than if the column was only made of steel Figure (4-7. b). The column acquired strength due to the concrete's compressive strength. When the column worked as a single section, the ultimate load reached 300 kN and the capacity decreased compared to sample (CHS2) as shown in figures (4-7.a) by 178.3 % due to the steel tube was not able to carry compressive stress. The ultimate failure load reached in empty specimen (CHS7) at displacement 8 mm in second cycle of repeated loading while the

(CHS2) failed at last cycle (11mm). This belong to absence sandwich concrete the tube cannot sustain the compressive stress longitudinally.

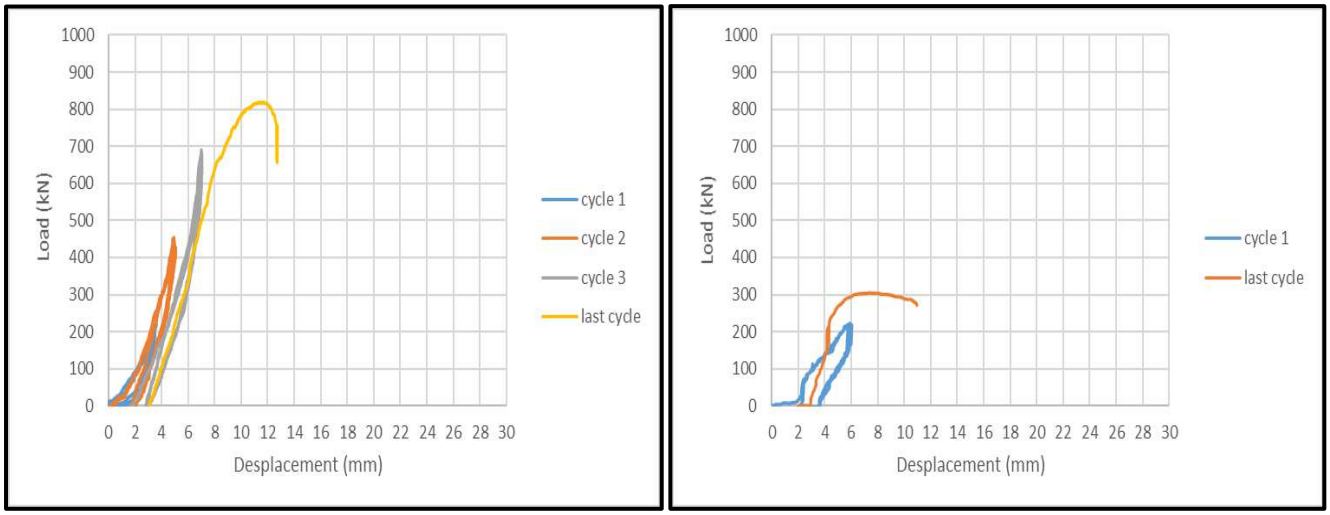

(a) **(b)**

Figures (4-7) (a) Load-deformation curve for CHS2 1.5 ,(b) Load-deformation curve for CHS7 and only steel tubing

4.4.2 Square Section

4.4.2.1Influence of steel fiber

Steel fibers were used in two different percentages in high-strength concrete mixtures (RPC). Figures (4.8.a) and (4.8.b) show that the first and second percentages were 0.5 and 1.5 %, respectively. The increase in the compressive strength of the section increased the it stiffness.The volumetric expansion of the concrete was reduced as the compressive strength of the concrete increased. As a result, delayed concrete crushing in the tube and local buckling are reduced. The section's compressive strength increased steadily from (SHS1) 73.3 to (SHS2) 90.32, leading to an increase of 3.33 % in strength. Where (SHS1) had a maximum load of 775kN and (SHS2) had a maximum load of 750kN. The deformation of the (SHS1,SHS2) sample was nearly equal in the first and second loading cycles, the displacement of cycle one ,two and three was 2,4,and 5.7mm for (SHS1),but 1.7,2.7,and 5mm respectively for the sample (SHS2).

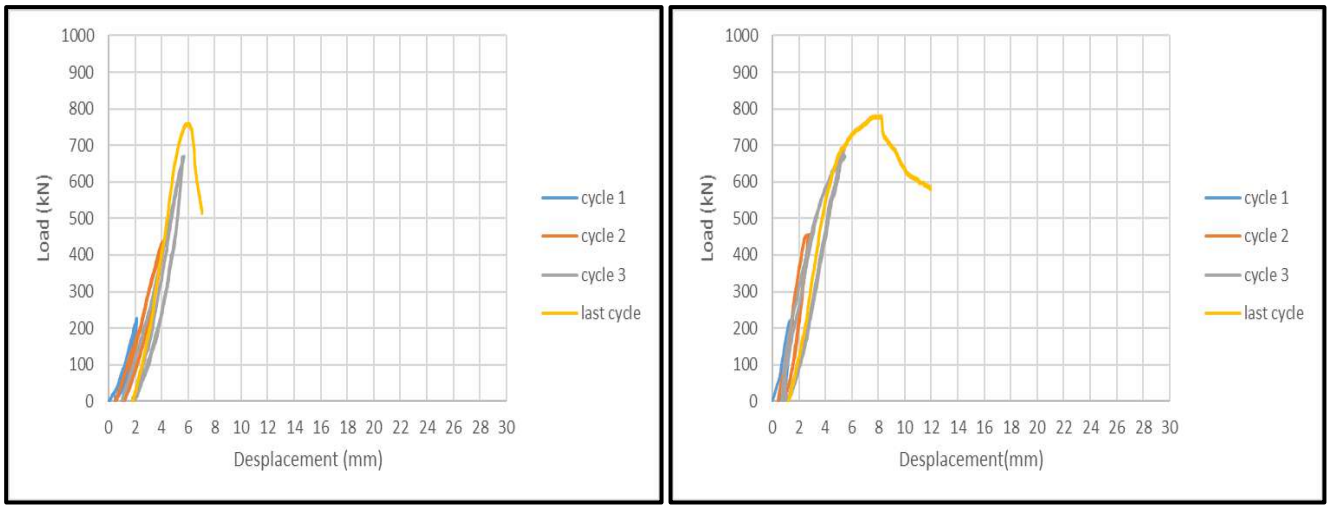

(a) **(b)**

Figure (4-8) (a) Load-deformation curve for SHS1 0.5, (b)Load-deformation curve for SHS2 1.5

4.4.2.2 Effect of shape of the inner tube

The effect of the inner of concrete area for square section was showed in the following Figures (4-9.a) and, (4-9.b),by placing the inner tube of the sample in a circular section, where the concrete area was increased from 6639 mm to 7176

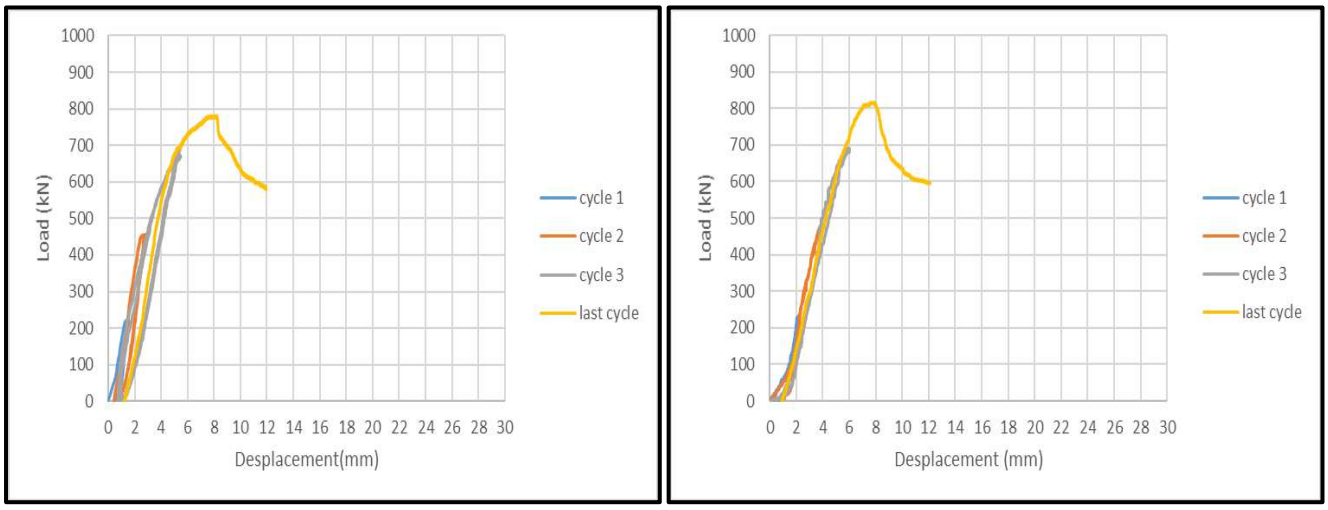

(a) **(b)**

Figure (4-9) (a) Load-deformation curve for SHS2 1.5, with square inner tube, (a)Load-deformation curve for SHS3 1.5 ,with circular inner tube

mm. This resulted in a 5.16 % increase in the bearing capacity of the final capacity. The failure strength of column (SHS3) was 815 kN after the value was

higher in the endurance in sample (SHS2).During the first, second, and third loading cycles, the sample (SHS3) showed deformation of 2,4, and 6 mm, respectively. During the first three cycles, the sample (SHS2) was deformed by 1.7,2.7, and 5. Whereas the value for deflection at ultimate load in the sample (SHS1, and SHS2) reached about 8for each one.

4.4.2.3 Effect of Aspect Ratio (L/B)

For the same concrete mixture used in samples (SHS2, SHS4) with steel fibers 1.5 %, the effect of the L/B ratio on the bearing capacity of the column was investigated. The ultimate load of (SHS4) was 850 kN which is higher than the ultimate load for column (SHS2) with a ratio of length / width of 8, and showed lower ductility than (SHS2) that had a sudden drop of curve failure, as shown in Figures (4-10.a) and (4-10.b).

In addition, the (SHS4) appeared to be higher by 9.67 % than (SHS2). The first and second cycles had displacements of about 3.5 and 5mm, respectively, but the third cycle had a displacement of 6.3mm (SHS4), On the contrary, the sample (SHS2) had 1.7,2.7, and 5mm.It can be also concluded that greater length to width ratio, gives lower bearing capacity of the composite column. It can be also concluded that greater length to width ratio, gives lower bearing capacity of the composite column. The ultimate load increase when the slenderness was started less and, the confinement of steel is high due to increase capacity of column

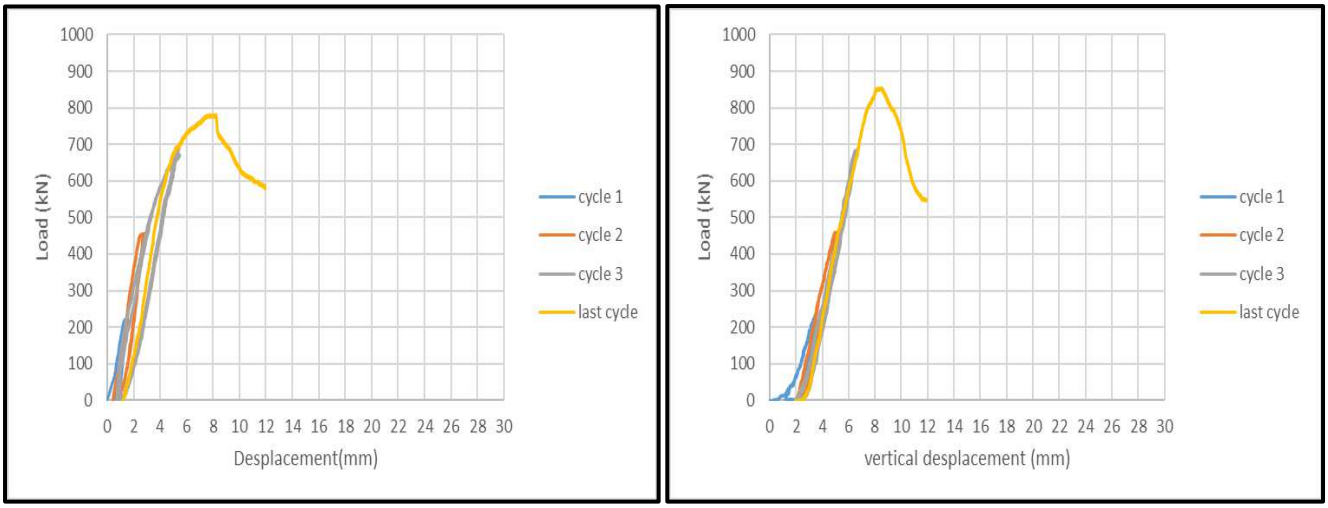

(a) **(b)**

Figure (4-10) (a) Load-deformation curve for SHS2 1.5 ,with (L/B) =8, (b) Load-deformation curve for SHS4 1.5 with (L/B) =7

4.4.2.4 Effect of Shear Connector

According to those who developed the composite column in accordance with the European code for shear stud distribution, the columns with connectors had significantly greater endurance than the sample with no shear stud. The use of connections enhanced the axial capacity load of the CFDST columns. This was due to the fact that as the number of shear connectors increased, thus, the load transferred to the pipe will increase .Load distribution was substantially impacted by shear connectors, as shown in Figures (4-11.a) and (4.11.b).These enhancements help in reducing the impact of the applied loads and, as a result, increasing capacity. So, one of the primary tasks in this form of connection is to delay the fracture of concrete. When comparing specimens (SHS2) and (SHS5), it was revealed that (SHS5) had a maximum load of 888 kN at a deformation of 9 mm, whereas sample (SHS2) had deformation at a maximum load of 8 mm. The percentage of the increase in this type (SHS5) was strengthen was 14.5%.

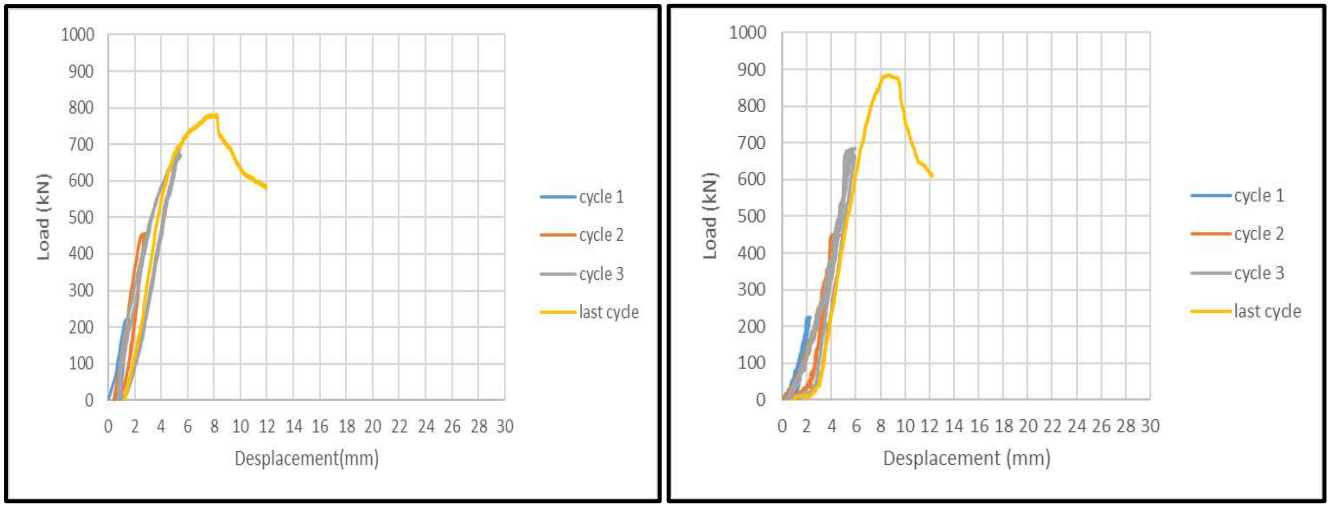

(a) **(b)**

Figures (4-11) (a)Load-deformation curve for SHS2 1.5, without shear connector ,(b) Load-deformation curve for SHS5 1.5 with shear connector

4.4.2.5 Effect of Type Filled Concrete

When compared (SHS21.5) sample with the section filled with ordinary concrete (SHS6), the rates of increase in the final capacity of the column by 1.5 % for the column was 40.90% respectively. The greater compressive strength, lead to the sudden failure curve. On opposite in which appeared a curved high ductility (SHS6) of the column as shown in Figures (4-12.a), (4-12.b).The value for deflection at ultimate load in the sample (SHS2,and SHS6) reached about 8,and 19mm respectively.

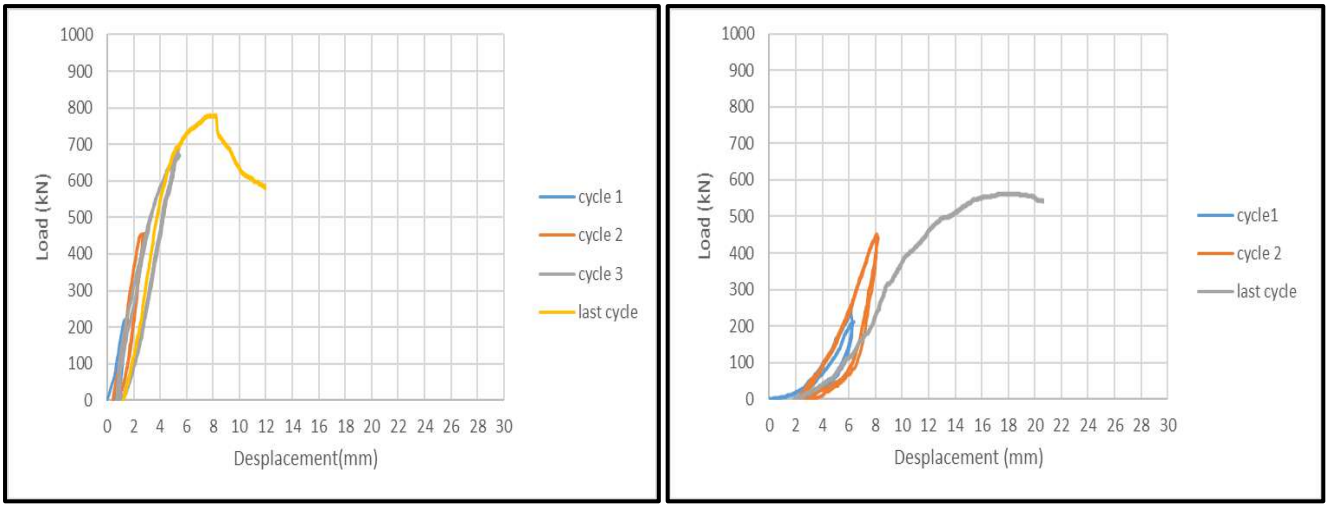

(a) **(b)**

Figure (4-12) (a) Load-deformation curve for SHS2 1.5 specimen, (b) Load-deformation curve for SHS6N specimen

4.4.2.6 Effect of Removed Filled Concrete

The result showed that the added concrete to steel tube provides greater strength than a steel-only column (4-13), where column gained force as a result of the concrete's compressive strength. Highest load of column developed in single type of section steel (SHS7), reached about 340 kN, and the capacity reduced by 56.1% when compared to the sample (SHS2).The ultimate failure load was obtained in the empty specimen (SHS7) at displacement 12 mm in the second cycle of repeated loading, while the (SHS2) failed in the last cycle (8mm).

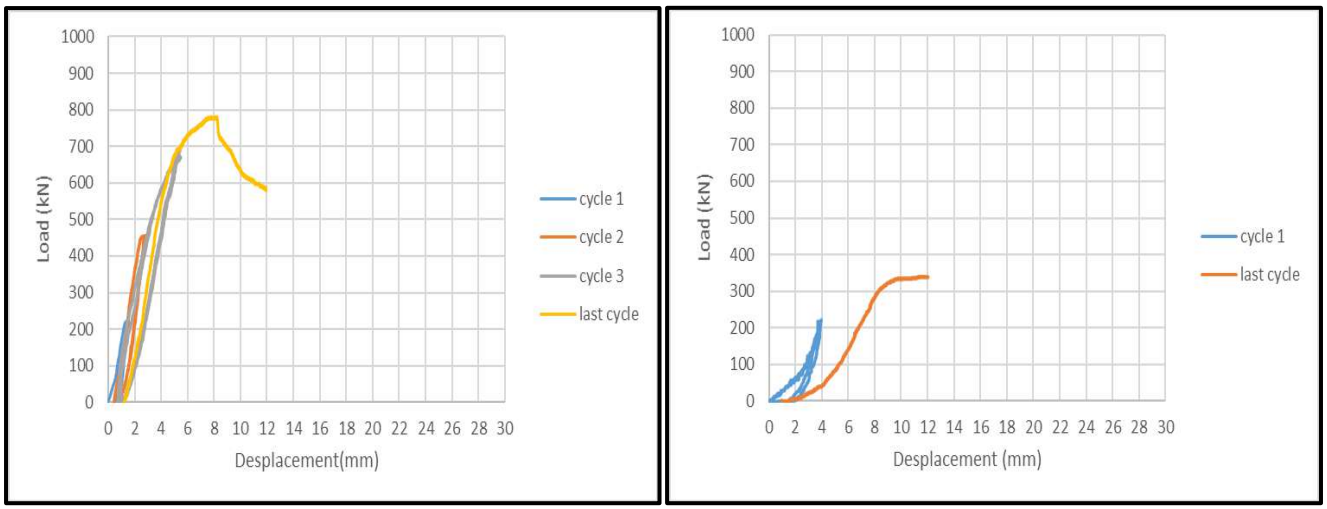

(a) **(b)**

Figures (4-13) (a) Load-deformation curve for SHS2 1.5 ,(b) Load-deformation curve for SHS7 and only steel tubing

4.5 Longitudinal Steel Strain Gauge Sensors

Each column contains four strain gauge, which are distributed in a way to insure reading of each side of the column, where two strain gauges were installed in the upper part, each one with a perpendicular direction to the other, and another two in the mid of the column in two perpendicular directions as well. Each strain gauge was numbered in the column from 1 to 4. Where number 1 and 2 were on one side, 3 and 4 are on transvers side, as shown in the Plate (3-27). They were linked to the Lab View program to record data logger of axial load versus longitudinal strain. The strain gauges continued to record data until the last moment of loading the column, and no one of them was damaged during the testing.

4.5.1 Longitudinal Strain Against Loading Ratio for Circular Section

In this section, which dealt with the difference between the samples containing the proportion of steel fiber 0.5% and 1.5% as shown in Figures (4-14) to (4-21),in strain number (1) at the top of specimen for each one, where recorded maximum strain of both columns was after the concrete reached the highest level

of capacity, the sample (CHS2) recorded strain value in station (1) was 10000 με at last cycle, while the sample (CHS1) recorded a maximum strain was 1640 με in the same location. This indicates that the percentage of steel fiber led to increase in the longitudinal tensile strain by increases of ultimate loading. On the opposite side of the strain gauge in position number (3) in each column, such as strain (3) for sample (CHS1) and (CHS2) where were reached values of the ultimate strain 1040 με and 2160 με respectively. Remembering that the yield stress of the steel coupon was 344.6 MPa and E=201065 MPa (Table 3-1) so

yielded value strain was 1713 μƐ, therefore 1&3 strain of tube column (CHS2) reached yield but (CHS1) did not yield.

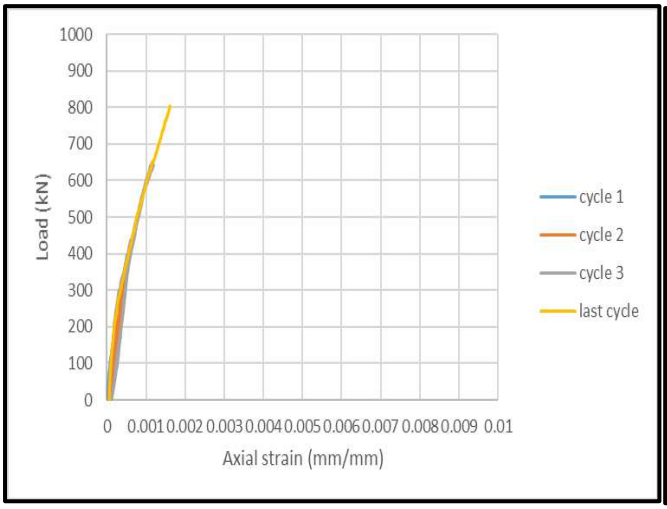

Figure (4-14) Top strain no. (1) of the specimen (CHS1)

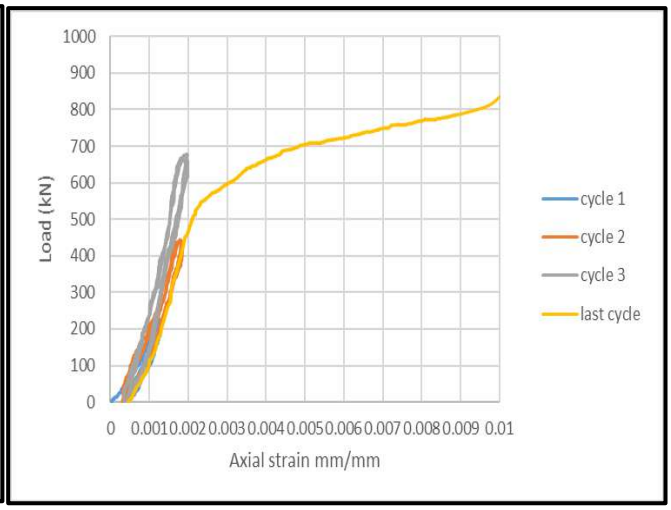

Figure (4-15) Top strain no. (1) of the specimen (CHS2)

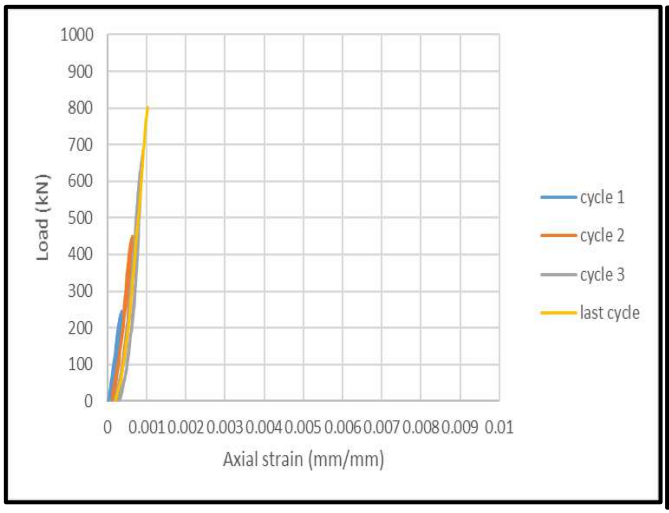

Figure (4-16) Top strain no. (3) of the specimen (CHS1)

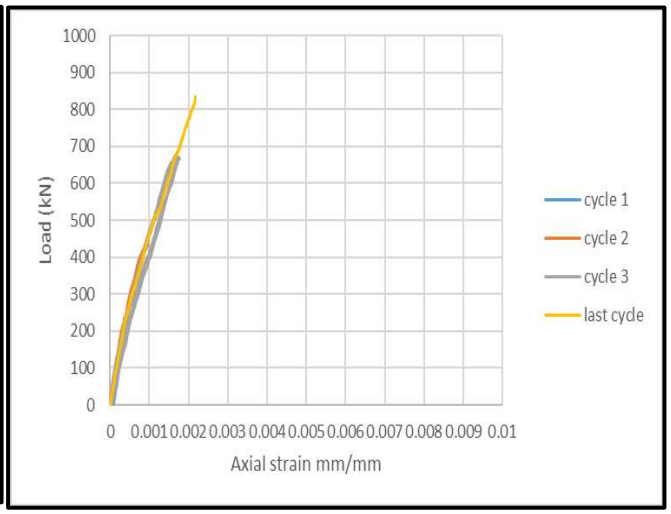

Figure (4-17) Top strain no. (3) of the specimen (CHS2)

While the maximum tensile strain in the middle of this columns in site (2&4), it recorded values higher than the strain values in the strain (1&3) for each column, where the values of the average strain in the middle for column (CHS1) were 2530 μƐ,2350 μƐ for (2&4) location respectively at the ultimate load. While the strain values for sample (CHS2) were 2630 μƐ and 2830 μƐ in the same point. The abrupt jump in the strain readings beyond to high is attributed to formation

of a buckle near the strain gage, which produced continued differences between the strain values. Some points appeared yield value for strain during second and third cycle, while the first cycle did not reach yielding in all columns.

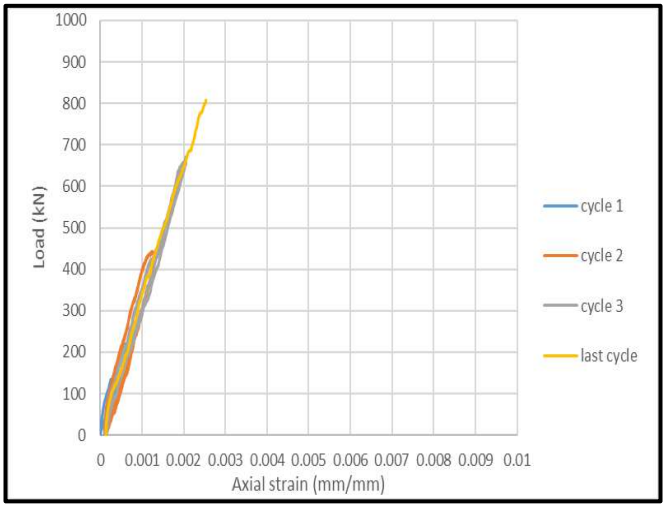

Figure (4-18) Mid strain no. (2) of the specimen (CHS1)

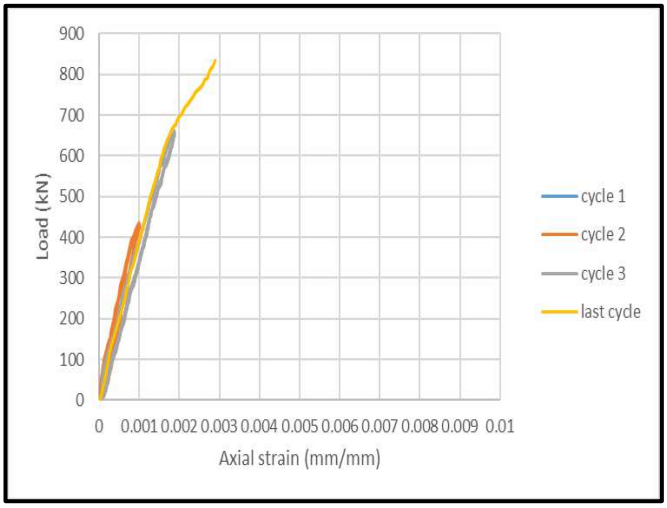

Figure (4-19) Mid strain no. (2) of the specimen (CHS2)

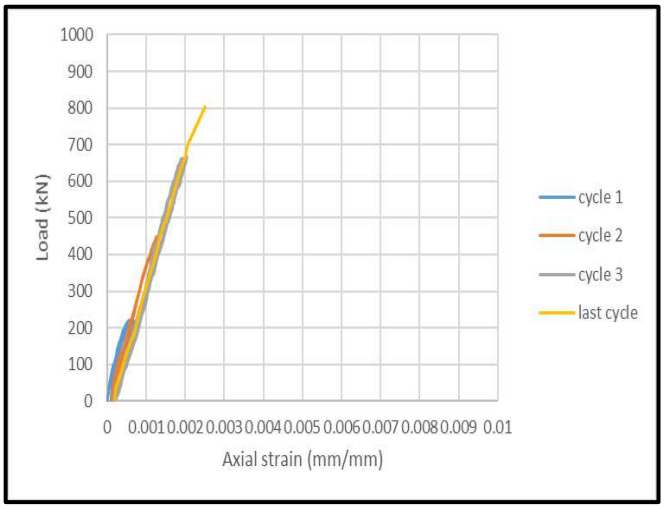

Figure (4-20) mid strain no. (4) of the specimen (CHS1)

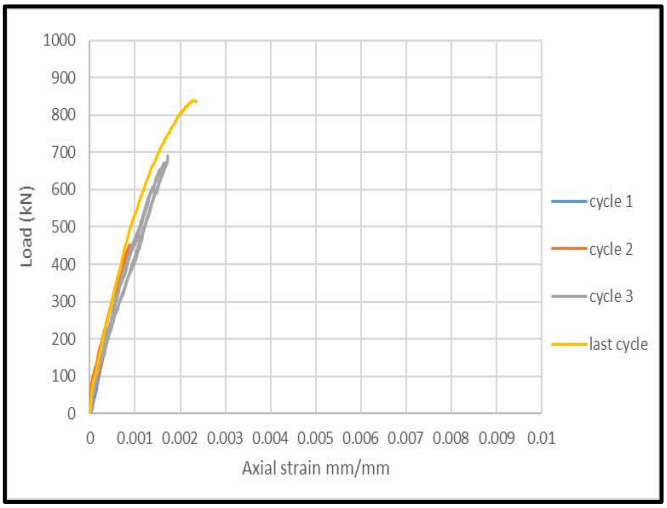

Figure (4-21) mid strain no. (4) of the specimen (CHS2)

When the ultimate load decrease (775kN) for column (CHS3),the strain recorded values less than (CHS2) except location (3).Figures (4-22) to (4-29) show a comparison between data recorded from steel tensile strain gauges in columns (CHS2) and (CHS3) for point (1 & 3), which were tested under repeated loading. The readings of strain gauges number (1&3) for columns (CHS2) and (CHS3) at ultimate load were 10000, 2160,6310, and 2714 μƐ respectively. It is clear that both strains of tube column (CHS3) was yielded. The ultimate strain value (1&3) for (CHS3) was attributed to formation of a buckle near the region of applied loading. Whereas the mid location gauges (2&4) did not record any yield strain for (CHS3) and less than occurred in (CHS2). Where the value of strain gauges number (2 & 4) in columns (CHS2) and (CHS3) described in Figures (4-25) to (4-28), and recorded value was 2830,2630, 955 and 991μƐ respectively. One of the gauges was recorded strain greater than the yield in the top of column in the cycle second cycle (450kN) for column (CHS2), and all strains were reach yielded in the third cycle (675kN) in the same column. While one strain gauge reach yield in the cycle (3) for (CHS3), and the others did not yield.

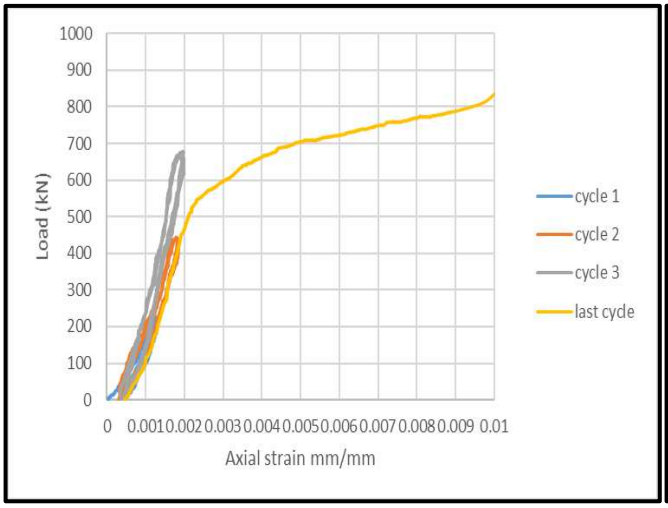

Figure (4-22) Top strain no. (1) of the specimen (CHS2)

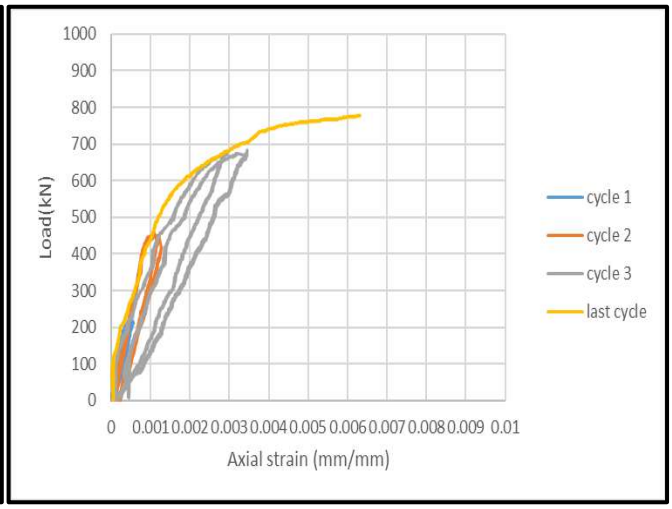

Figure (4-23) Top strain no. (1) of the specimen (CHS3)

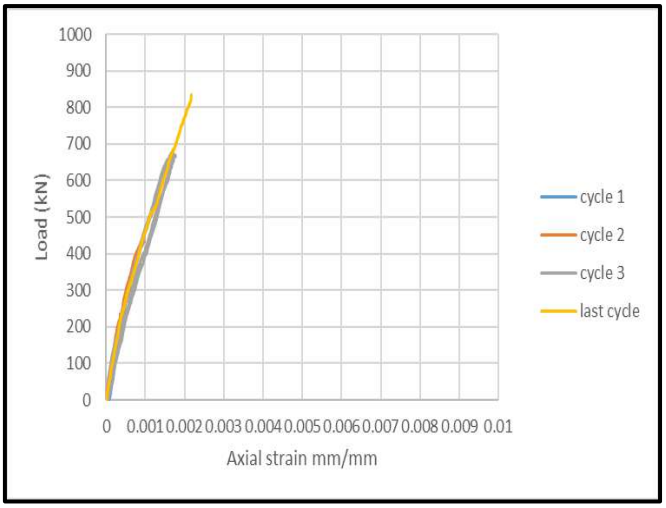

Figure (4-24) Top strain no. (3) of the specimen (CHS2)

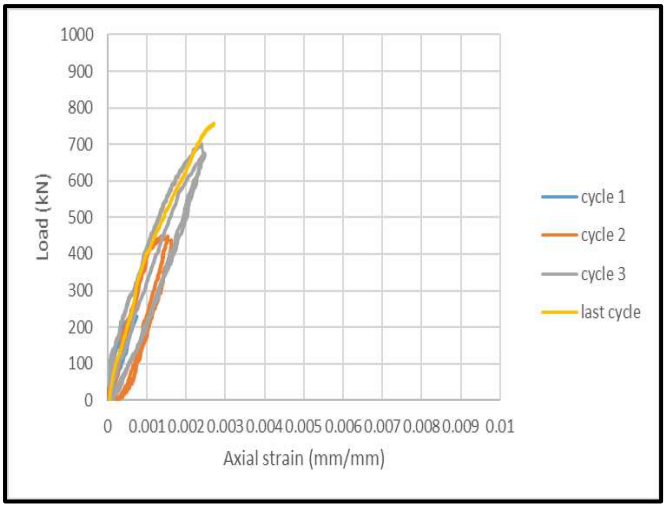

Figure (4-25) Top strain no. (3) of the specimen (CHS3)

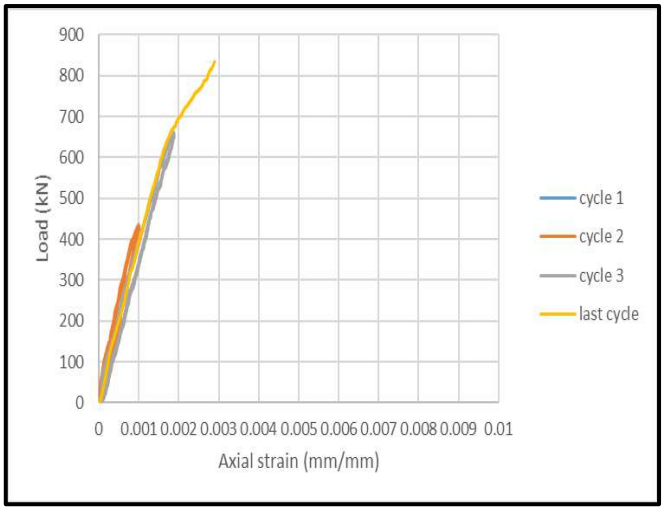

Figure (4-26) Mid strain no. (2) of the specimen (CHS2)

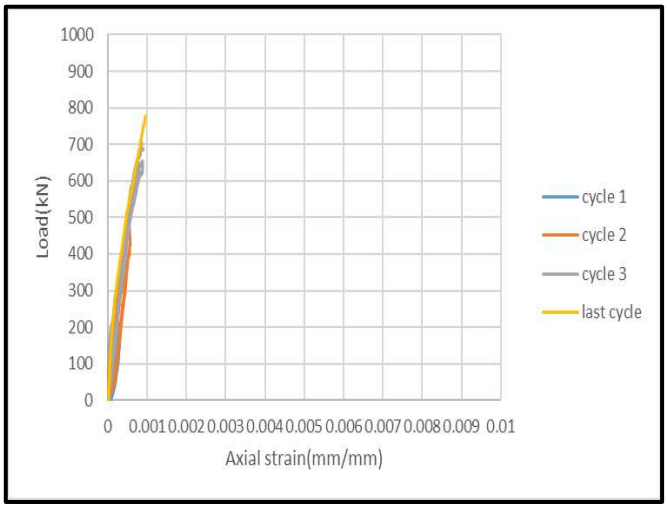

Figure (4-27) Mid strain no.(2) of the specimen (CHS3)

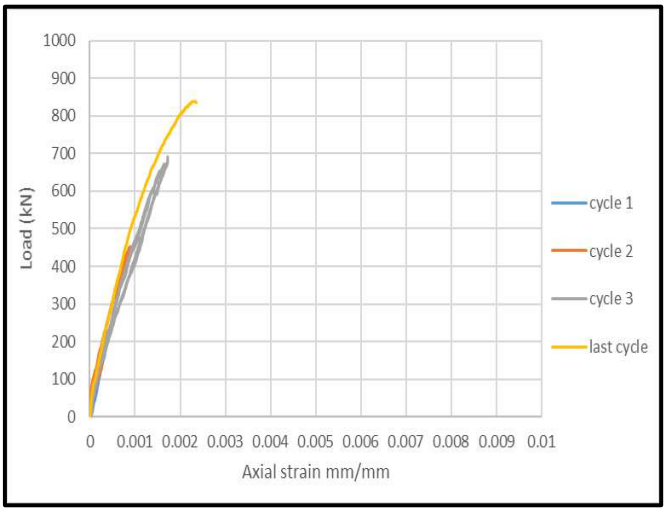

Figure (4-28) Mid strain no. (4) of the specimen (CHS2)

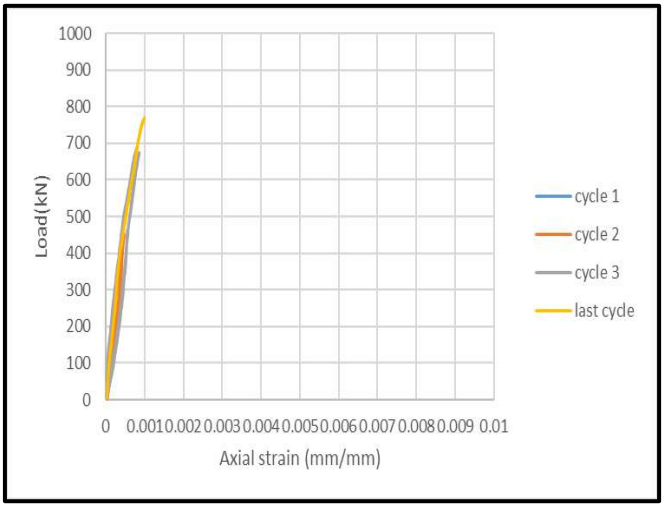

Figure (4-29) Mid strain no. (4) of the specimen (CHS3)

Steel strain gauges readings curves for columns(CHS2),and (CHS4) are drawn in Figures (4-30) to (4-37),which deals with the difference in longitudinal tensile strain of the samples containing global ratio (L/B(D)) equal 8 and 7. Due to slenderness effect, the columns of L/D = 70 reached a strain of about 3790 με,and 3550 at the top of the column for points (1&3) respectively, while specimens with L/D =80(CHS2), presented axial strain with magnitude 10000 με and, greater than specimens (CHS4) in the strain number (1).Whereas the other strain (3) of specimen (CHS2) had lower value than position (3) for (CHS4) and was 2160 με. On the other hand, the maximum strain in the mid height of the column (CHS4) had values greater than this developed in the upper part. The strain reached for (2&4) points was approximately 10700 and 3600 με respectively, as well as greater than the values of strain in column (CHS2) for the same point (2630&2830) με. This increase was due to the large ultimate load when the length of column was shorted and failure mode appeared local buckling in this region. All strain gauges placed to measure axial strain obtained values higher than 1713 με (yield strain) at the peak load. This indicate the beginning of the local buckling process for the short columns. All recorded value for strain when L/D=70 reach yielded in third cycle (675Kn) but except one.

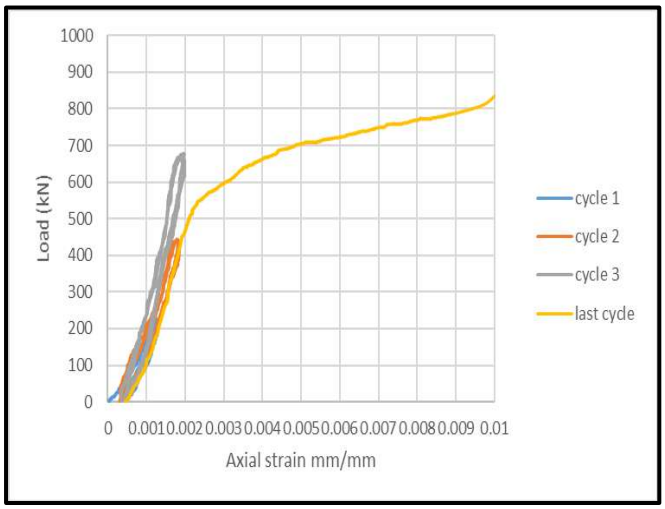

Figure (4-30) Top strain no. (1) of the specimen (CHS2)

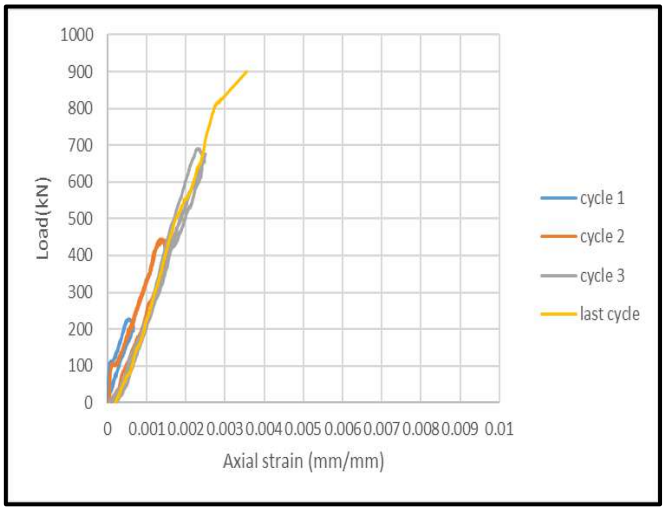

Figure (4-31) Top strain no. (1) of the specimen (CHS4)

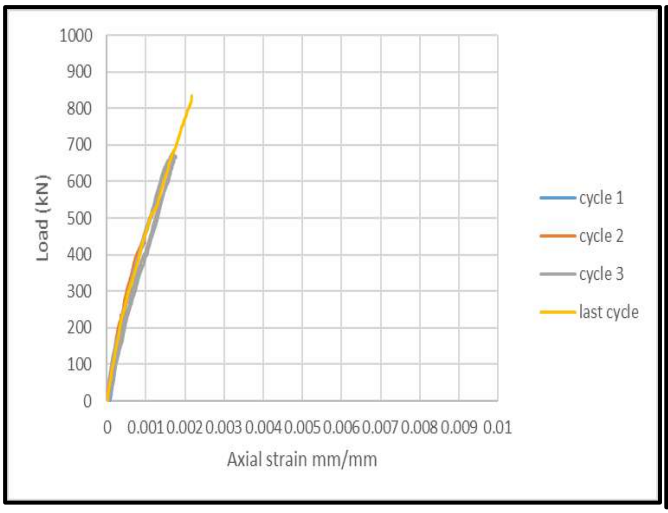

Figure (4-32) Top strain no. (3) of the specimen (CHS2)

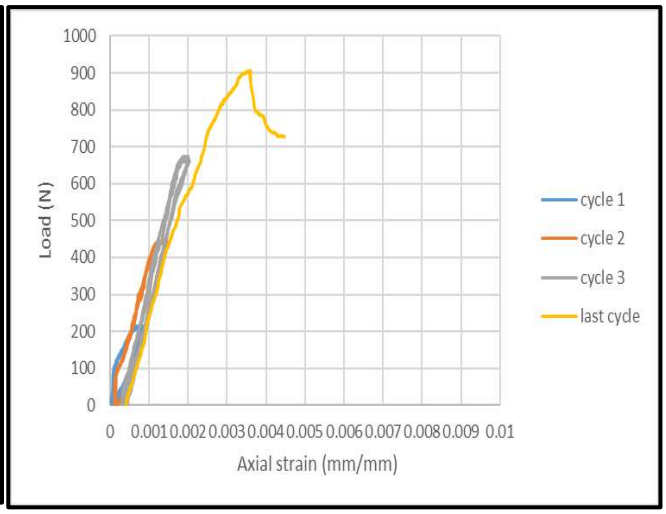

Figure (4-33) Top strain no. (3) of the specimen (CHS4)

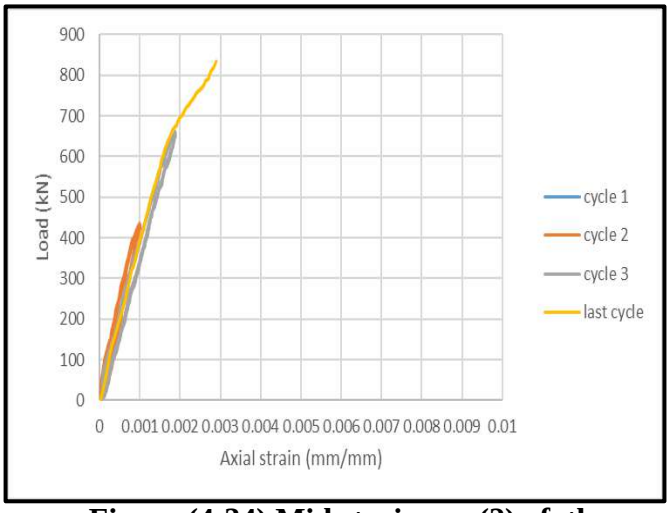

Figure (4-34) Mid strain no. (2) of the specimen (CHS2)

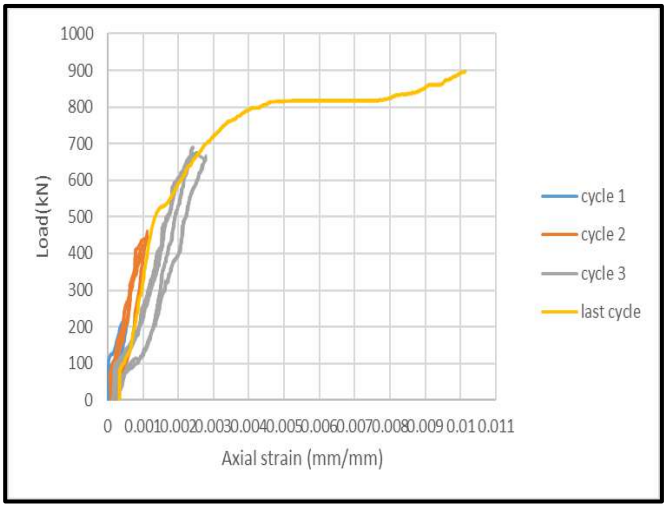

Figure (4-35) Mid strain no. (2) of the specimen (CHS4)

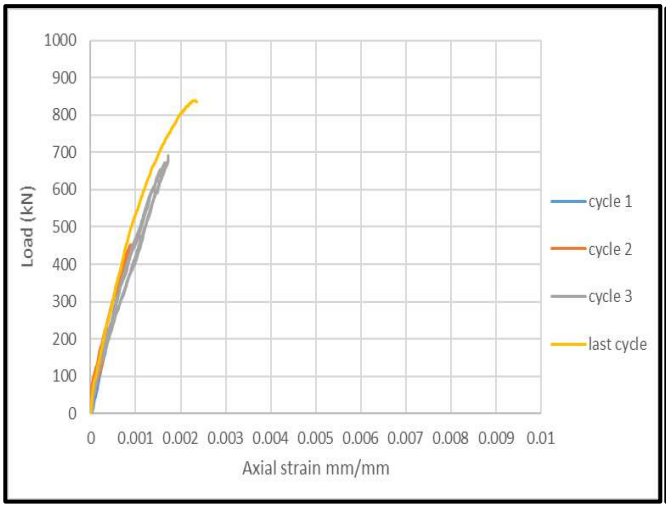

Figure (4-36) mid strain no. (4) of the specimen (CHS2)

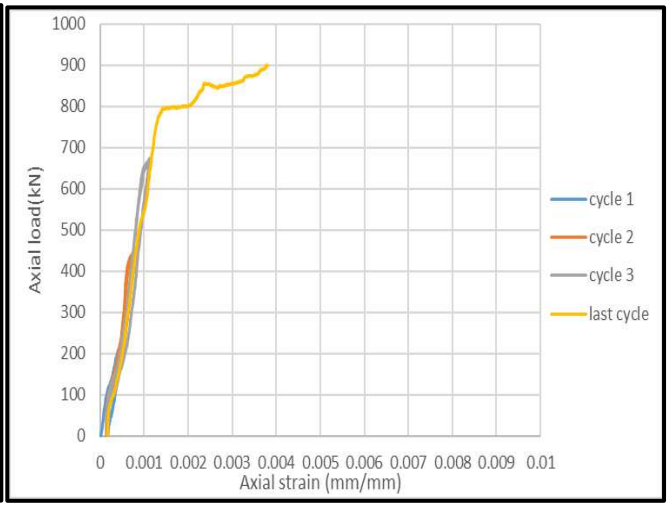

Figure (4-37) mid strain no. (4) of the specimen (CHS4)

Figures No. (4-38) (4-45) show the strain readings for steel strain in the upper and lower positions for six cycles and the last cycle for column (CHS5). It was found by increasing of the loads,and due to the presence of shear connectors which forced the steel tube and the concrete core to interact and deform as one unit. The measured longitudinal strains at peak load (910kN) for sample (CHS5) were 1991με and 875 με for points (1&3), while the strain values for the sample (CHS5) in the upper part (1&3) were less than values of the strain in the middle height (2 & 4) was 2500 and 3000 με respectively. But one of the two top strain gauges for sample (CHS5) was not reached to the maximum stress.when the shear connectors are used and larger spacing of shear connectors preventing progresses increase of hoop strains due to less expansion of concrete leading to less stress in this region . All the longitudinal strains in specimen (CHS5) when compare with (CHS2) were slightly lower and did not record any yield value thruogh the three cycle first.

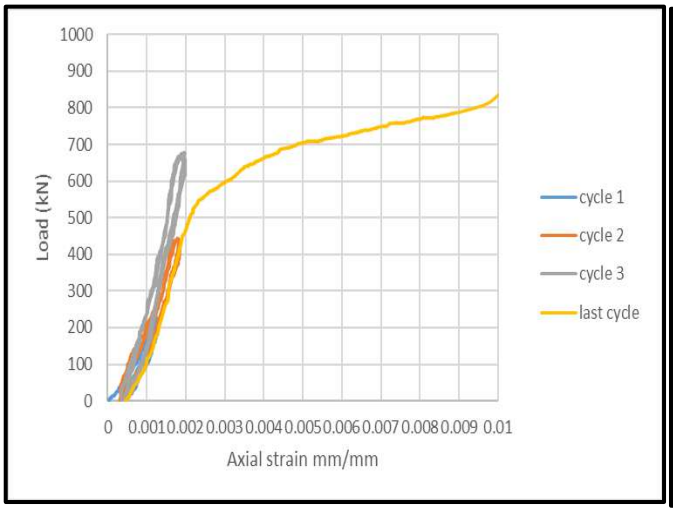

Figure (4-38) Top strain no. (1) of the specimen (CHS2)

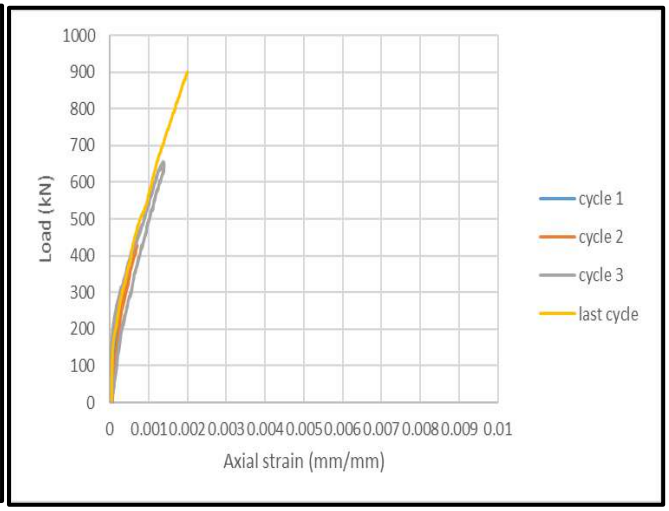

Figure (4-39) Top strain no. (1) of the specimen (CHS5)

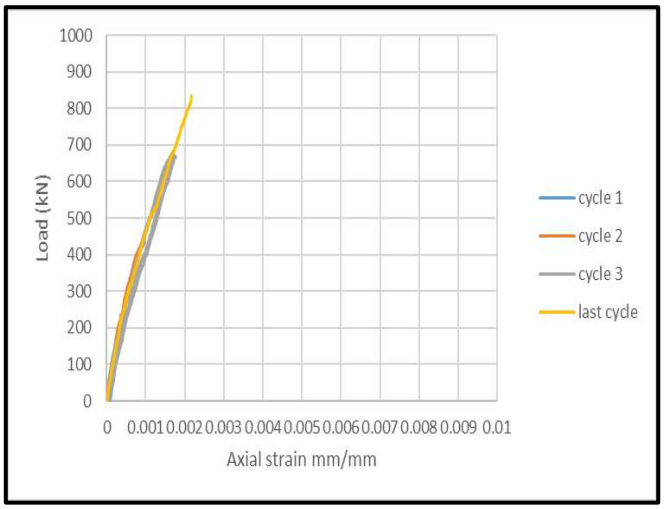

Figure (4-40) Top strain no. (3) of the specimen (CHS2)

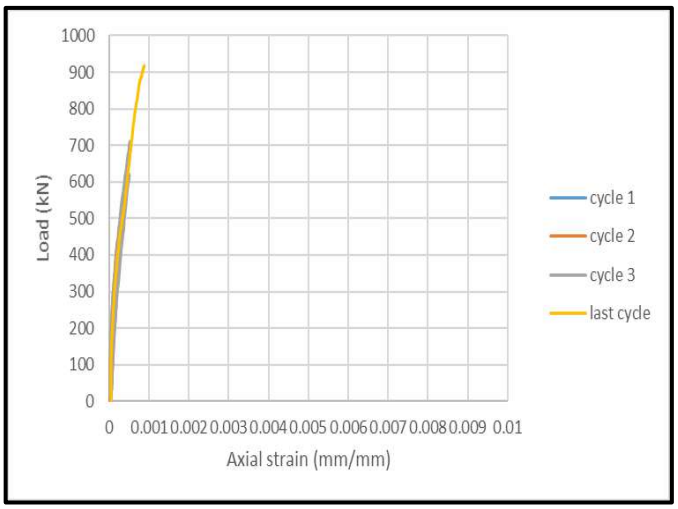

Figure (4-41) Top strain no. (3) of the specimen (CHS5)

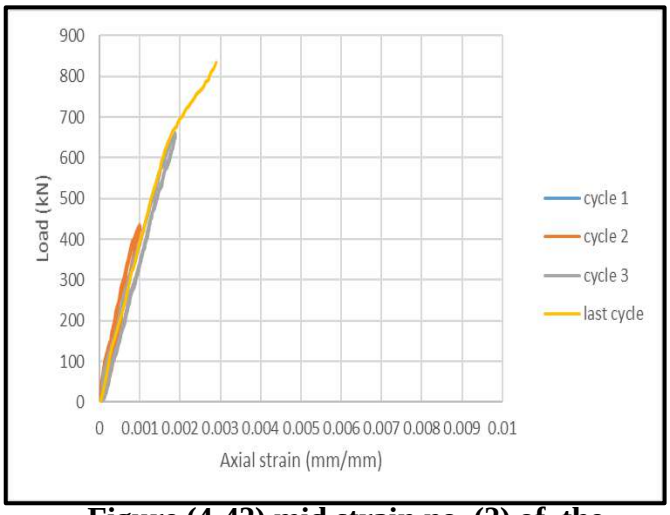

Figure (4-42) mid strain no. (2) of the specimen (CHS2)

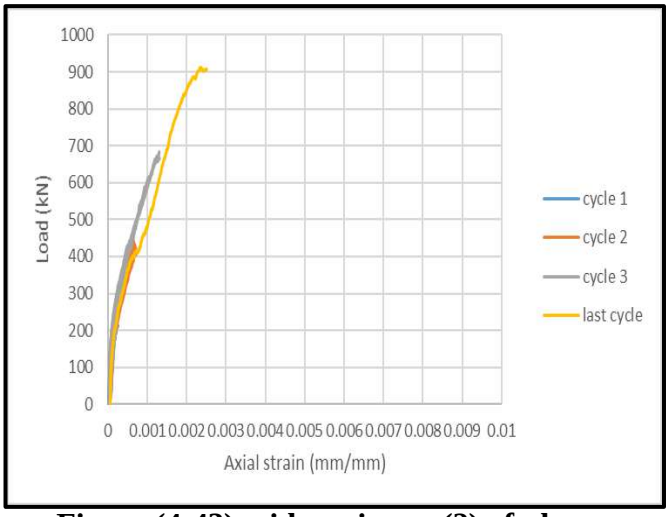

Figure (4-43) mid strain no. (2) of the specimen (CHS5)

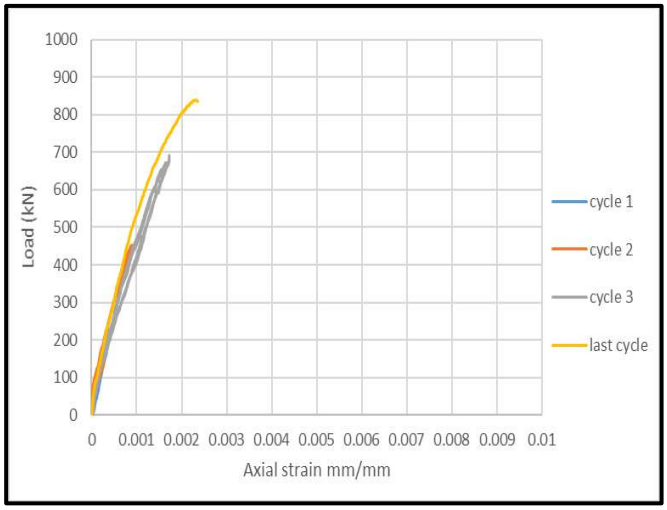

Figure (4-44) mid strain no. (4) of the specimen (CHS2)

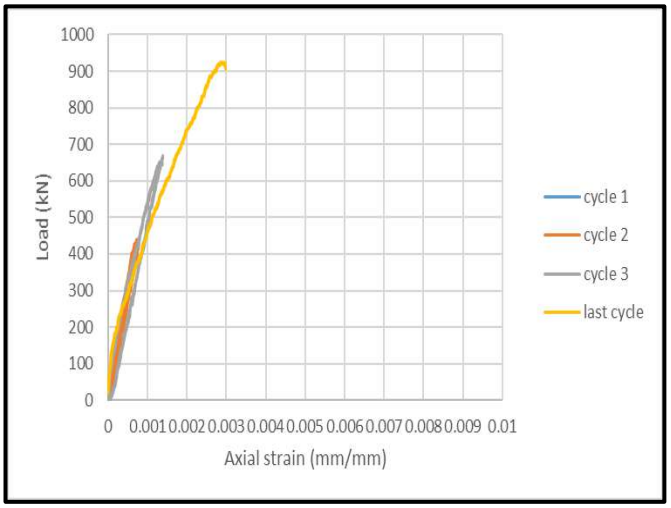

Figure (4-45) mid strain no. (4) of the specimen (CHS5)

Also studied the behavior of tensile strain curve when compressive strength 90.32 Mpa and 30.83 Mpa .Through Figures (4-46) to (4-53),it was noticed the normal concrete (CHS6)strains at site (1 & 3) were 1233 and 1305 μƐ respectively, and they were less than recorded values at sites (2 & 4),which was reached 2459 and 4166 μƐ respectively.All strain for sample (CHS6) was not recorded any value grater than yeild strain (1713 μƐ) during the three cycle first until reaching ultimate strain .The mid height strain value for (CHS6) was jumped and become graeter than this occurred in the middle of specimen (CHS2) due to sudden buckle. It was concluded that the effects of the bond between the concrete and the steel tube was more critical for high-strength concrete. For normal strength concrete, the reduction on the axial capacity due to the loss of bonding between steel and concrete was very small.This specimen was filled with normal concrete failed in the third cycle of loading.

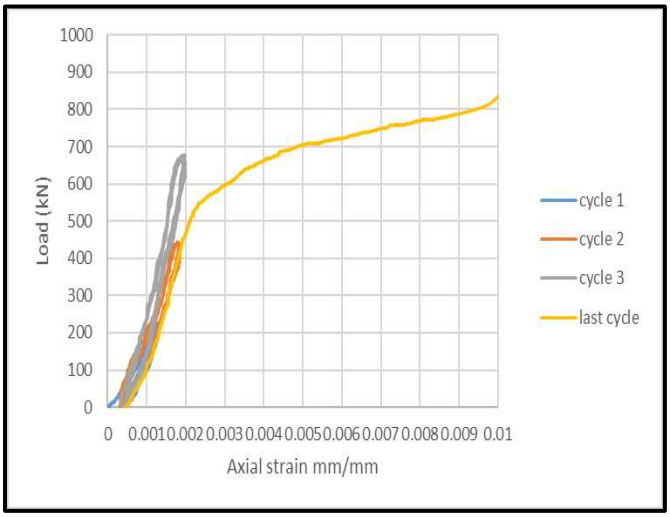

Figure (4-46)Top strain no. (1) of the specimen (CHS2)

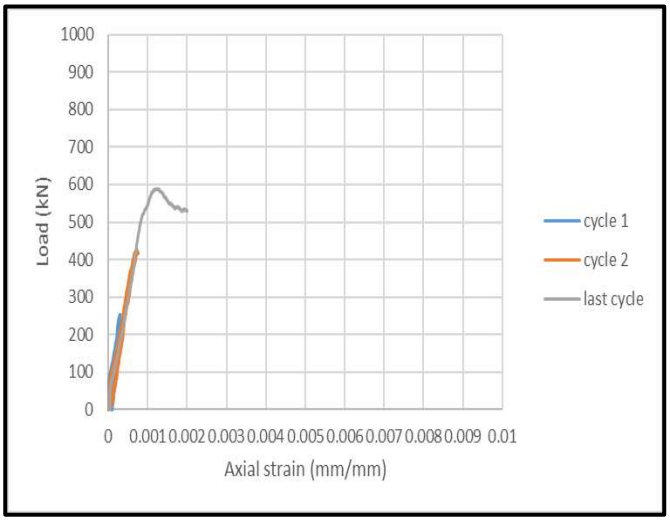

Figure (4-47) Top strain no. (1) of the specimen (CHS6)

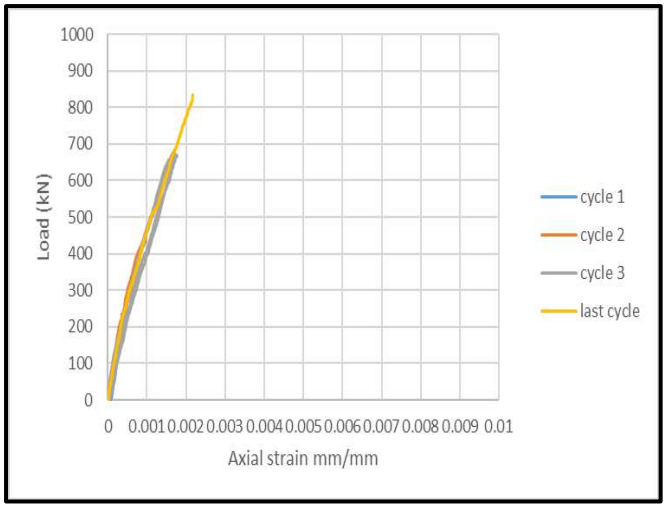

Figure (4-48) Top strain no. (3) of the specimen (CHS2)

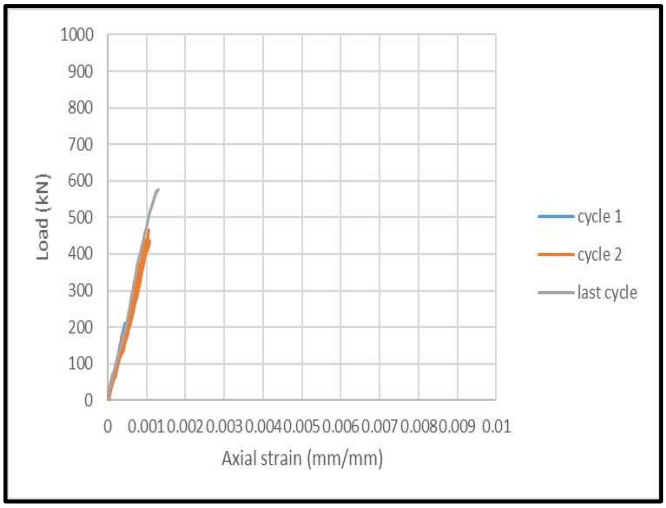

Figure (4-49) Top strain no. (3) of the specimen (CHS6)

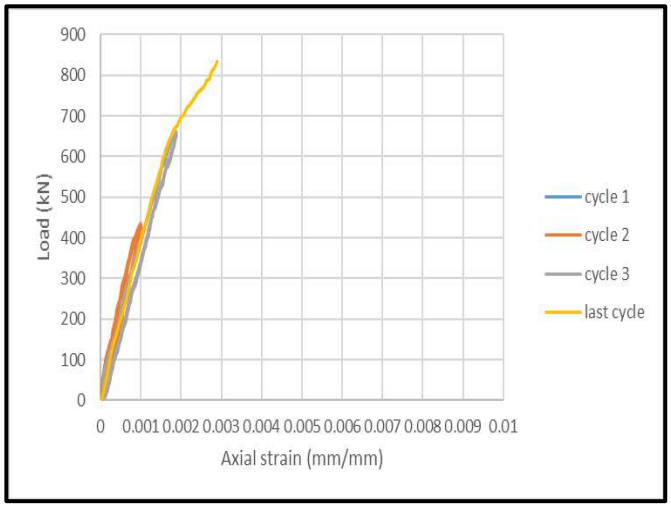

Figure (4-50) mid strain no. (2) of the specimen (CHS2)

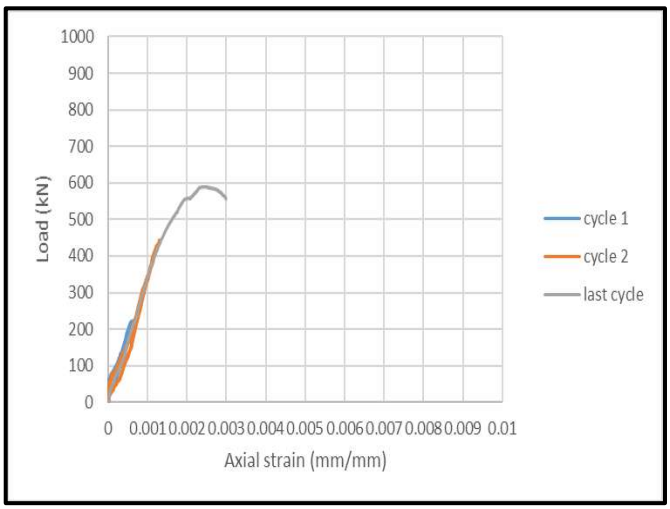

Figure (4-51) mid strain no. (2) of the specimen (CHS6)

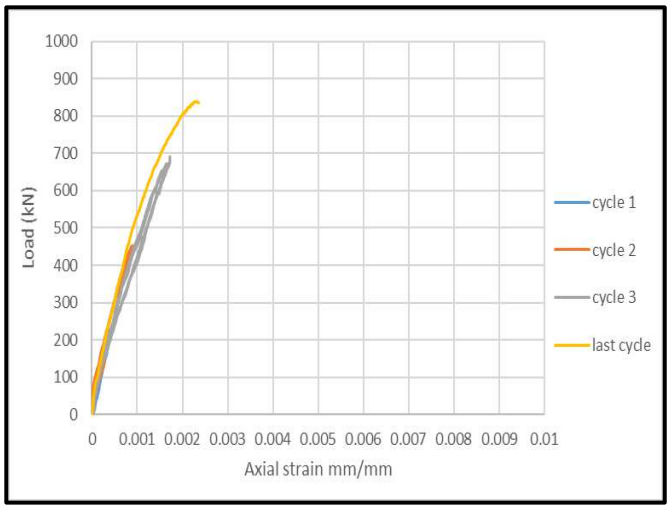

Figure (4-52) mid strain no. (4) of the specimen (CHS2)

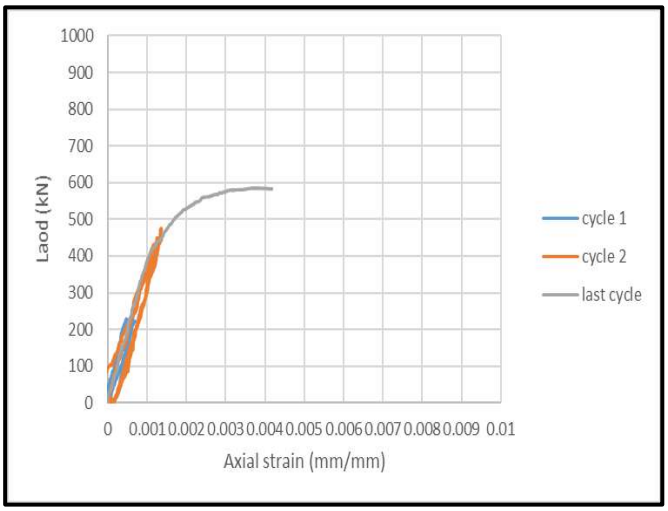

Figure (4-53) mid strain no. (4) of the specimen (CHS6)

And, also the Figures (4-54) to (4-61) described the stresses of the sample (CHS7) were less compared to the section filled with concrete. The sample (CHS7) failed in the second cycle of loading at the ultimate load 320 kN. Also, the strain was very high because the concrete was reducing the axial shortening and restricting the steel tube. The sample had strain at position (1 & 3) were 9320,2500με respectively, while the mid height location (2 & 4) was reached values 4516,2596 με respectively at the value of the maximum load. But the Hoop tension strain values measured in (CHS7) are higher compared to the specimen (CHS2) in position (2&3) due to steel tube expands in the radial direction during the compressive loads in its longitudinal direction by magnitude value (670 and 1886 με).

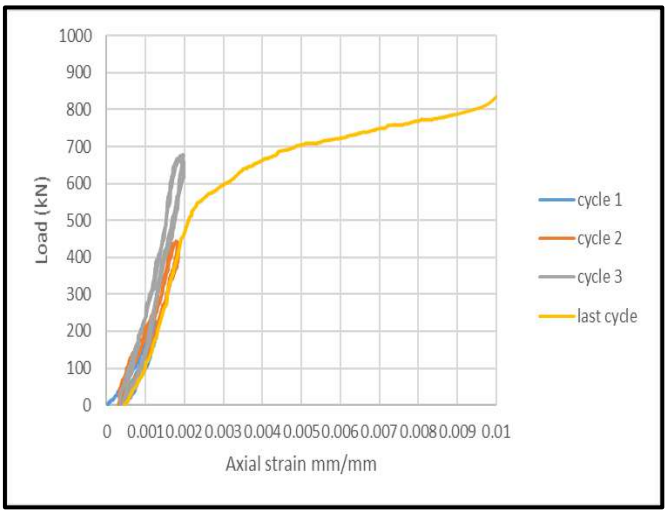

Figure (4-54) Top strain no. (1) of the specimen (CHS2)

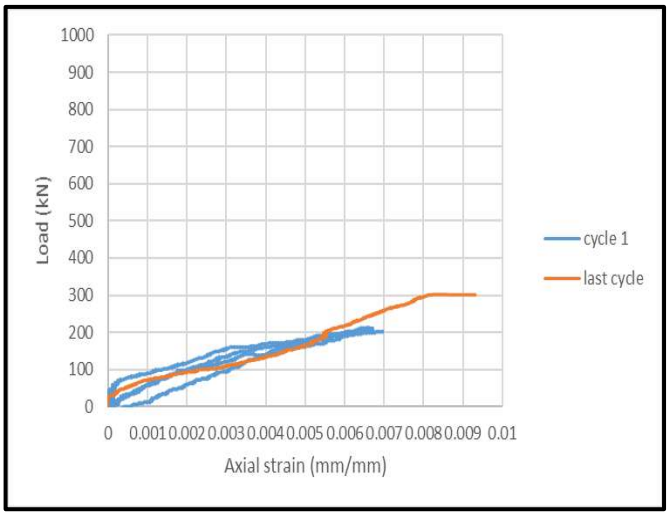

Figure (4-55) Top strain no. (1) of the specimen (CHS7)

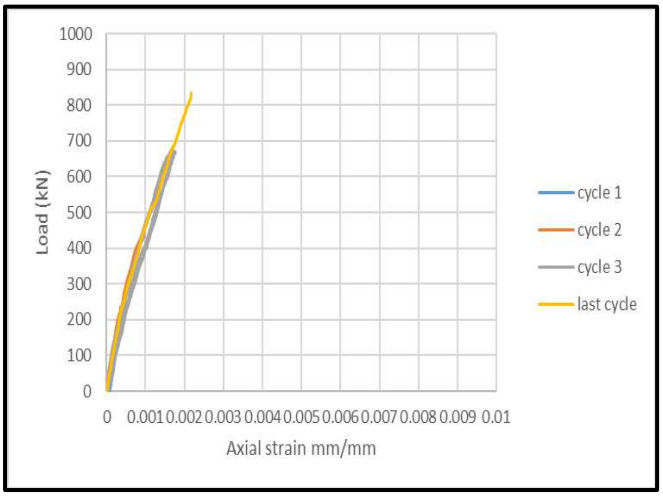

Figure (4-56) Top strain no. (3) of the specimen (CHS2)

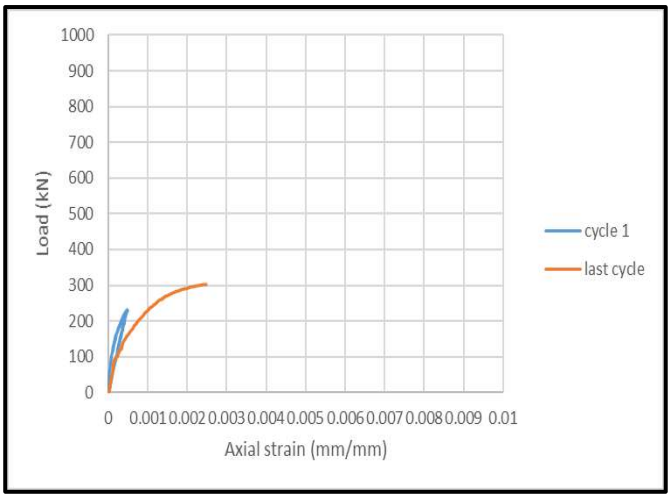

Figure (4-57) Top strain no. (3) of the specimen (CHS7)

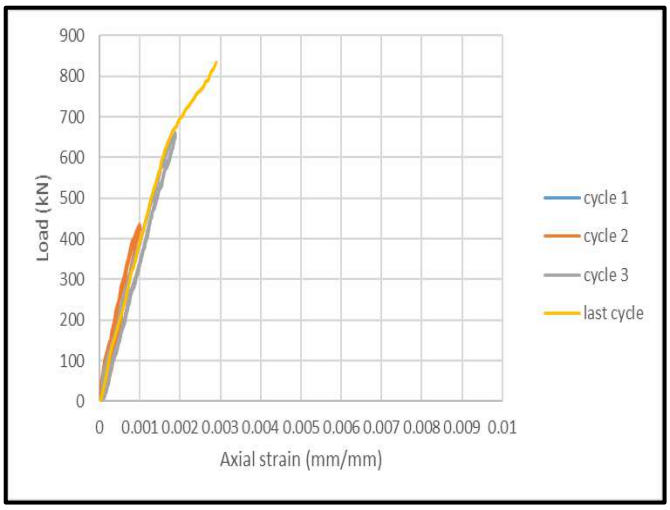

Figure (4-58) mid strain no. (2) of the specimen (CHS2)

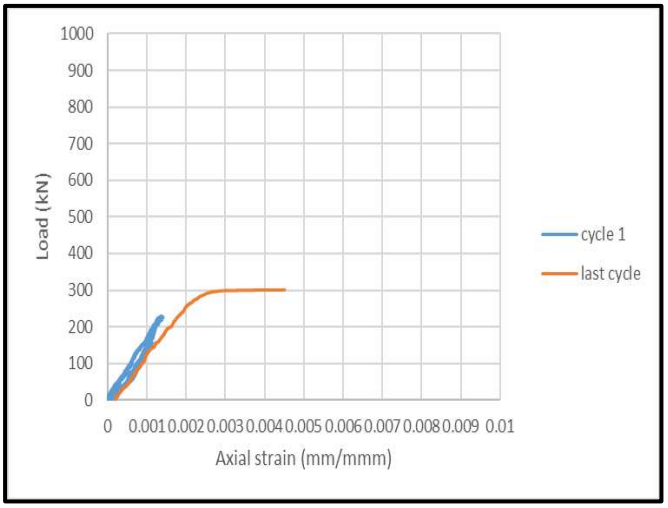

Figure (4-59) mid strain no. (2) of the specimen (CHS7)

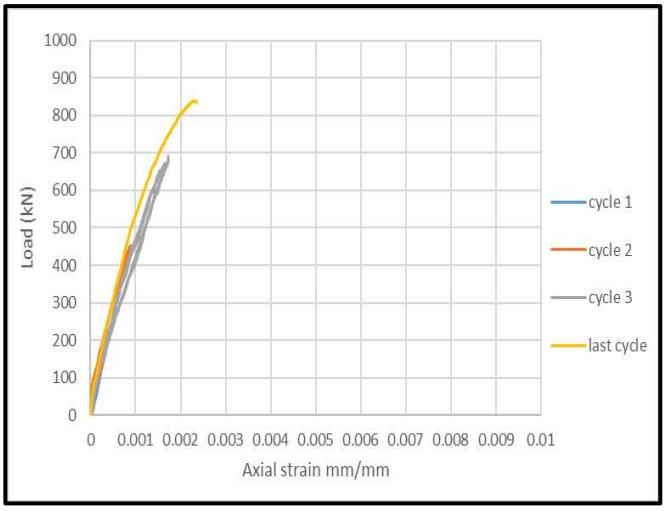

Figure (4-60) mid strain no. (4) of the specimen (CHS2)

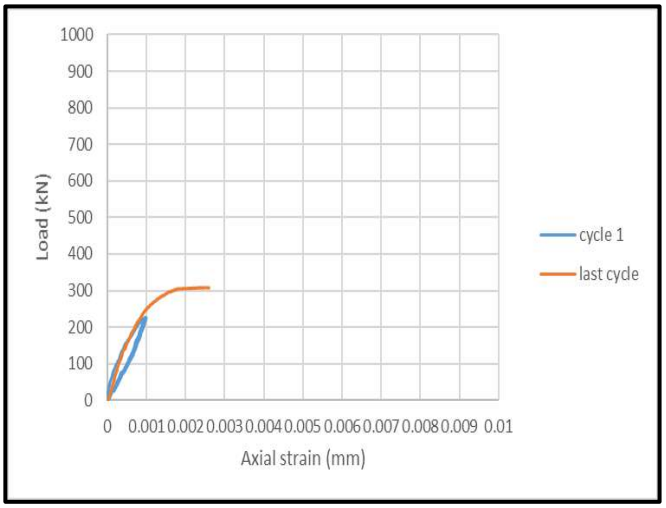

Figure (4-61) mid strain no. (4) of the specimen (CHS7)

4.5.2 Longitudinal Strain Against Loading Ration for Square Section

In this section, samples of column (SHS1) and (SHS2) was discussed. The difference between them the first column contained proportion of steel fiber 0.5% and the seconder 1.5% steel fiber ratio respectively as shown in Figures (4-62) to (4-69). The ultimate load for each column approximetally equall ,which was in the sample (SHS1) reached (775 kN),and the other (750kN) in last cycle of reapeted loading.The form of failure was local buckling for both them, but in the sample (SHS1) local buckle was occurred in the lower part of the height ,while this occurred in the upper part for sample (SHS2) was due to the difference in stresses region on length of samples. The longitudinal strain was recorded value in the sample (SHS1) at site (1 & 3) 1351,1877 με respectively, but recorded in sites (2 & 4) values smaller than the top points which (1078,1650 με).On the contrary to the sample (SHS2),the highest tensile strain in the failure zone (1 & 3) reached about 1752,5649 με near the buckle tube, while it was 1317,803 με in the points (2 & 4) . Some points appeared yield value for strain during the last cycle such as point (3) for (SHS1) and points (1&3) for (SHS2) sample, while the three cycle first did not reach yielding in this columns.

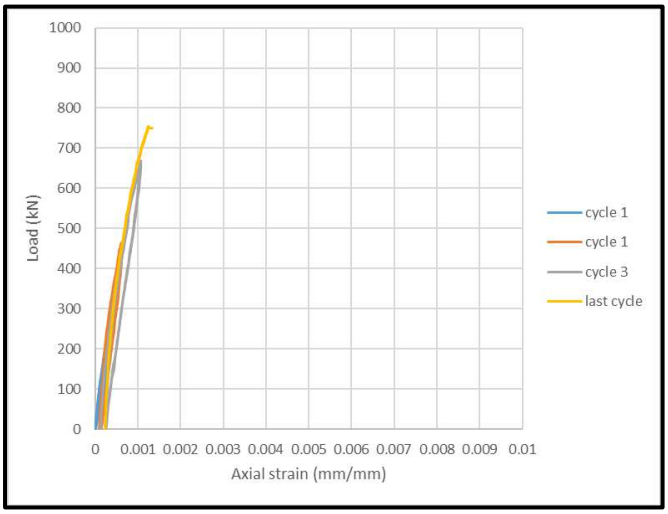

Figure (4-62) top strain no. (1) of the specimen (SHS1)

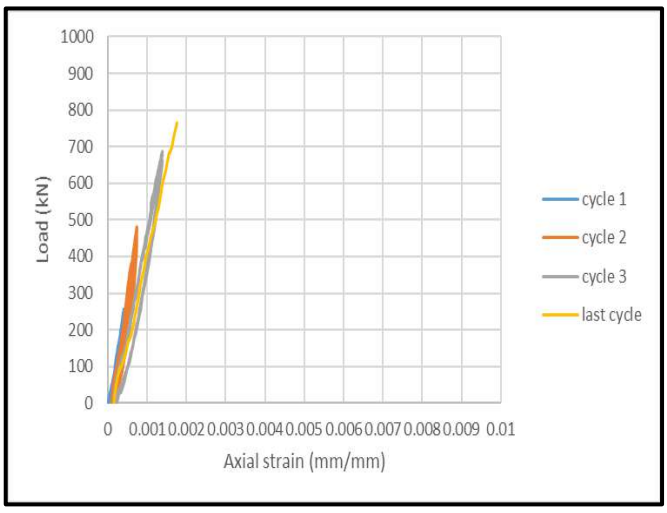

Figure (4-63) top strain no. (1) of the specimen (SHS2)

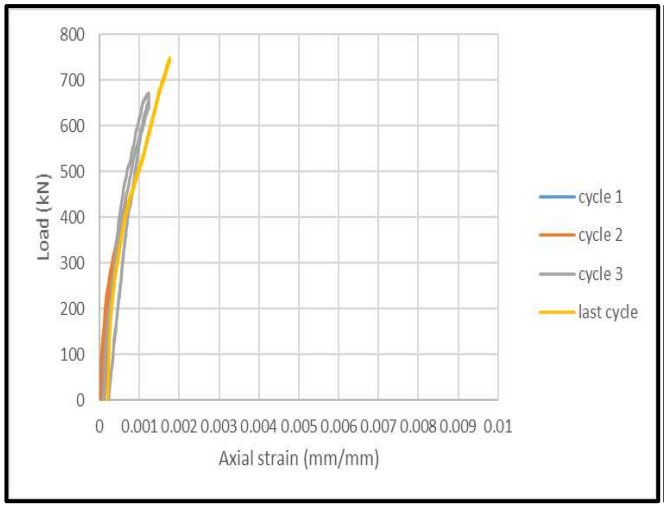

Figure (4-64) top strain no. (3) of the specimen (SHS1)

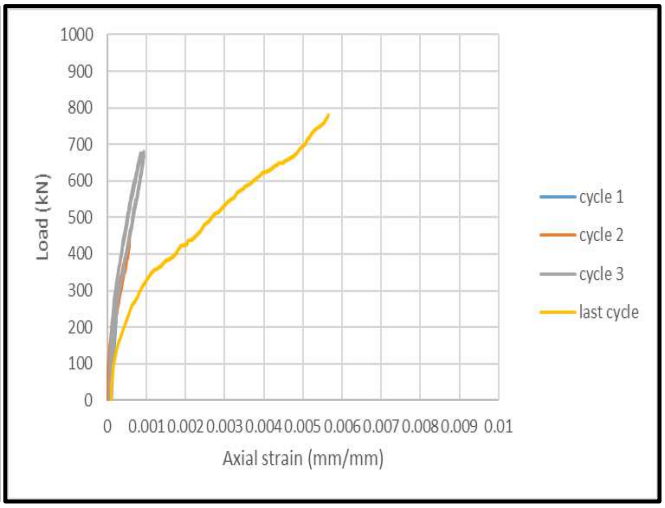

Figure (4-65) top strain no. (3) of the specimen (SHS2)

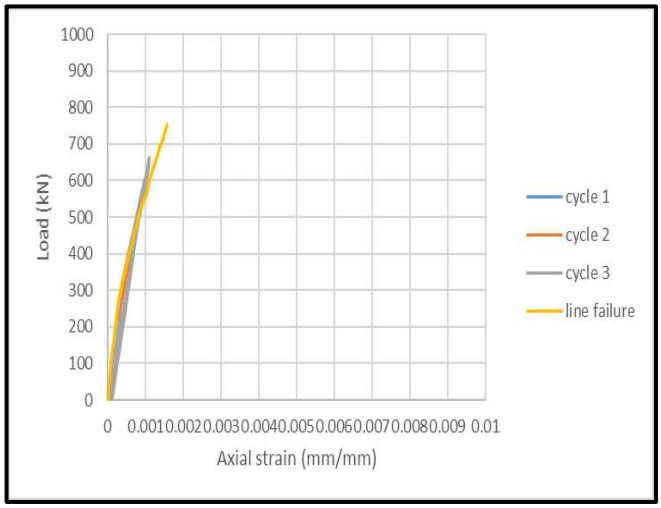

Figure (4-66) mid strain no. (2) of the specimen (SHS1)

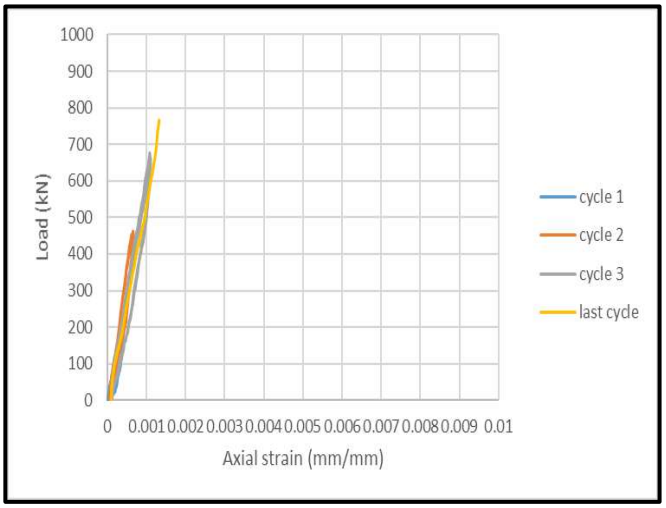

Figure (4-67) mid strain no. (2) of the specimen (SHS2)

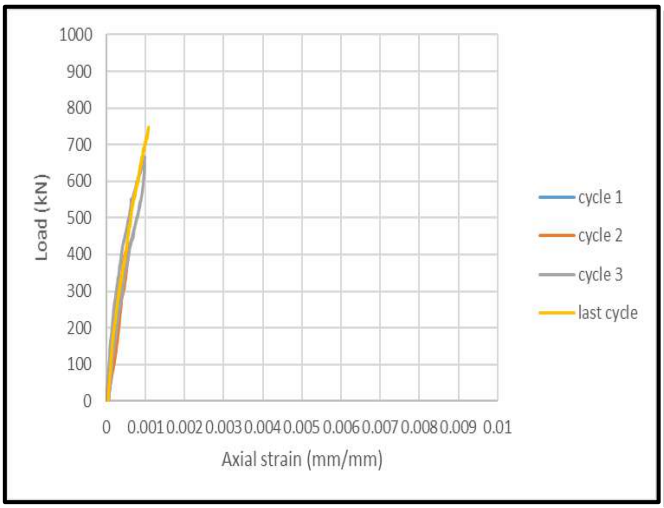

Figure (4-68) mid strain no. (4) of the specimen (SHS1)

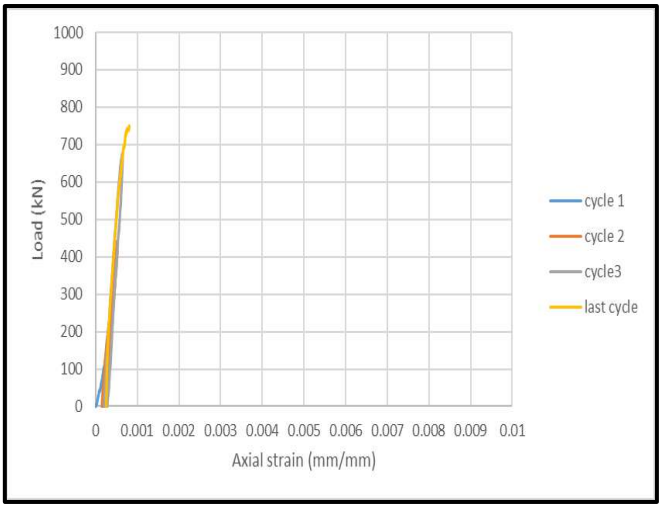

Figure (4-69) mid strain no. (4) of the specimen (SHS2)

When the ultimate load increase (815kN) for column (SHS3),the strain recorded values more than (1713με) except location (3).Figures (4-70) to (4-77) show a comparison between data recorded from steel tensile strain gauges in columns (SHS2) and (SHS3) for point (1 & 3), which were tested under repeated loading. The readings of strain gauges number (1&3) for columns (SHS2) and (SHS3) at ultimate load were 1752, 5949, 4520, and 1078με respectively. It is clear that one of the strains for tube column (SHS3) was yielded. The ultimate strain value (1&3) for (SHS3) was attributed to formation of a buckle near the region of applied loading. Whereas the mid location gauges (2&4) did not record any yield strain for (SHS3) and more than occurred in (SHS2). Where the value of strain gauges number (2 & 4) in columns (SHS2) and (SHS3) described in Figures (4-25) to (4-28), and recorded value was 1317, 803, 1531,1348με respectively. One of the gauges was recorded strain greater than the yield in the top of column in the third cycle (675kN) for column (SHS3), and the others did not yield. This indicates that the greater area of concrete in the column (SHS3) was increased the vertical load and leading to increase the expansion tube.

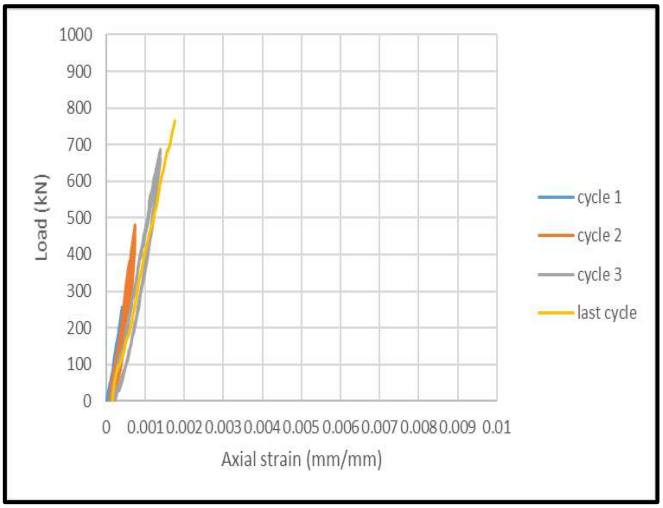

Figure (4-70) top strain no. (1) of the specimen (SHS2)

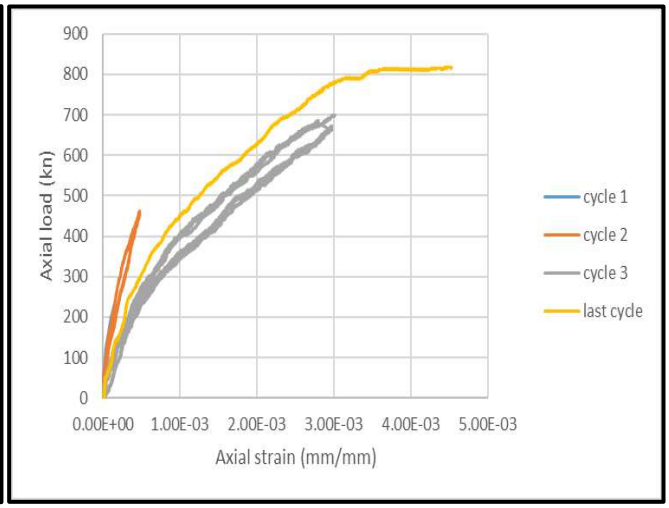

Figure (4-71) top strain no. (1) of the specimen (SHS3)

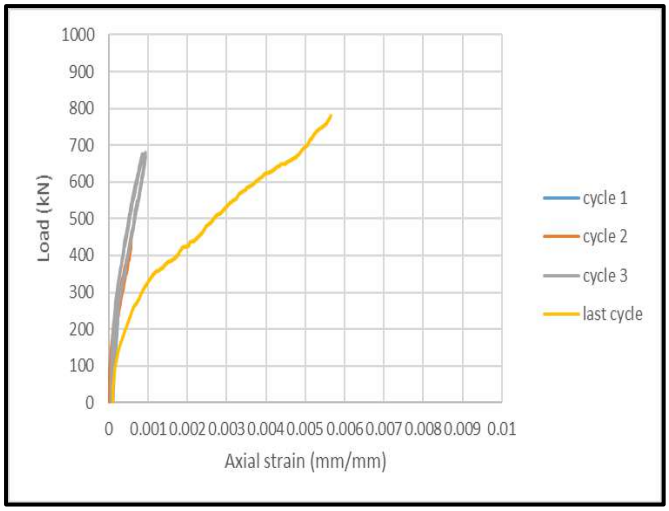

Figure (4-72) top strain no. (3) of the specimen (SHS2)

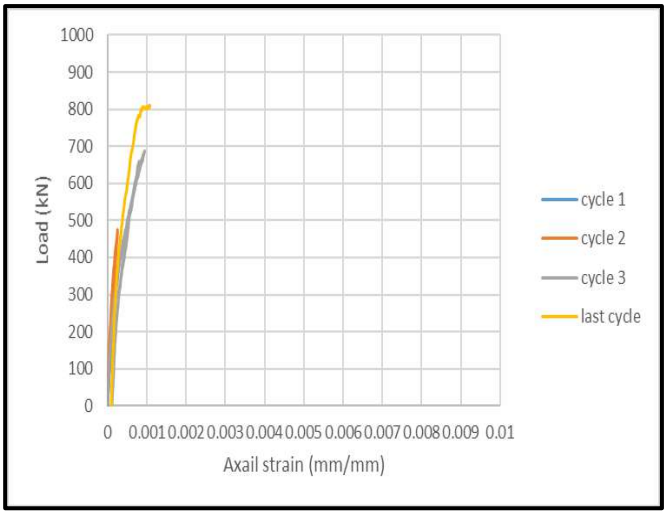

Figure (4-73) top strain no. (3) of the specimen (SHS3)

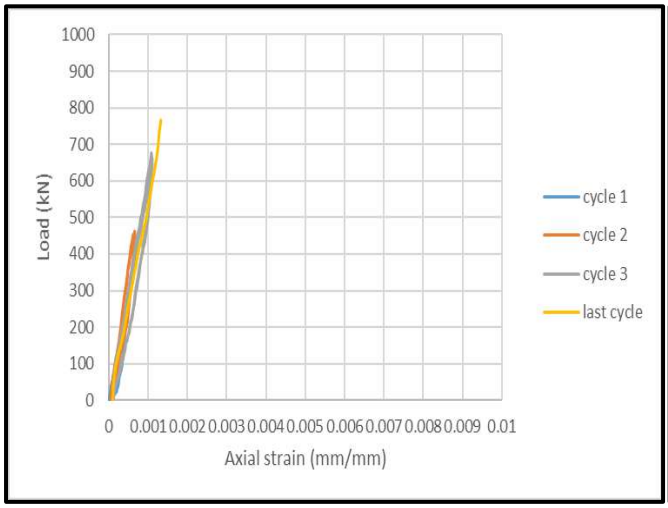

Figure (4-74) mid strain no. (2) of the specimen (SHS2)

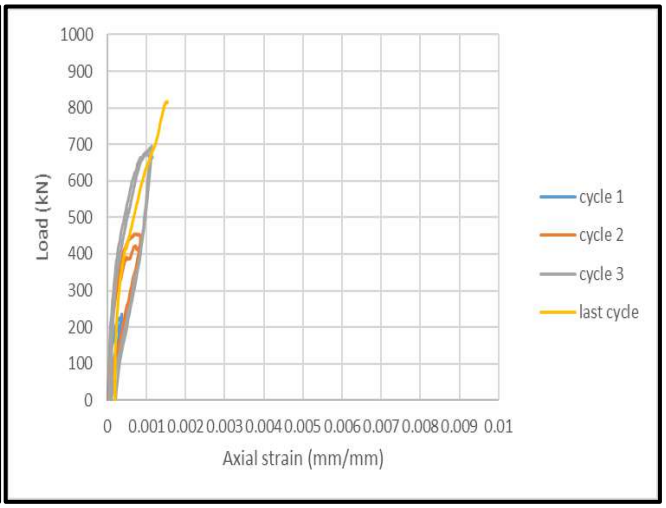

Figure (4-75) mid strain no. (2) of the specimen (SHS3)

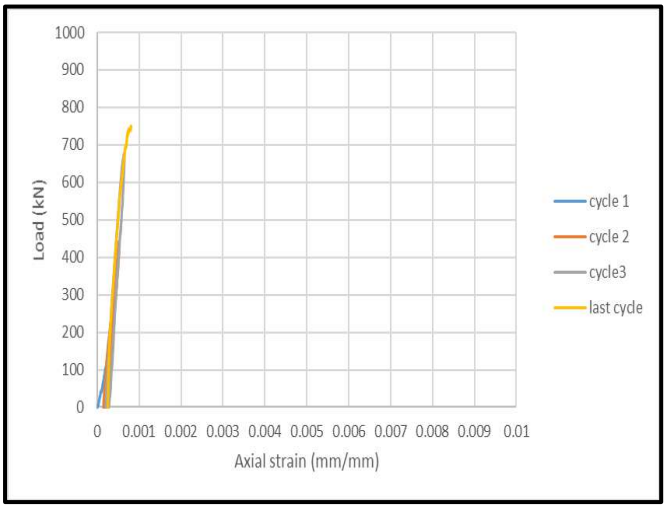

Figure (4-76) mid strain no. (4) of the specimen (SHS2)

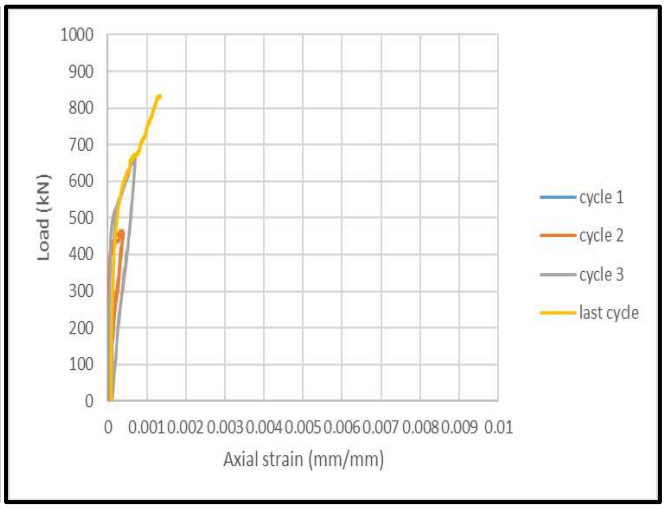

Figure (4-77) mid strain no. (4) of the specimen (SHS3)

Steel strain gauges readings curves for columns(SHS2),and (SHS4) are drawn in Figures (4-78) to (4-85),which deals with the difference in longitudinal tensile strain of the samples containing global ratio (L/B(D)) equal 80 and 70. Due to slenderness effect, the column of L/B = 70 reached a strain of about 2019 μƐ,and 2297 at the top of the column for points (1&3) respectively, while specimens with L/D =80 (SHS2), presented axial strain with magnitude 5949 μƐ and, greater than specimens (SHS4) in the strain number (3).Whereas the other strain (1) of specimen (SHS2) had lower value than position (1) for (SHS4) and was 1752 μƐ. On the other hand, the maximum strain in the mid height of the column (SHS4) had values smaller than this developed in the upper part. The strain reached for (2&4) points was approximately 1700 and 1713 μƐ respectively, as well as greater than the values of strain in column (SHS2) for the same point (1317, 803) μƐ. This increase was due to the large ultimate load when the length of column was shorted and failure mode appeared local buckling in this region. All strain gauges placed to measure axial strain obtained values higher than 1713 μƐ (yield strain) at the peak load of sample (SHS4). This indicate the beginning of the local buckling process for the short columns. All recorded value for strain when L/D=70 did not reach yielded in three cycle first.

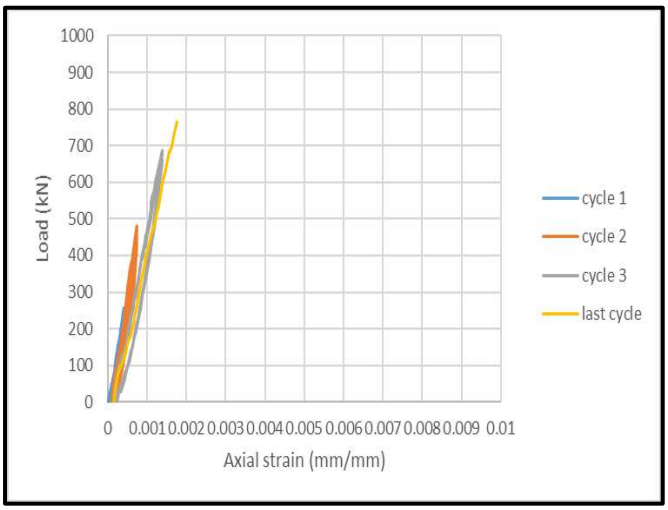

Figure (4-78) top strain no. (1) of the specimen (SHS2)

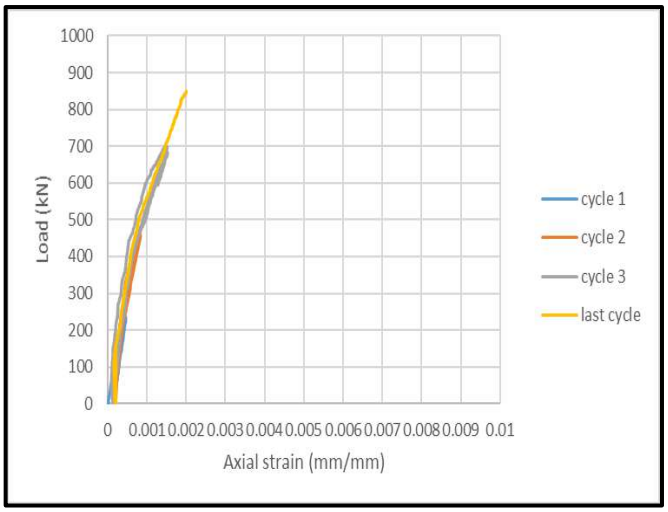

Figure (4-79) top strain no. (1) of the specimen (SHS4)

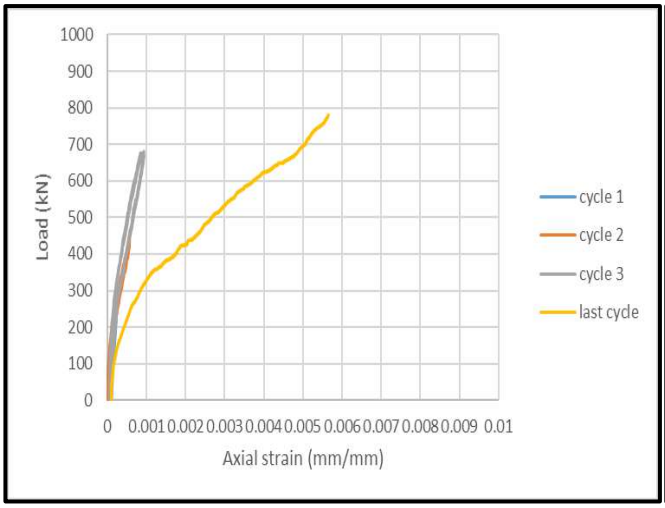

Figure (4-80) top strain no. (3) of the specimen (SHS2)

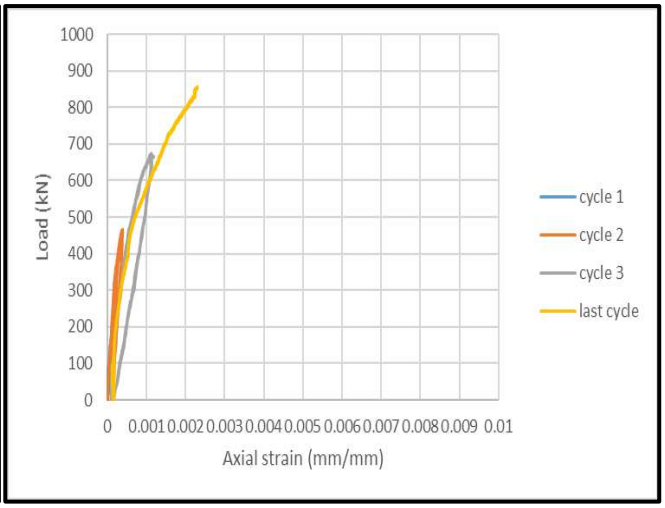

Figure (4-81) top strain no. (3) of the specimen (SHS4)

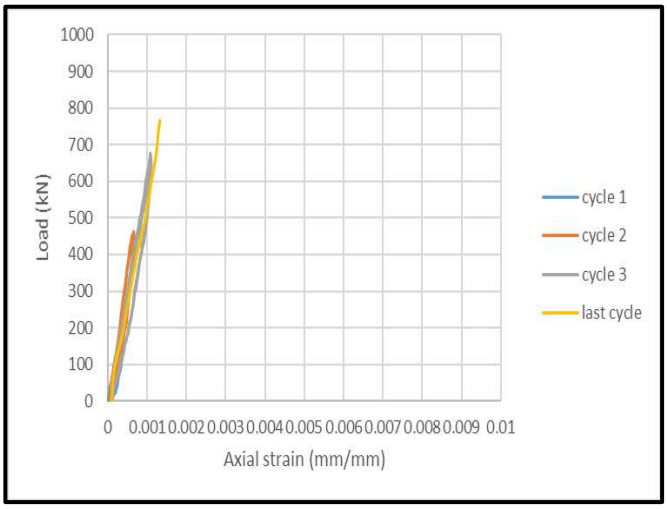

Figure (4-82) mid strain no. (2) of the specimen (SHS2)

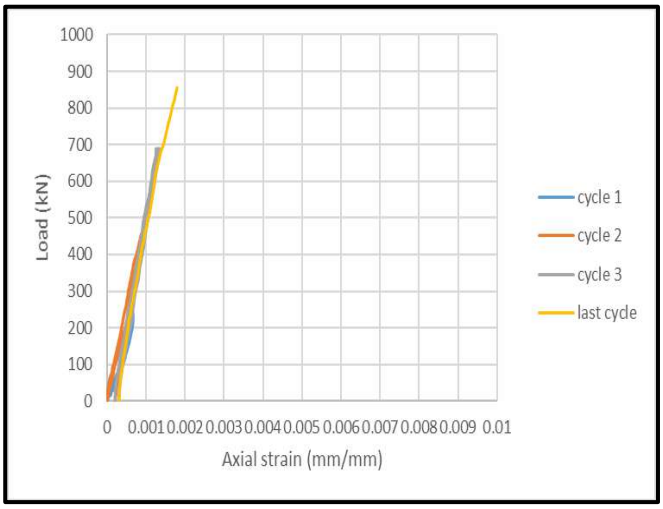

Figure (4-83) mid strain no. (2) of the specimen (SHS4)

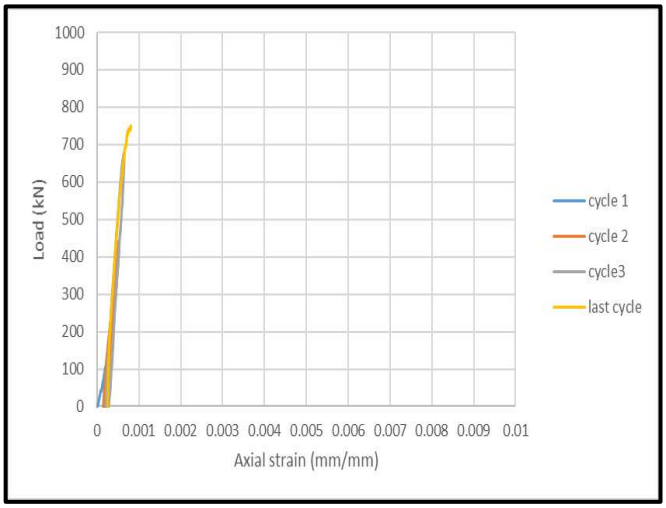

Figure (4-84) mid strain no. (4) of the specimen (SHS2)

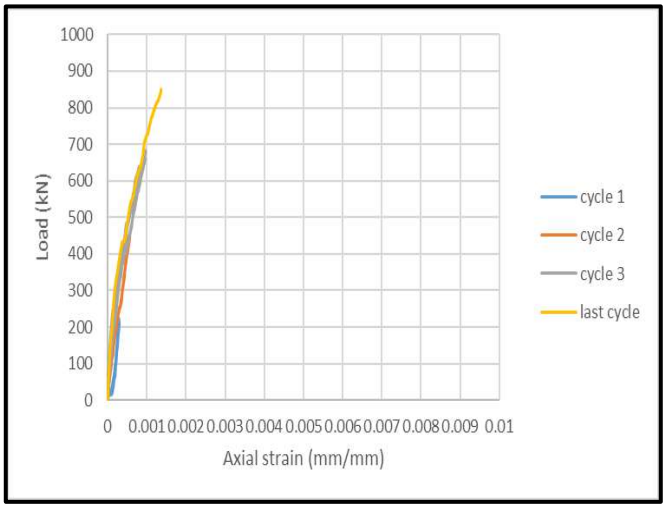

Figure (4-85) mid strain no. (4) of the specimen (SHS4)

Figures No. (4-86) to (4-93) show the strain readings for steel strain in the upper and lower positions for six cycles and the last cycle for column (SHS5). It was found by increasing of the loads, and due to the presence of shear connectors which forced the steel tube and the concrete core to interact and deform as one unit. The measured longitudinal strains at peak load (888kN) for sample (SHS5) were 4805 με and 2170 με for points (1&3), while the strain values for the sample (SHS5) in the upper part (1&3) were more than values of the strain in the middle height (2 & 4) was 1900 and 1754 με respectively. But one of the two top strain gauges for sample (SHS5) was small than the maximum strain in sample (SHS2) 5949με. when the shear connectors are used and larger spacing of shear

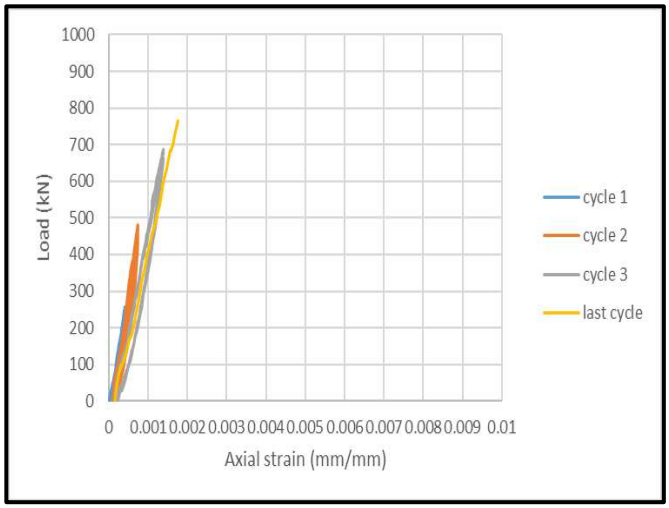

Figure (4-86) top strain no. (1) of the specimen (SHS2)

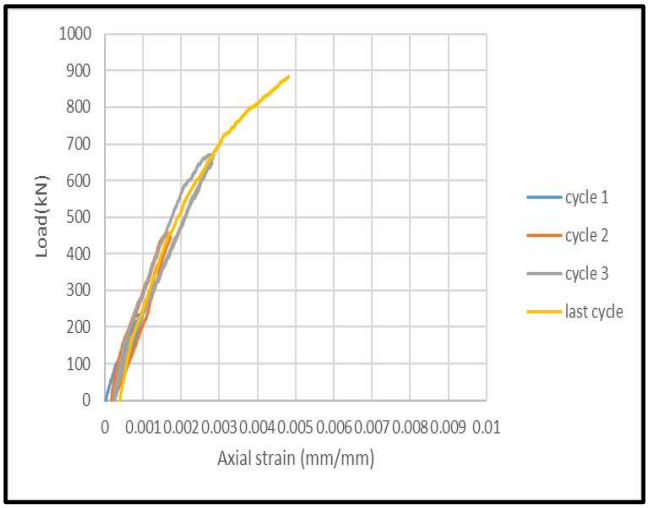

Figure (4-87) top strain no. (1) of the specimen (SHS5)

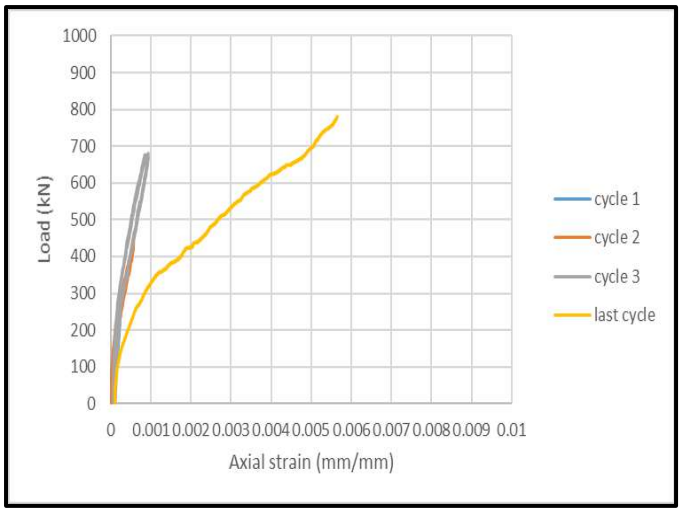

Figure (4-88) top strain no. (3) of the specimen (SHS2)

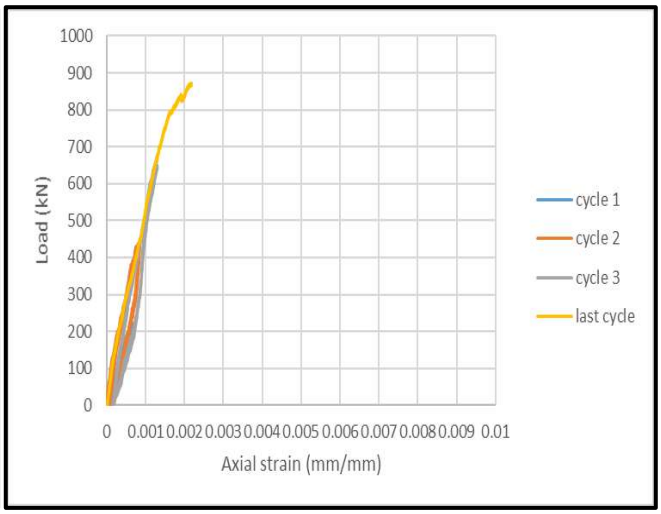

Figure (4-89) top strain no. (3) of the specimen (SHS5)

connectors not preventing progresses of hoop strains on the contrary from circular section. All the longitudinal strains in specimen (SHS5) when compare with (SHS2) were more and record yield value during the third cycle in point (1&3). The longitudinal deformation and strain gauge value were both increased as a result of this peak load.

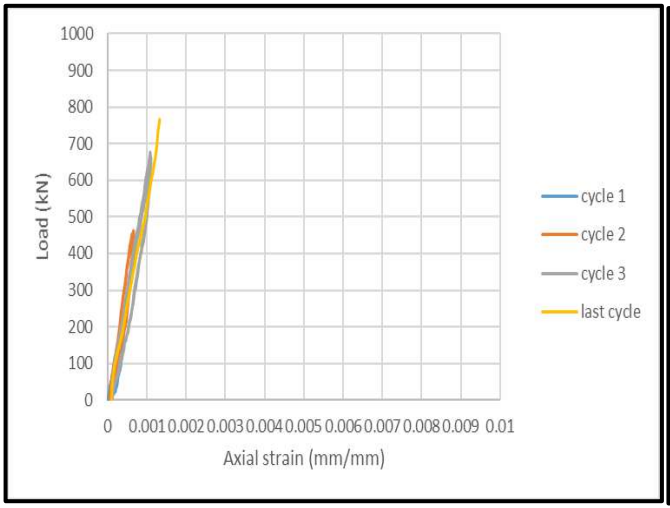

Figure (4-90) mid strain no. (2) of the specimen (SHS2)

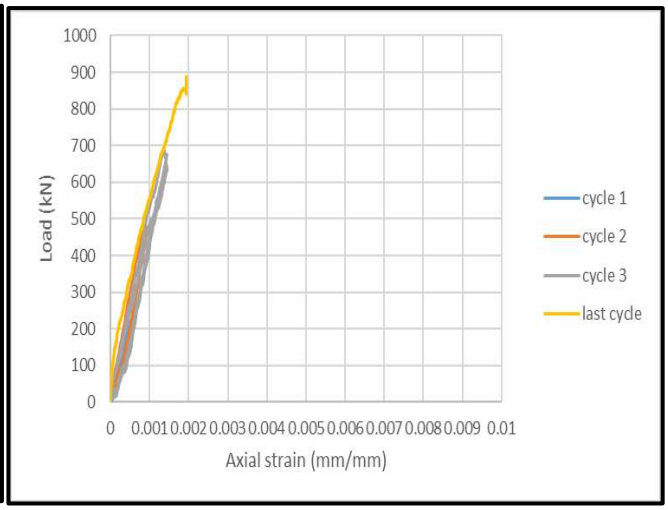

Figure (4-91) mid strain no. (2) of the specimen (SHS5)

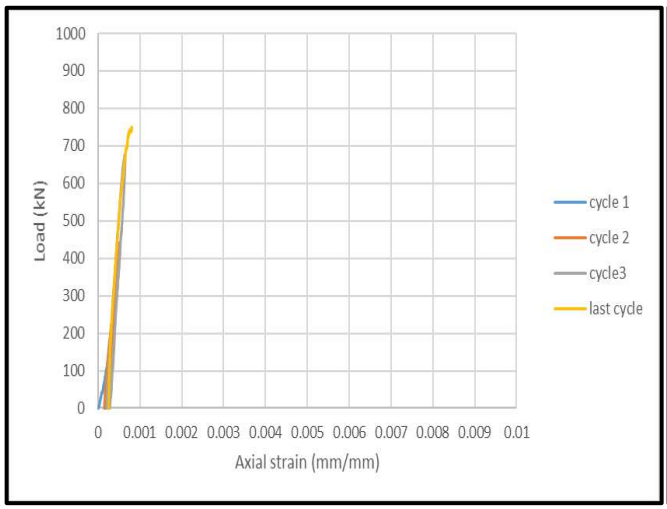

Figure (4-92) mid strain no. (4) of the specimen (SHS2)

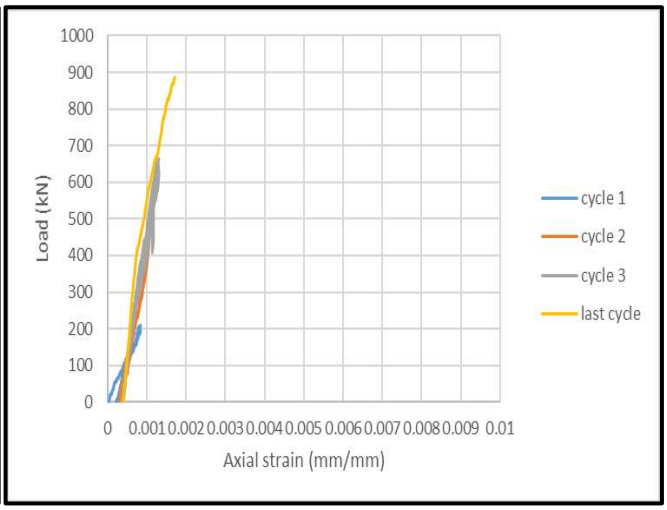

Figure (4-93) mid strain no. (4) of the specimen (SHS5)

Also studied the behavior of tensile strain curve when compressive strength 90.32 Mpa and 30.83 Mpa .Through Figures (4-94) to (4-101),it was noticed the normal concrete (SHS6)strains at site (1 & 3) were 1588,and 2588με respectively, and

they were more than recorded values at sites (2 & 4),which was reached 1000 and 400 με respectively. All strain for sample (SHS6) was not recorded any value greater than ultimate strain for specimen (SHS2) during the three cycle first of loading until reaching ultimate strain. The top strain value for (SHS6) was jumped and become greater than this occurred in the middle sites (2&4) due to sudden buckle. It was concluded that the effects of the bond between the concrete and the steel tube was more critical for high-strength concrete.For normal strength concrete, the reduction on the axial capacity due to the loss of bonding between steel and concrete was very small. The strain gauge in site (4) for normal concrete specimen had failed in the first cycle of loading (225kN).

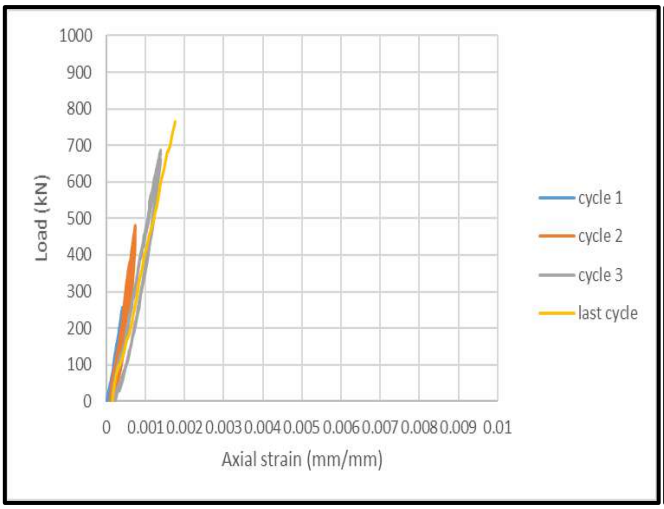

Figure (4-94) top strain no. (1) of the specimen (SHS2)

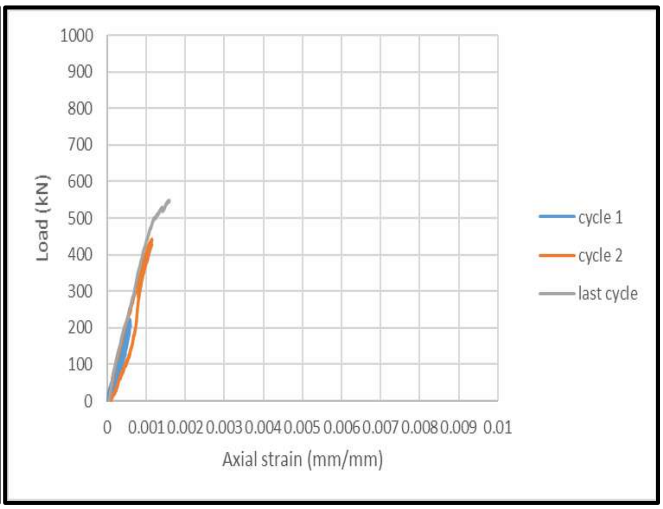

Figure (4-95) top strain no. (1) of the specimen (SHS6)

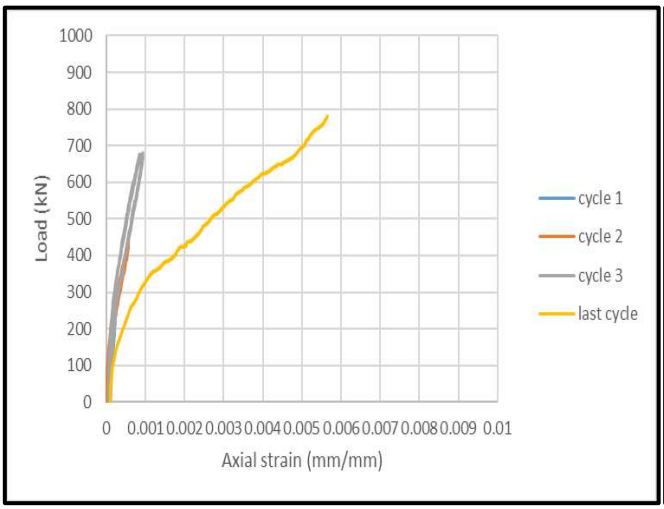

Figure (4-96) top strain no. (3) of the specimen (SHS2)

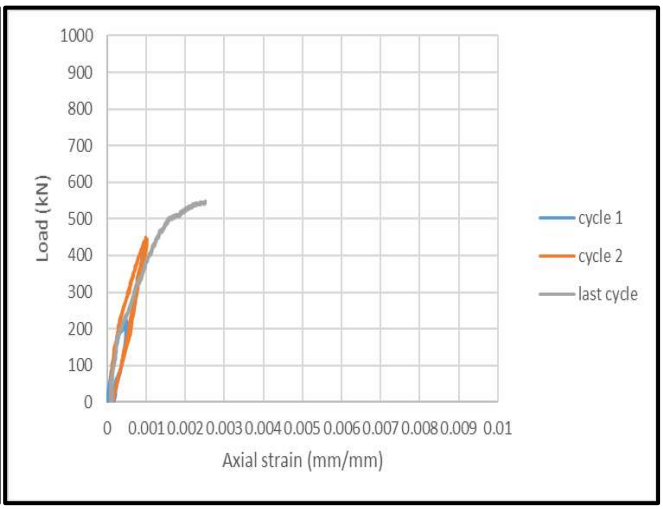

Figure (4-97) top strain no. (3) of the specimen (SHS6)

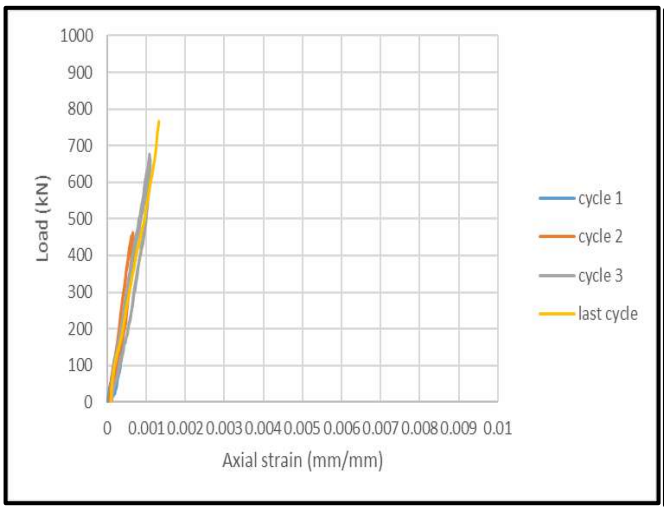

Figure (4-98) mid strain no. (2) of the specimen (SHS2)

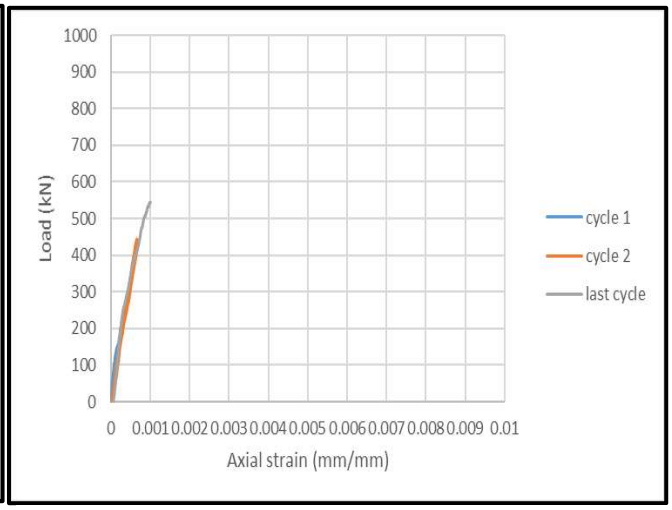

Figure (4-99) mid strain no. (2) of the specimen (SHS6)

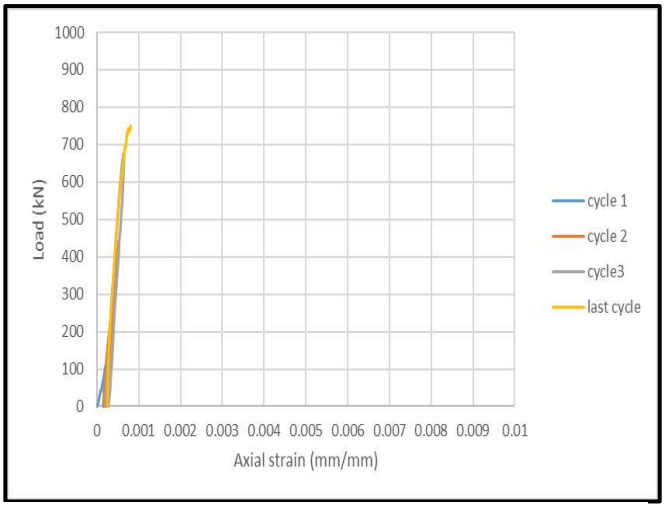

Figure (4-100) mid strain no. (4) of the specimen (SHS2)

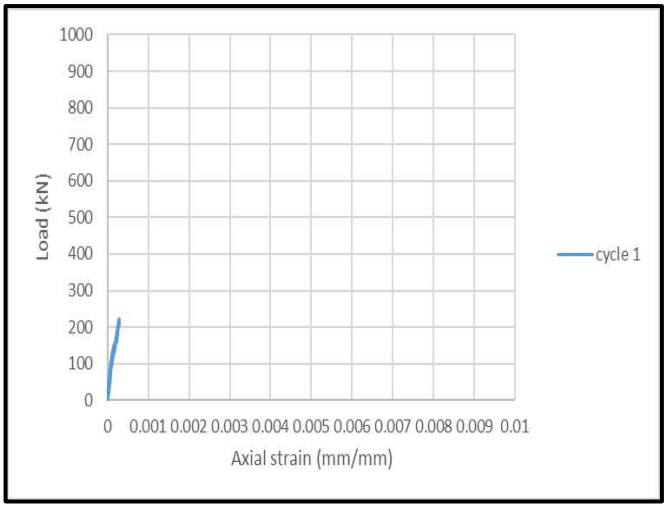

Figure (4-101) mid strain no. (4) of the specimen (SHS6)

And, also the Figures (4-102) to (4-109) described the axial load of the sample (SHS7) were less compared to the section filled with concrete. The sample (SHS7) failed in the second cycle of loading at the ultimate load 320 kN. Also, the strain was very high because the concrete was reducing the axial shortening and restricting the steel tube compare with specimen (SHS2).The sample had strain at position (1 & 3) were 2592, 1678με respectively, while the mid height location (2 & 4) was reached values 1122, 1601 με respectively at the value of the maximum load. But the Hoop tension strain values measured in (SHS7) are higher compared to the specimen (SHS2) in position (1&4) due to steel tube expands in the radial direction during the compressive loads in its longitudinal

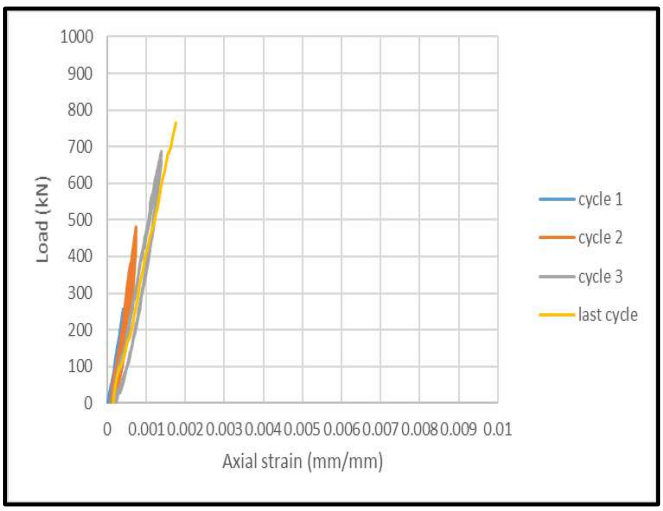

Figure (4-102) top strain no. (1) of the specimen (SHS2)

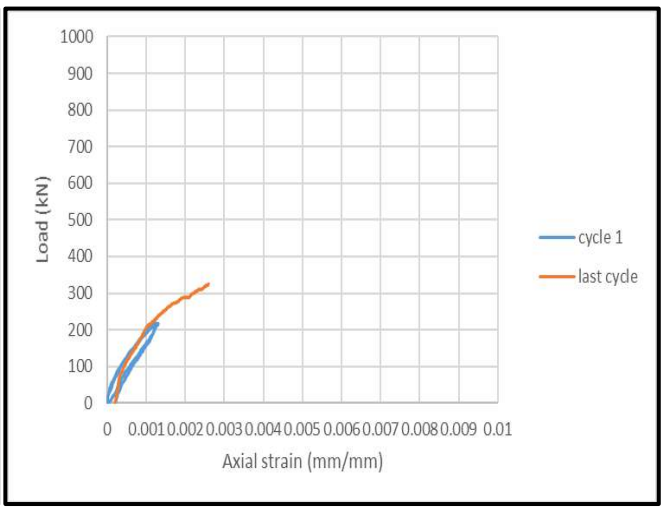

Figure (4-103) top strain no. (1) of the specimen (SHS7)

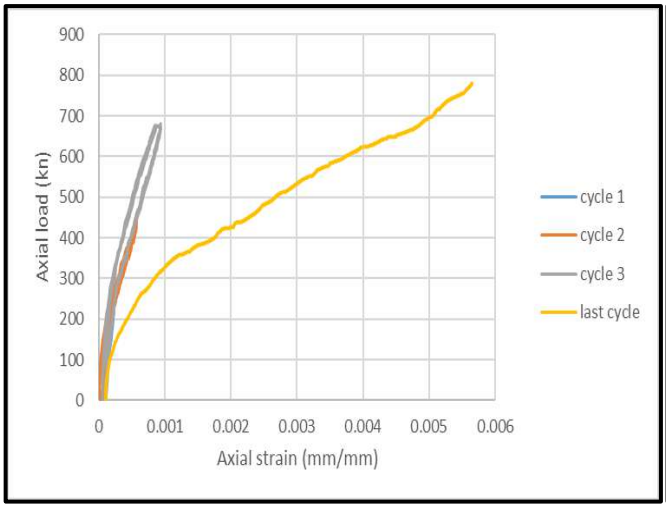

Figure (4-104) top strain no. (3) of the specimen (SHS2)

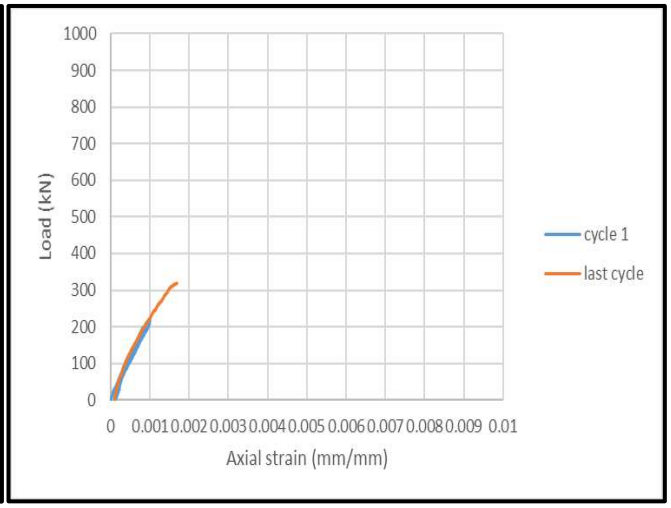

Figure (4-105) top strain no. (3) of the specimen (SHS7)

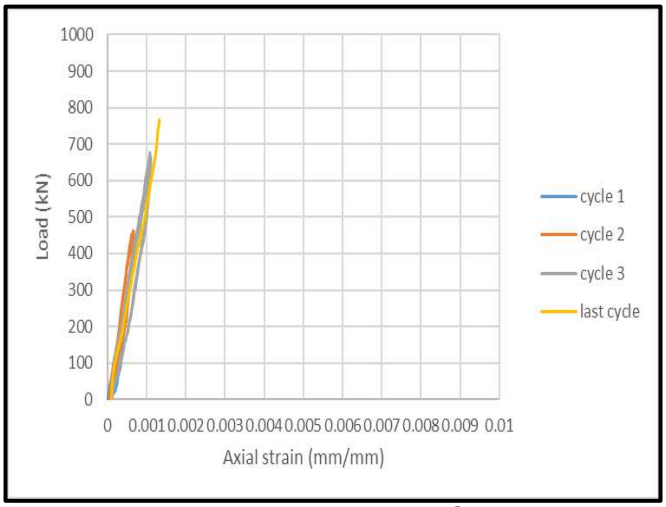

Figure (4-106) mid strain no. (2) of the specimen (SHS2)

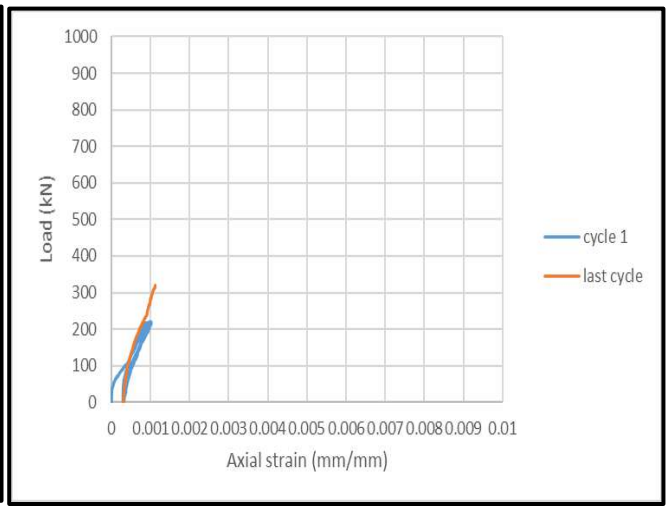

Figure (4-107) mid strain no. (2) of the specimen (SHS7)

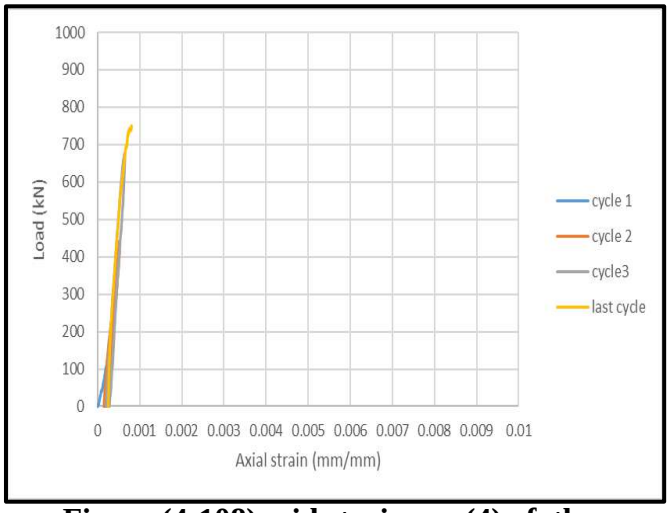

Figure (4-108) mid strain no. (4) of the specimen (SHS2)

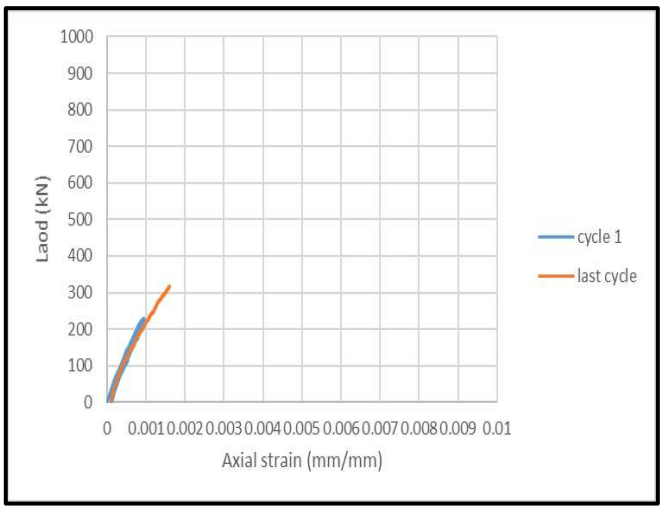

Figure (4-109) mid strain no. (4) of the specimen (SHS7)

4.6 Strength index (SI)

strength index (SI) defined by (Hussein, and Talha) [100] (2019) is the ratio between the theoretical cross-sectional capacity and the actual ultimate load. It helps to measure the synergy existing between the two components (steel tube and concrete core) of the CFST column. It was calculated for each column by means of:

Strength index (SI) = p_u / p_o ……. (4.3)

Where:

p_u = Ultimate load of the tested column.

p_o = As fy + 0.85f′cAc ……. (4.4)

Table (4.5) presents Strength index (SI) of test columns. This table also shows the effects of concrete compressive strength (f′c), cross-sectional concrete area and global slenderness ratio (L/B(D)) on the strength index (SI) of the CFDST columns.

Table (4.5) Strength index (SI) of test columns.

Specimen	fc′ (Mpa)	(L/B)	Area of concrete	P(exp)	P(th)	(SI)Pexp/Pth	Ratio of difference (%)
CHS1	**73.3**	**8**	5211	**800**	**592**	**1.35**	–
CHS2	**90.32**	**8**	5211	**835**	**672**	**1.24**	**-11%**
CHS3	**90.32**	**8**	4675	**775**	**669**	**1.15**	**-9%**
CHS4	**90.32**	**7**	5211	**900**	**672**	**1.33**	**+ 9%**
CHS5	**90.32**	**8**	5211	**910**	**672**	**1.35**	**+11%**
CHS6	**30.83**	**8**	5211	**580**	**457**	**1.26**	**+2%**
CHS7	**Not fill**	**8**	-	**300**	**346**	**0.86**	**-38%**
SHS1	**73.3**	**8**	6639	**750**	**754**	**0.99**	–
SHS2	**90.32**	**8**	6639	**775**	**856**	**0.90**	**-9%**

SHS3	**90.32**	**80**	**7176**	**815**	**858**	**0.94**	**+4%**
SHS4	**90.32**	**70**	6639	**850**	**856**	**0.99**	**+9%**
SHS5	**90.32**	**80**	6639	**888**	**856**	**1.03**	**+13%**
SHS6	**30.83**	**80**	6639	**540**	**582**	**0.92**	**+2%**
SHS7	**Not fill**	**80**	**-**	**340**	**441**	**0.77**	**-13%**

*** First ratio of difference in table = ratio of difference (CHS2,SHS2)-ratio of difference (CHS1,SHS1)**

***Rest ratio of difference in table = ratio of difference (CHS3,SHS3)-ratio of difference (CHS2,SHS2)**

4.6.1 Effect of concrete compressive strength (fc′)

As shown in Figure (4.110), SI decreases by 11% and 9% for circular and square column respectively when the concrete compressive strength increases from 73.3 MPa to 90.32 MPa. This may be attributed to the fact that the confining effect by the steel tube for higher strength concrete filled tube columns is much less than the medium or low strength concrete ones. When the concrete compressive strength is increased from 73.3 MPa to 90.32 MPa, the strength index (SI) is found to be reduced from 1.35 to 1.24 for circular and 0.99 to 0.90 for square column respectively.

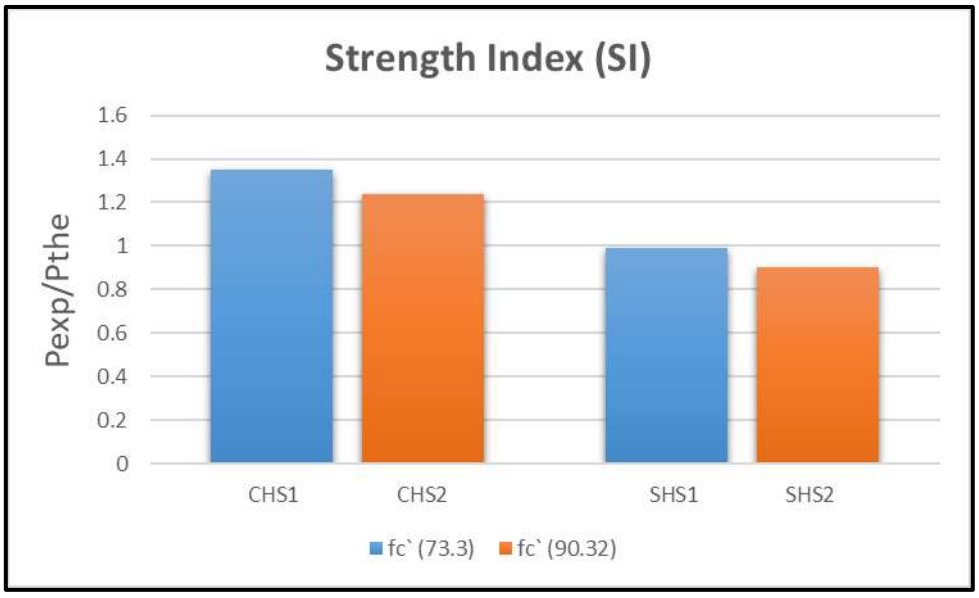

Figure (4-110) strength index for differnt compreesive strength

4.6.2 Effect of shape of the inner tube

In the following Figure (4-111), SI decreases by 9% when the inner concrete area of the circular section was reduced from 5211 mm to 4675 mm after replaced the inner tube by a square section, as well as SI increases by 4% when the area increased from 6639 mm to 7176 mm for square section when replaced the inner tube of the sample by a circular section. This is belong to the larger area of concrete bear higher pressure loading .

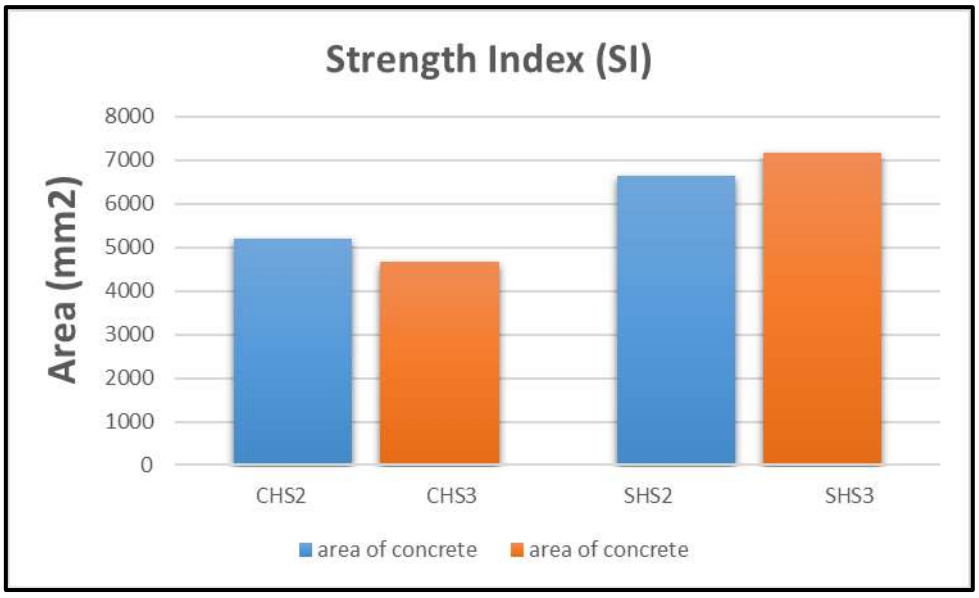

Figure (4.111) strength index for differnt concrete area

4.6.3 Effect of global slenderness ratio (L/B(D))

The strength index (SI) of the columns were determined by varying the column slenderness ratio ranging from 70 to 80 and the results are presented in figure (4.112) The figure indicates that the column slenderness has a pronounced effect on the ultimate axial strengths of CFDST columns. The strength index (SI) is significantly increased by 9% for circular and square column by decreasing the column slenderness ratio from 80 to 70. This is because of the fact that the columns having higher overall slenderness ratio, buckle much earlier before gaining its full capacity.

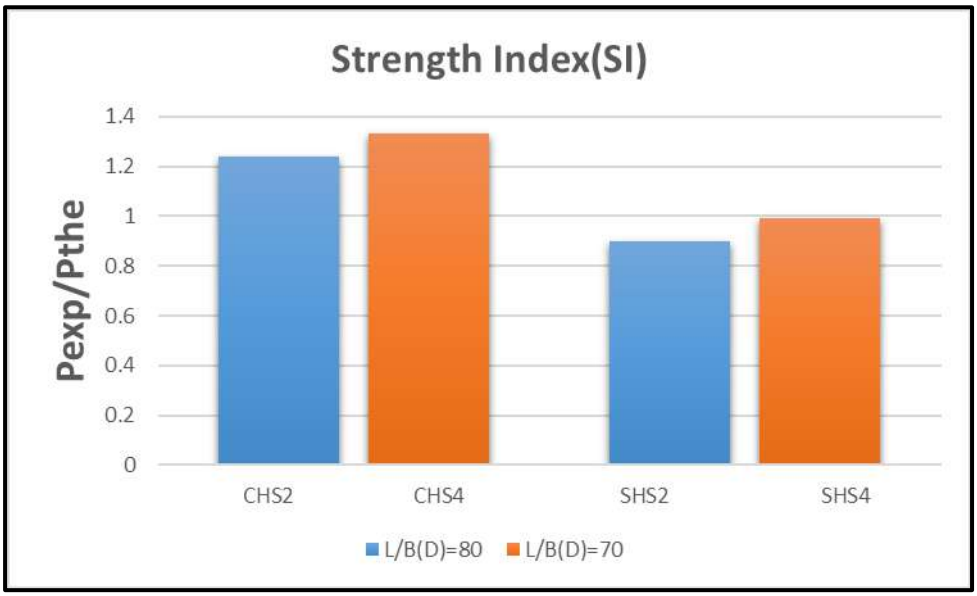

Figure (4.112) strength index for differnt L/B (D)

4.7 Ductility Factor

Ductility is a mechanical property of materials which indicates the degree of plastic deformation, which consider one of the efficient properties of each material.Concrete is non homogenous material, so calculate the ductility index to evaluate this property of the concrete. Furthermore, ductility index can be defined as the ratio of the total displacement of RPC column to displacement up to 80 % of the failure load each column (Jain et al., (2017) as shown in Figure (4-113). This property without units of dimensions μ, as shown in Equation (4-5) proposed by (Jain et al., (2017) [101]

$$\mu = \frac{\Delta \mathbf{u}}{\Delta \mathbf{y}} \qquad \ldots\ldots\ldots\ldots\ldots\ldots\ldots\ldots\ldots\ldots\ldots\ldots\ldots\ldots\ldots\ldots \text{(4-5)}$$

Which

Δu : the displacement at peak load

Δ y : the yield displacement at 0.8 of ultimate load

which is the most feasible evaluation of Δy and Δu. All results are described in Table (4-6).

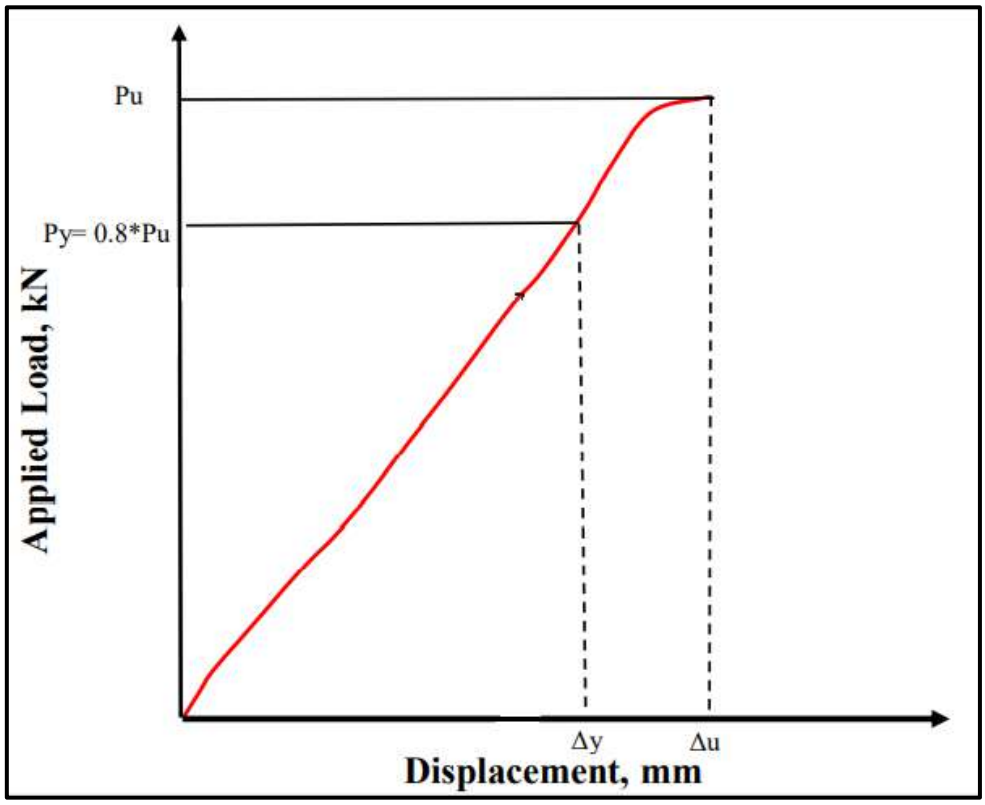

Figure (4-113) Ductility index produced by Jain [101]

Table (4-6) ductility factor of specimen

Specimen		According to Jain (2017) Approach			
		Pu (exp)	Δu	Δy	Ductility(μ)
Groupe one	**CHS1**	800	8.6	5.6	1.53
	CHS2	835	11.7	8.3	1.40
	CHS3	775	6.2	4.3	1.44

	CHS4	900	10.7	8.6	1.24
	CHS5	910	10.4	7.8	1.33
	CHS6	580	24.1	13	1.85
	CHS7	300	7.9	4.5	1.75
Groupe two	**SHS1**	750	5.9	4.8	1.22
	SHS2	775	8	4.7	1.7
	SHS3	815	8	5.2	1.53
	SHS4	850	8.7	6.8	1.27
	SHS5	888	9	6.6	1.36
	SHS6	540	19	11	1.72
	SHS7	340	12	7.7	1.55

Through previous research to measure ductility index for all laboratory columns, it was found that this indicator is important for the stage after the yield of endurance. Through the calculations, it was found that for samples circular filled with reactive powder concrete, the ductility was decreased rapidly with the increase in the axial force ratio of reference (CHS2) when compare with (CHS1),and (CHS3).Whereas the index ductility was change from (1.53 to 1.40) for (CHS1) and (CHS2),respectively and from (1.44 to 1.4) for (CHS3) and (CHS2).As well as for (CHS4) and (CHS5) specimen when compare with (CHS2) sample .The reason for this is that in the case of increasing the endurance of the column, a sudden crushing in the concrete happened that leads to an unexpected failure at any point of loading, except the normal concrete filled tube (CHS6) and the empty tube (CHS7) exposed to loading, the value of the ductility index was 1.85 and 1.75 respectively for circular columns due to softening the normal concrete mixture and steel tube . Also, as the case with square sections, the values

of ductility index were approximately greater than in circular section which indicates ductile best performance for square section. In general, the greater the bearing strength of the composite columns, the less the amount of ductility index, especially in high-strength concrete filling steel pipes.

4.8 Comparative Study with Practical Results

There are many equations that have been proposed over the years to predict the axial capacitance of composite columns. For example, there are those who take an increase in the resistance of concrete, unlike those who ignore this form of increase. Conceptually, the American Concrete Institute (ACI 2014) [102] uses concrete that is reinforced without any significance to the effects of confined concrete. Whereas the American Institute of Steel (AISC) [103] Structures directly relies on structural steel. But the combination of these two concepts for designing composite structures was taken into consideration in the European Code Eurocode-4 [104]. In this study, the aforementioned design criteria were applied to find out the final capacity of the laboratory samples. After that, the expected final capacity was compared with the practical results, where the expected values calculated by the standards give a different prediction about the final strength of the column. In the design calculations, the safety factors were suggested and also for determine the experimental process errors the practical results were divided with the expected capacities of the columns. All formula of designs described in Appendix (B). The fourteen experimental tests with standard codes are given in Table (4-7) and (4-8).

For circular section the AISC code was the most conservative, while Eurocode 4 and ACI presented values approaching to the experimental results with error range from lower than the experimental results. The Eurocode 4 and ACI was gave values approximately equal, the sectional capacity is about 3-24 % lower than the experimental results for Eurocode, while reach about 13-26% in ACI code as shown in Table (4-7). As well as the sectional capacity is about 14-26%

lower than the experimental results for AISC code. But the steel empty testing appears unconservative than experimental value by 9.3% and as well as reach 0.6 and 15.3% for Eurocode 4 and ACI respectively.

Table (4-7) Code calculation results of circular column

Sample	Pu (exp)	Pu AISC	Ratio of difference (%)	Pu EC4	Ratio of difference (%)	Pu (ACI)	Ratio of difference (%)
CHS1	800	588	26.5	615	23.1	592	26
CHS2	835	669	19.8	684	18	672	19.5
CHS3	775	663	14.4	751	3	669	13.6
CHS4	900	679	24.5	706	21.5	672	25.3
CHS5	910	669	26.4	684	24.8	672	26.1
CHS6	580	448	22.7	462	20.3	457	21.2
CHS7	300	328	9.3	302	0.6	346	15.3

For square section the AISC code was the most unconservative ,with Eurocode 4 and ACI which presented values approaching to the experimental results with small error range for the square column with more than the experimental results in most column. The Eurocode 4 and ASIC were giving values approximately equal, the sectional capacity is about 2-14 % than the experimental results for Eurocode, while reach about 0.11-22% in ACI code. In general, the codes unsafe, particularly for square columns as shown in Table (4-7).As well as The sectional capacity is about 0.36-53% difference than the experimental results for AISC code

Table (4-8) Code calculation results of square column

Sample	Pu (exp)	Pu AISC	Ratio of error (%)	Pu EC4	Ratio of error (%)	Pu (ACI)	Ratio of error (%)
SHS1	750	724	34.6	793	5.4	754	0.53
SHS2	775	819	53.7	910	14.8	856	9.4
SHS3	815	818	0.36	919	11.3	858	5
SHS4	850	828	2.5	929	8.5	856	0.11
SHS5	888	819	7.7	910	2.4	856	3.6
SHS6	540	561	3.7	607	11	582	7.2
SHS7	340	424	24.7	370	8.1	441	22.9

To be specific, the maximum safe error for the modified AISC 360 design method is 1.36, and the maximum safe error for the ACI design method is 1.35. Lastly, Eurocode 4 formulae exhibits a maximum safe error of 1.33 for circular, which is smaller than the modified AISC 360 design method and the ACI design method. Moreover, the average Pu(exp)/Pu (EC4) value of (EC4) formulae is 0.97, and 1.08,1.03 for AISC and ACI respectively which is quite close to 1.00 during the three design methods for square column .This also indicates that the above three design methods (AISC-360, Eurocode 4, and ACI formulae) are quite appropriate for predicting the ultimate strength of CFSDT short columns with double circular steel tubes compared with those with double square steel tubes.

CHAPTER FIVE

CHAPTER FIVE

CONCLUSIONS AND RECOMMENDATIONS

6.1 Introduction

The experimental investigations of the effect of reactive powder concrete in double skin tabular columns subjected to variable repeated loading are presented. The experimental program consisted of manufacturing and testing twelve double skin columns filled with concrete and two without concrete divided into three groups. The first group was filled with reactive concrete, second group filled with normal concrete and third group not was filled. All columns had dimensions of 100mm width(diameter), and 800mm in length. The present study revealed several important points in the philosophy of composite columns. Based on the experimental results of the double skin column, the main points have been concluded as follows:

6.2 Conclusions

As previous results was concluded:

1-The typical failure mode of the all specimens was characterized by local buckling of the steel tube and crushing of concrete. while the failure of the specimens of circular sections filled with normal concrete exhibited global buckling. Specimens with square cross section showed more pronounced outward buckling.

2-The ultimate strength of the composite columns filled reactive powder concrete (RPC) of 1.5% and 0.5% steel fiber show an increase of 42.24% and 37.39% respectively compared with columns filled normal concrete (NC).This great difference means that the high strength concrete is effective for increasing the

bearing capacity of such composite column. RPC filled steel tubular columns can achieve ultra-high compression capacities, but their post peak load behavior is quite brittle

3- The ultimate capacity of the tested columns decreased with the decrease of concrete core area, and L/B ratio of the specimen whilst they increased with the increase of concrete compressive strength.

4- The welded shear bolts improved the bearing capacity of the columns significantly and clearly, as the strength increased by 8.98 % and 14.58% for the circular and square sections respectively compared with these without shear connectors.

5-The external confinement with steel tube can provide sufficient lateral support to the concrete core and significantly increase the strength of the specimens under axial loading. The experimental results clearly demonstrate that steel can enhance the structural performance of concrete columns under axial loading.

6- The longitudinal strain was uniform along the length and was high near the failure region and decreased gradually far from the failure region.

7-In general, the circular tubes filled with high strength concrete give higher bearing than square sections under the same engineering properties and loading conditions.

8- Repeated loading/unloading cycles have a cumulative effect on the permanent strain and stress deterioration.

9- The failure mode of the outer SHS was similar to that observed for SHS fully filled with concrete. The failure mode for the inner CHS was found different from that for empty CHS.

6.3 Recommendation for Future Studies

1. Study the effects of other types of shear connectors (such as angle, plates … etc.) on the behavior of the composite CFDST column with reinforced bar.

2-A comparison between CFDST columns and RC columns, showing the advantages and disadvantages of both (including construction costs).

3- Further testing is recommended on concrete filled double skin column with high slenderness ratio under repeated loads.

4-Strengthen the specimens' ends with FRP jackets may change the failure in the top height region of the samples.

REFERENCE

Reference

[1]Tao, Z., L.-H. Han, and X.-L.J.J.o.C.s.r. Zhao, *Behaviour of concrete-filled double skin (CHS inner and CHS outer) steel tubular stub columns and beam-columns.* 2004. **60**(8): p. 1129-1158.

[2]Tao, Z. and L.-H.J.J.o.C.S.R. Han, *Behaviour of concrete-filled double skin rectangular steel tubular beam–columns.* 2006. **62**(7): p. 631-646.

[3]Han, L.-H., W. Li, and R.J.J.o.C.S.R. Bjorhovde, *Developments and advanced applications of concrete-filled steel tubular (CFST) structures: Members.* 2014. **100**: p. 211-228

[4] F. M. Ren, Y. W. Liang, J. C. M. Ho, and M. H. Lai, "Behavior of FRP tube-concrete-encased steel composite columns," Compos. Struct., vol. 241, 2020, doi: 10.1016/j.compstruct.2020.112139.

[5] R. Cosenza, E., and Zandonini, "'Composite Construction,'" Struct. Eng. Handbook, CRC Press LLC, 1999.

[6] M. M.-A. K. Mohi-Aldeen, "Nonlinear finite element analysis of plane frame composed of composite members," Univ. Babylon/college Eng. Dep., 2008.

[7] C. C. and L. NJ., "Analytical model for predicting axial capacity and behavior of concrete encased steel composite stub columns.," J. Constr. Steel, vol. 62(5), pp. 424–433, 2006.

[8] E. E. and Y. B., "Numerical simulation of concrete encased steel composite columns.," J. Constr. Steel Res., vol. 67(2), pp. 211–222, 2011.

[9] E.-T. S. and D. GG, "Strength and Ductility of Concrete Encased Composite Columns.," J. Struct. Eng., vol. 125(9), pp. 1009–1019, 1999.

[10] M. Hüsem, M. M. Nasery, F. Y. Okur, and A. C. Altunişik, "Experimental evaluation of damage effect on dynamic characteristics of concrete encased composite column-beam connections," Eng. Fail. Anal., vol. 91, no. April, pp. 129–150, 2018, doi: 10.1016/j.engfailanal.2018.04.030.

[11] M. M.-A. K. Mohi-Aldeen, "Nonlinear finite element analysis of plane frame composed of composite members," Univ. Babylon/college Eng. Dep., 2008.

[12] B. Ștefan-Marius and C.-G. CHIOREAN, "ADVANCED ANALYSIS OF STEEL–CONCRETE COMPOSITE STRUCTURES."

[13] B. S. Prickett and R. G. Driver, "Behaviour of partially encased composite columns made with high performance concrete," Struct. Eng. Rep., no. 262, pp. 1–235, 2006.

[14] T. Sheehan, X. H. Dai, T. M. Chan, and D. Lam, "Structural response of concrete-filled elliptical steel hollow sections under eccentric compression," Eng. Struct., vol. 45, pp. 314–323, 2012, doi: 10.1016/j.engstruct.2012.06.040.

[15] J. A. Packer, "Concrete-Filled Double-Skin Tubes," pp. 1–5, 2010.

[16] Zhao, X.-L., L.-H. Han, and H. Lu, Concrete-filled tubular members and connections. 2010: CRC Press

[17] Han, L.-H., et al., Concrete-filled double skin steel tubular (CFDST) beam–columns subjected to cyclic bending. 2006. 28(12): p. 1698-1714 .

[18] Ebrahim, F.B., Comparative investigation into the behavior of concrete filled steel tubular CFT columns concrete filled double skin steel tubular CFDST columns steel reinforced concrete filled steel tubular columns SR CFT. 2016 .

[19] Schneider, S.P. and Y.M.J.J.o.C.S.R. Alostaz, Experimental behavior of connections to concrete-filled steel tubes. 1998. 45(3): p. 321-352.

[20] Ricles, J., S .Peng, and L.J.J.o.S.E. Lu, Seismic behavior of composite concrete filled steel tube column-wide flange beam moment connections. 2004. 130(2): p. 223-232 .

[21] Ferguson, P.M.; Breen, J.E. and Jirsa, J.O., Reinforced Concrete Fundamentals, Fourth Edition, John Wiley and Sons, New York, 1981, pp. 694.

[22] ACI Committee. (2014). Building Code Requirements for Structure Concrete and Commentary ACI 318M. American Concrete Institute, Michigan

[23] BIS, I. (2000). 456: 2000, Plain and reinforced concrete code of practice ‖ Bureau of Indian Standards. Fourth revision.

[24] Module 10 Compression Members (2010). Short Compression Members under Axial Load with Uniaxial Bending. Lesson 23, Version 2 CE IIT, Kharagpur.

[25] Chaallal, O.; Shahawy, M. and Hassan, M.," Performance of Axially Loaded Short Rectangular Columns Strengthened with Carbon Fiber-Reinforced Polymer Wrapping" (ASCE) Journal of Composites for Construction, Vol. 7, No. 3, August 2003, pp. 200-208.

[26] Pessiki, S.; Harries, K.A.; Kestener, J.T; Sause, R., and Ricles, J.M., "Axial Behavior of Reinforced Concrete Columns Confined with FRP Jackets", (ASCE) Journal of Composite for Construction, Vol.5, No.4, November 2001, pp.237- 245.

[27]. Hajjar, J.F.J.P.i.S.E. and Materials, Concrete-filled steel tube columns under earthquake loads :)1 (2 .2000 .p. 72-81 .

[28] Rodera García, A., Design of composite beams using light steel sections. 2004.

[29]. Liu, S., et al., Numerical and experimental study on pull-out behaviour of stud shear connector embedded in concrete. 2008. 38(71): p. 13-19 .

[30]. McCormac, J.C., Structural Steel Design-LRFD Method. Clemson University. 1995, HarperCollins College Publishers .

[31]. Sadrekarimi, A.J.J.o.A.C.T., Development of a light weight reactive powder concrete. 2004. 2(3): p. 409-417 .

[32] Hannawayya, S., Behavior of reactive powder concrete beams in bending. 2010, Ph. D. Thesis, Building and Construction Engineering Department, University

[33]. Saeed, M.M, 2010. Shear Behavior of Reactive Powder Concrete Beams. Ph.D Thesis, University of Technology, pp.205

[34] Portoles, J., et al. (2013). "Influence of ultra-high strength infill in slender concrete-filled steel tubular columns." Journal of Constructional Steel Research 86: 107-114 .

[35] Zeghiche, J. and K. Chaoui (2005). "An experimental behaviour of concrete-filled steel tubular columns." Journal of Constructional Steel Research 61(1): 53-66.

[36] SCHNEIDER, S. P. (1998). “Axially loaded concrete-filled steel tubes”.Journal of Structural Engineering, 124(10), 1125–1138.

[37] EN 1994-1-1:2004. Eurocode 4 : Design of composite steel and concrete structures Part 1-1 : General rules and rules for buildings. Eur Comm Stand 2004:1–117. doi:10.1680/dgte4.31517.

[38] DBJ/T 13-51-2010 2010. Technical specification for concrete-filled steel tubular structures. Department of Housing and Urban-Rural Development of Fujian Province, Fuzhou, China.

[39] AIJ (2008). “Recommendations for design and construction of concrete filled steel tubular structures”. Architectural Institute of Japan, Tokyo, Japan.

[40] AISC-LRFD (2010), "AISC Manual for Steel Construction”. American Institute for Steel Construction, USA.

[41] AS5100 (2004), “Bridge Design-steel and Composite Construction”. Australian Standard.

[42] TAO, Z., HAN, L. H. & ZHAO, X. L. (2004). “ Behaviour of concrete filled double skin (CHS inner and CHS outer) steel tubular stub columns and beam-columns”. Journal of Constructional Steel Research, 60(8), 1129–1158.

[43] ZHAO, X. L. & GRZEBIETA, R. (2002). “Strength and ductility of concrete filled double skin (SHS inner and SHS outer) tubes”. Thin-Walled Structures, 40(2), 199– 213.

[44] TAO, Z., HAN, L. H. & WANG, Z. B. (2005). “Experimental behavior of stiffened concrete-filled thin-walled hollow steel structural (HSS) stub columns”. Journal of Constructional Steel Research, 61(7), 962–983.

[45] HAN, L. H., REN, Q. X. & LI, W. (2010). “Tests on inclined, tapered and STS concrete-filled steel tubular (CFST) stub columns”. Journal of Constructional Steel Research, 66(10), 1186–1195.

[46] LI, W., REN, Q. X., HAN, L. H. & ZHAO, X. L. (2012). “Behavior of tapered concrete-filled double skin steel tubular (CFDST) stub columns.” Thin Walled Structures, 57, 37–48.

[47] UY, B. (2001). “Strength of short concrete filled high strength steel box columns. ” Journal of Constructional Steel Research, 57(2), 113–134.

[48] MURSI, M. & UY, B. (2004). “Strength of slender concrete filled high strength steel box columns.” Journal of Constructional Steel Research, 60(12), 1825–1848.

[49] YOUNG, B. & ELLOBODY, E. (2006). “Experimental investigation of concretefilled cold-formed high strength stainless steel tube columns.” Journal of Constructional Steel Research, 62(5), 484–492.

[50] Uy, B., Tao, Z., and Han, L.-H. (2011). “Behaviour of short and slender concretefilled stainless steel tubular columns.” Journal of Constructional Steel Research, 67(3), 360–378.

[51] VARMA, A. H., RICLES, J. M., SAUSE, R. & LU, L. W. (2002). “Experimental behavior of high strength square concrete-filled steel tube beamcolumns. ” Journal of Structural Engineering, 128(3), 309–318.

[52] YU, Q., TAO, Z. & WU, Y. X. (2008). “ Experimental behaviour of high performance concrete-filled steel tubular columns. ” Thin-Walled Structures, 46(4), 362–370.

[53] XIONG, D. X. (2012). “Structural behaviour of concrete filled steel tubes with high strength materials. ” PhD thesis, National University of Singapore

[54] YANG, Y. F. & HAN, L. H. (2006). “Experimental behaviour of recycled aggregate concrete filled steel tubular columns.” Journal of Constructional Steel Research, 62(12), 1310–1324.

[55] TAM, V. W., WANG, Z. B. & TAO, Z. (2014). " Behaviour of recycled aggregate concrete filled stainless steel stub columns". Materials and Sructures, 47(1), 293– 310.

[56] FU, Z. Q., JI, B. H., LV, L. & ZHOU, W. J. (2011). " Behaviour of lightweight aggregate concrete filled steel tubular slender columns under axial compression". Advanced Steel Construction, 7(2), 144–156.

[57] Uy, B., Tao, Z., and Han, L.-H. (2011). "Behaviour of short and slender concrete filled stainless steel tubular columns." Journal of Constructional Steel Research, 67(3), 360–378.

[58] Portolés J M, Serra E and Romero M L (2013), "Influence of ultra-high strength infill in slender concrete-filled steel tubular columns", Journal of Constructional Steel Research, Vol. 86, July, pp. 107-114.

[59] Essopjee, Y. and M. J. C. S. Dundu (2015). "Performance of concrete filled double-skin circular tubes in compression." 133: 1276-1283

[60] SANS (SANS 10162-1). (2000). The structural use of steel Part 1: Limit state design of hot-rolled steelwork. Pretoria: Standards South Africa.

[61] Mahgub, M., Ashour, A., Lam, D., and Dai, X. (2017). "Tests of self compacting concrete filled elliptical steel tube columns." Thin-Walled Structures, 110, 27–34.

[62] Elchalakani, M., et al. Experimental tests and design of rubberised concrete-filled double skin circular tubular short columns. in Structures. 2018. Elsevier.

[63] T. Ekmekyapar and H. Ghanim Hasan, "The influence of the inner steel tube on the compression behaviour of the concrete filled double skin steel tube (CFDST) columns," Mar. Struct., vol. 66, no. December 2018, pp. 197–212, 2019, doi: 10.1016/j.marstruc.2019.04.006.

[64] Eom, S.-S., et al. (2019). "Flexural behavior of concrete-filled double skin steel tubes with a joint." 155: 260-272.

[65] Yuan, F., et al. (2019). "Effect of stiffeners on the eccentric compression behaviour of square concrete-filled steel tubular columns." 135: 196-209

[66] X. F. Yan and Y. G. Zhao, “Compressive strength of axially loaded circular concrete-filled double-skin steel tubular short columns,” J. Constr. Steel Res., vol. 170, p. 106114, 2020, doi: 10.1016/j.jcsr.2020.106114.

[67] V. I. Patel, Q. Q. Liang, and M. N. S. Hadi, “Numerical analysis of circular double-skin concrete-filled stainless steel tubular short columns under axial loading,” Structures, vol. 24, no. February, pp. 754–765, 2020, doi: 10.1016/j.istruc.2020.02.001.

[68] Soutsos, M. N., Millard, S.G., and Karaiskos, K. “Mix Design, Mechanical Properties, and Impact Resistance of Reactive Powder Concrete (RPC)” Department of Civil Engineering, University of Liverpool, Liverpool, UK 2001, pp. 1-10

[69] Nematollahi, B., Saifulnaz, R., Jaafer, M.S. and Voo, Y.L., “A Review on Ultra High Performance Ductile Concrete (UHPdC) Technology”, International Journal of Civil and Structural Engineering, Vol.2, No.3, 2012, pp.1003-1018

[70] Batoz, J.F. and Behloul, M., “UHPFRC Development on the Last Two Decades: An Overview”, Proceedings of UHPFRC, Nov.17-18, 2009, Marseille, France, 13pp

[71] Richard, P. and Cheyrezy, M., 1995. Composition of reactive powder concretes. Cement and concrete research, Vol. 25, No 7, pp.1501-1511.

[72] Hassan , H.F.,2012. Punching shear behavior of Normal and Modified Reactive powder concrete slabs. Ph.D Thesis, Al-Mustansiryia University , pp.236.

[73]AL-Amery S. M., “Influence of Using Ultra Fine Steel Fiber on the Behavior of Reactive Powder Concrete Slabs”, MSc. Thesis, University of Babylon, Iraq 2013

[74] K. H. Hoang, P. Hadl, and A. T. N. V., "A New Mix Design Method for UHPC based on Stepwise Optimization of Particle Packing Density," First International Interactive Symposium on UHPC, 2016.

[75] Abdulrahman. M., Al-Atta. A. and Ahmad.M., 2014 . Effect of different curing conditions on the mechanical properties of reactive powder concrete. Tikrit University.

[76] J.F.Sima, P.Roca and C.Molins, "Cyclic constitutive model for concrete," Engineering Structures, vol. 30, pp. 695-706, 2008.

[77] Iraqi Specification, No. 5/1984, "Portland Cement". وزارة التخطيط والجهاز المركزي للتقييس والسيطرة النوعية.

[78] Iraqi Specification, No. 45/1984, "Aggregate from Natural Sources for Concrete and Construction " , وزارة التخطيط والجهاز المركزي للتقييس والسيطرة النوعية

[79] Iraqi Specification, No. 45/1984, "Aggregate from Natural Sources for Concrete and Construction " , وزارة التخطيط والجهاز المركزي للتقييس والسيطرة النوعية

[80] Megaadd MS company "Densified micro silica " construction chemical,Sharjah UAE-Tel: 0097165314155, email: conmix@conmix.com

[81] ASTM C 1240-05, "Standard Specification for the Use of Silica Fume as a Mineral Admixture in Hydraulic Cement Concrete, Mortar, and Grout", Vol 04.02, 2005, pp. 1-7.

[82] Sika ViscoCrete® -5930," High Performance Superplasticizer Concrete Admixture", product Data Sheet, Edition 02, 2015. Version no. 12.2014.

[83]ASTM C494-99,"Chemical Admixture for Concrete", Annual Book of ASTM Standards American Society for Testing and Materials, Vol.04-02, 1999, PP. 245-252..

[84] ASTM A1058, "Standard Test Methods and Definitions for Mechanical Testing of Steel Products," ASTM International, 2004.

[85] ASTM A370, ''Standard Test Method and Definitions for Mechanical Testing of Steel Products" American Society for Testing and Materials, 1977.

[86]AL-Amery S. M., “Influence of Using Ultra Fine Steel Fiber on the Behavior of Reactive Powder Concrete Slabs”, MSc. Thesis, University of Babylon, Iraq 2013.

[87] Kindeel, Z. “Ultimate Strength Capacity and the Bond-Slip Behavior of Composite Ultra- High Performance Concrete-Steel Beams” Ph.D. Thesis, University Of Babylon-Iraq, 2015.

[88] Wille, K., Naaman, A.E., Parr-Montesinos, G.J., 2011. "Ultra-High Performance Concrete with Compressive Strength Exceeding 150MPa (22ksi): A Simpler Way", ACI Materials Journal, Vol.108, No.1, January February 2011, pp.46-54.

[89]Abd Aoun, A, “Comparative Study for Different Types of Reinforced Concrete Spliced Girders”, MSc. Thesis, University of Kerbala, Iraq 2018.

[90] Grout, F. J. M. c. s. a. "Grout for pressure-injection grouting shall be a high-strength, nonshrink, cementitious, adhesive grout conforming with ASTM C1107, Grade C, or a high-strength, non-shrink, manufactured epoxy adhesive grout." 28

[91] T. P. E-1007D, “Strain Gauge,” Tokyo, 2017.

[92] ASTM C 143/C 143M-05a, 2005 "Standard Test Method for Slump of Hydraulic-Cement Concrete", Book of ASTM Standards, American Society for Testing and Materials, pp. 1-4.

[93] Standard Practice for Selecting Proportions for Normal, Heavyweight, and Mass Concrete (ACI 211.1-15)

[94] B.S. 1881, part 116, 1989 "Method of Determination of Compressive Strength of Concrete Cubes", British Standards Institution, 1989, 3pp.

[95] ASTM C496/C496M-04, “Standard Test Method for Splitting Tensile Strength of Cylindrical Concrete Specimens”, Vol. 04.02, 2004, 5p.

[96] ASTM C 469-02, “Standard Test Method for Static Modulus of Elasticity and Poisson’s Ratio of Concrete in Compression”, 2002, 5pp.

[97] ACI Committee 318M-318RM, "Building Code Requirements for Structural Concrete and Commentary”, American Concrete Institute, Farmington Hills, Michigan, 2011, 503 pp.

[98] Graybeal, B.A"Compressive behavior of ultra-high-performance fiber-reinforced concrete", ACI materials journal, 2007. 104(2): p. 146.

[99] Mahgub M, Ashour A, Lam D, Dai X. Tests of self-compacting concrete filled elliptical steel tube columns. Thin-Walled Struct 2017;110:27–34.

[100] Hasan, Hussein Ghanim, Talha Ekmekyapar, and Bashar A %J Marine Structures Shehab 2019 Mechanical performances of stiffened and reinforced concrete-filled steel tubes under axial compression. 65:417-432.

[101] Jain, S., Chellapandian, M., & Prakash, S. S. (2017). Emergency repair of severely 113 damaged reinforced concrete column elements under axial compression: An experimental study. Construction and Building Materials, 155(0), 751–761.

[102] A. C. 318, Building Code Requirements for Structural Concrete (ACI 318-14)[and] Commentary on Building Code Requirements for Structural Concrete (ACI 318R-14). 2014.

[103] AISC, “Specification for Structural Steel Buildings,” American Institute of Steel Construction ANSI/AISC 360-16, Chicago, Illinois, 2016.

[104]CEN, “Design of composite steel and concrete structures – Part 1-1: General rules and rules for buildings,” EN 1994-1-1 Eurocode 4, Brussels, 2004

Appendixes

Appendix A

1. Silica Fume Properties

Construction Chemicals

CON MIX

MegaAdd MS(D)

Densified Microsilica

DESCRIPTION

MegaAdd MS(D) is a very fine pozzolanic, ready to use high performance mineral additive for use in concrete. It acts physically to optimize particle packing of the concrete or mortar mixture and chemically as a highly reactive pozzolan.

MegaAdd MS(D) in contact with water, goes into solution within an hour. The silica in solution forms an amorphous silica rich, calcium poor gel on the surface of the silica fume particles and agglomerates. After time the silica rich calcium poor coating dissolves and the agglomerates of silica fume react with free lime ($Ca(OH)_2$) to form calcium silicate hydrates (CSH). This is the pozzolanic reaction in cementitious system.

STANDARDS

ASTM C 1240

USES

MegaAdd MS(D) can be used in a variety of applications such as concrete, grouts, mortars, fibre cement products, refractory, oilgas well cements, ceramics, elastomer, polymer applications and all cement related products.

ADVANTAGES

- High to ultra high strength
- High resistance to chlorides and sulfates
- Protection against corrosion
- Increased durability, longer service life for structures
- Enhanced rheology, control of mixture segregation and bleed
- Greater resistance to chemicals

TYPICAL PROPERTIES at 25°C

PROPERTY	TEST METHOD	VALUE
State	Amorphous	Sub-micron powder
Colour	-	Grey to medium grey powder
Specific Gravity	-	2.10 to 2.40
Bulk Density	-	500 to 700 kg/m³
Chemical Requirements		
Silicon Dioxide (SiO_2)	-	Minimum 85%
Moisture Content (H_2O)	-	Maximum 3%
Loss on Ignition (LOI)	-	Maximum 6%
Physical Requirements		
Specifi Surface Area	-	Minimum 15 m²/g
Pozzolanic Activity Index, 7 days	-	Maximum 105% of control
Over size particles retained on 45 micron sieve	-	Maximum 10%

COMPATIBILITY

MegaAdd MS(D) is suitable for use with all types of cement and cementitious materials.

With Admixtures :

MegaAdd MS(D) is compatible to use with all types of water reducing plasticisers / superplasticisers and poly carboxylate based superplasticiser.

DOSAGE

The normal dosage of **MegaAdd MS(D)** is 5 - 8% by weight of cement, but it can be used up to 10%. Site trials should be carried out to establish the optimum dosage for the mix to be used as the dosage varies depending on application.

Construction Chemicals

CONMIX

MegaAdd MS(D)

BATCHING	Batch **MegaAdd MS(D)** into the concrete mixer and mix thoroughly with the other mixture ingredients, adopting a procedure that ensures full dispersion of the product.	
PACK SIZE	600 Kgs and 1200 Kgs Jumbo bags	
GENERAL INFORMATION	**Shelf Life**	12 months from date of manufacture when stored under warehouse conditions in original unopened packing. Extreme temperature / humidity may reduce shelf life.
	Cleaning	Clean all equipments and tools with water immediately after use.
HEALTH and SAFETY	**PPE's**	Gloves, goggles and suitable mask must be worn.
	Precautions	Contact with skin, eyes, etc. must be avoided.
	Hazard	Regarded as non-hazardous for transportation.
	Disposal	Do not reuse bags. To be disposed off as per local rules and regulations.
	Additional Information	Refer MSDS. (Available on request.)
TECHNICAL SERVICE	**CONMIX Technical Services** are available on request for onsite support to assist in the correct use of its products.	

2- Chemical Admixture properties

Construction

Sika ViscoCrete® -5930

High Performance Superplasticiser Concrete Admixture

Product Description

Sika ViscoCrete® -5930 is a third generation super plasticizer for concrete and mortar. It meets the requirements for super plasticizer according to ASTM-C- 494 Types G and F and BS EN 934 part 2: 2001.

Uses

Sika ViscoCrete® -5930 is suitable for the production of concrete.

Sika ViscoCrete® -5930 facilitates extreme water reduction, excellent flowability at the same time optimal cohesion and highest self compacting behaviour.

Sika ViscoCrete® -5930 is used for the following types of concrete:

- Precast concrete.
- Ready Mix Concretes.
- Concrete with highest water reduction (up to 30%).
- High strength concrete.
- Hot weather Concrete.
- Self compacting concretes.

High water reduction, excellent flowability, coupled with high early strengths, have a positive influence on the above mentioned applications.

Advantages

Sika ViscoCrete® -5930 acts by different mechanisms. Through surfaces adsorption and sterical separation effect on the cement particles, in parallel to the hydration process, the following properties are obtained:

- Strong self compacting behaviour. Therefore suitable for the production of self compacting concrete.
- Extremely high water reduction (resulting in high density and strengths).
- Excellent flowability (resulting in highly reduced placing - and compacting efforts)
- Increase high early strengths development.
- Improved shrinkage- and creep behaviour.
- Reduced rate of carbonation of the concrete.
- Improved Water Impermeability.

Sika ViscoCrete® -5930 does not contain chloride or other, steel corrosion promoting ingredients, it may therefore be used without any restrictions for reinforced and prestressed concrete construction.

Technical Data

Basis	Aqueous solution of modified Polycarboxylate
Appearance	Turbid liquid
Density	1.095 kg/lt. (ASTM C494)
Packaging	5 Kg, 20 Kg pails 200 kg drums Bulk Tanks are available upon request.
Storage/ Shelf Life	In unopened, undamaged original container, protected from direct sunlight and frost at temperatures between + 5 °C and + 35°C. Shelf life at least 12 months from date of production.

Sika®

3.Steel Fibre Properties

河北宇森网类制品有限公司
Hebei YuSen Metal Wire Mesh Co., Ltd.
钢纤维质量证明书
Steel fibre quality certificate

地址(ADDRESS)：河北省安平县丝网大世界开发区
Wire Mesh World Anping, Hengshui, Hebei, P. R. China
电话（TEL）：+86-318-7758858
传真（FAX）：+86-318-5288858
网址（WEB）：www.china-steelfiber.com.cn
邮箱(EMAIL)：yusen01@metalmesh.com.cn

名称：Description	微丝镀铜钢纤维(Micro copper coated straight steel fiber)	订单号：Order No.	20180226
规格：DIMENSIONS	0.2*13mm	质量证明书号：Certificate ID	YS-GQW18022803
执行标准：Executive Standard	ASTM A820-96, YB/T151-1999	签发日期：Date Of Issue	2018.02.28

检测项目 Detected items	等效直径 Diameter	长度 Length	抗拉强度 Tensile Strength	长径比 L/D	弯曲性能，变芯 3mm Bending Properties ,Bend Core 3mm	外观质量 Quality of Soating
标准值 Standard values	0.2mm-0.25 mm	13±10%	≥2850	30-100	冷弯 90°，9/10 不断 Cold bend 90°,9/10 have not broken	OK
检测值 Detected value	0.22mm	13.1	3005	59	10/10 不断 10/10 have not broken	OK

综合判定 Final Resrult	合 格 OK	1、质量证明书复印件不作有效证明文件。The copy of this certificate is invalid. 2、用户验货使用有异常及时告知编号，并保留实物及标志。The no. will be sent to ours in time by the customer,if the complain would happened after in section.Keep in the material and the marking card.	质量印章 SEAL	签证人 Inspector

4.Flo-Grout BP800 properties

Flo-Grout BP800

Non shrink cementitious bearing pads precision grout

Description

Flo-Grout BP800 is a pre-mixed, pre-packed, high strength, chloride and hydrogen free cementitious grout. Flo-Grout BP800 is compound of cement, selected additives, well graded fillers, and non-reactive aggregates designed to give excellent flow properties, shrinkage compensation, and high compressive strength.

Applications

Flo-Grout BP800 is ideally designed for grouting areas beneath bridge bearing pads, pile caps treatment, heavy stanchion bases and base plates where high strength grout is required.

Advantages

- Non-shrink grout.
- Suitable for use in hot climates.
- Extremely dense and low permeability.
- High initial and ultimate strength allowing for rapid installation.
- Good flow can be poured or pumped into variable thicknesses down to 10 mm.
- Easy to apply, single component, requires only addition of water.
- Hydrogen and chloride free.

Standards

Flo-Grout BP800 complies with U.S. Corps of Engineers Specifications CRD–CS88-79 and CRD – C621 and ASTM C1107, Grade C.

Method of Use

Substrate Preparation

The Substrate should be sound, clean and free from contamination. Surface Laitance should be removed by suitable mechanical means.

All surfaces should be pre-soaked with clean water for a minimum period of 4 hours prior to grouting.

Mixing

To ensure proper mixing, a mechanically powered mixer or drill fitted with suitable paddle should be used.

Technical Properties:

Compressive strength: ASTM C109/109M-11	30 MPa @ 1 day 60 MPa @7 days 80 MPa @ 28 days
Flexural strength: ASTM C348	> 10 MPa @ 28 days
Colour:	Grey
Plastic-expansion characteristics: ASTM C827/C827M-10	Up to 2%
Bleeding: ASTM C940	Nil
Hardening stage expansion: ASTM C1090	Up to 0.3% @ 28 days
Fresh wet density:	≈ 2.0 gm/ cm³

Note: Typical properties for Flo-Grout BP800 are obtained @ 3.75 litres/ 25 kg @ 25°C.
Compressive strength @ 1 day is under restrain.

Depending on the consistency required, 4.5 litres (Fluid) or 3.75 litres (Flowable) of clean water should be added to a clean container. The 25 kg powder is then added slowly to the water while mixing continuously with low speed mixer/drill (400 - 600 rpm). Mixing time should be continued for 4 to 5 minutes until a uniform consistency is obtained. Where the first 2 minutes of mixing the mixture will be stiff.

The mixed grout shall be poured immediately after mixing, the grouting operation must be carried out continuously.

Placing and Finishing

Enough material should be available to achieve continuous fill and to complete the work. Pouring of the mixed grout should be started from one side only to avoid air entrapment. To obtain maximum flow distance, a side shutter feed between 100mm to 250 mm high should be erected and used to build the required

Flo-Grout BP800

Formwork:
As the mixed grout possesses high fluidity characteristics, all formworks and shutters should be water tight.

This can be obtained by sealing underneath the formwork and at the joints by using appropriate mastic. The unrestrained areas should be kept to a minimum due to the expansion nature of Flo-Grout BP800.

Curing

As Flo-Grout BP800 is a cementitious material, it should be cured conventional means.

Curing can be conducted using a good concrete curing compound such as Setseal 44.

Notes:
- At low temperatures (below 8°C), warm water is recommended to achieve the early strength. Form work striking is to be delayed as necessary.
- At high temperatures (35°C and above), cold water (less than 20°C) must be used for mixing. Materials shall be stored in a cool shaded area prior to mixing, avoid application shall commence in early morning hours or after sunset where temperature is falling.

Cleaning

All tools should be cleaned immediately after application using fresh water. Hardened materials must be cleaned mechanically.

Packaging

Flo-Grout BP800 is available in 25 kg bags.

Thicknesses and Size Limitations

Flo-Grout BP800 can be applied in a single layer at thickness between 10 – 180 mm. For greater thicknesses, Flo-Grout BP800 (WWA) should be used. Flo-Grout BP800 (WWA) contains 8 – 12 mm well graded washed aggregates to minimize exothermic or 14 kg of washed aggregates should be added to 25 kg of Flo-Grout BP800.

Yield

Approximately 14 - 15 litres/ 25 kg bag depending on consistency.

Storage

Flo-Grout BP800 has a shelf life of 12 months if stored at temperatures between 2°C and 40°C in original unopened bags.

If these conditions are exceeded, DCP Technical Department should be contacted for advice.

Cautions

Health and Safety

Flo-Grout BP800 may cause irritation to skin or eyes.

In case of accidental contact with eyes, immediately flush with plenty of water for at least 10 minutes and seek medical advice if necessary.

For further information refer to the Material Safety Data sheet.

Fire

Flo-Grout BP800 is non-flammable.

More from Don Construction Products

A wide range of construction chemical products are manufactured by DCP which include:

- Concrete admixtures.
- Surface treatments
- Grouts and anchors.
- Concrete repair.
- Flooring systems.
- Protective coatings.
- Sealants.
- Waterproofing.
- Adhesives.
- Tile adhesives and grouts.
- Building products.
- Structural strengthening.

Appendix B

Design criteria of compressive strength for CFST columns by

1. **AISC 360 – 16**

The AISC 360-16 specification provides an approach for predicting the compressive strength of CFST columns within the specified limitations (TABLE I1.1a).The compressive strength of CFST columns is determined in accordance with the CFST section classification for local buckling, as shown in below:

where $\lambda p = 0.15\frac{Es}{Fy}$ (for a circular section) and $2.26\sqrt{\frac{Es}{Fy}}$ (for a square section), $\lambda r = 0.19\frac{Es}{Fy}$ (for a circular section) and $3.00\sqrt{\frac{Es}{Fy}}$ (for a square section).

For circular section

$\lambda = \frac{D}{t} = \frac{100}{2.2} = 45.45$

where $\lambda p = 0.15 * \frac{201065}{344.6} = 87.52$

and $\lambda r = 0.19 * \frac{201065}{344.6} = 110$

$\lambda \leq \lambda p$ The section is compact and less than $0.31* \frac{Es}{Fy} = 180$:. Ok

For a compact section, the compressive strength of the CFST section (pn_o) is equal to the plastic strength of section (p_p) as follows:

$\mathrm{Pno} = \mathrm{Pp\ (AISC)} = (\mathrm{Asfy}) + \mathrm{C2Acfc'}$

$$Pno = 344.6 * 675 + 344.6 * 330 + 0.95 * 5211 * 25$$

=470084N

According to American institute of steel construction, the theoretical load carrying capacity of CFST column is given by

(a) When $\frac{P_{no}}{P_e} \leq 2.25$

$$P_n = P_{no}\left(0.658^{\frac{P_{no}}{P_e}}\right)$$

(b) When $\frac{P_{no}}{P_e} > 2.25$

$$P_n = 0.877P_e$$

Moment of Inertia steel:

$$Is\ for\ outer\ tube\ = \frac{\pi\ (100^4 - 95.6^4)}{64}$$

=808162.34961 mm^4

$$Is\ for\ inner\ tube = \frac{\pi\ (50^4 - 45.6^4)}{64}$$

= 94507.2289mm^4

Moment of Inertia concrete:

$$Ic\ = \frac{\pi(95.6^4 - 50^4)}{64}$$

=3791447.028

Total Moment of inertia I = 4694116.607mm^4

Similarly, for Area of outer tube = 675 mm^2

Area of inner tube = 330 mm^2

Area of concrete = 5211mm^2

Total area of cross section composite column = 6216mm^2

Radius of gyration = $R_s = \sqrt{\left(\frac{Isc}{Asc}\right)}$

= 27.48

K=1

Slenderness ratio = $\frac{KL}{r} = \frac{1*800}{27.84}$

=29.11< 40 :. Short column

C3 =0.45 +3(As/Ag) ≤ 0.9

=0.45+3(330+675/330+675+5211) =0.9 ≤ 0.9

$E_c = 0.043(Wc)^{1.5} * F'c^{0.5}$

$=0.043(2400)^{1.5} * 25^{0.5}$

=25278 Mpa

$EI\ eff = Es * Is + C3 * Ec * Ic$

=((94507.2289+808162.34961)*201065+0.9 *3791447.028*25278)

$=2.63995* 10^{11}$Mpa

$p_e = \frac{\pi^2 EI\ eff}{(KL)^2}$

Pe=4124916.82N

$$\frac{p_{no}}{p_e} = 0.11 < 2.25$$

$p_{u=p_{no}} = (0.658^{\frac{p_{no}}{p_e}})$

Pu(AISC)=448188 N

For square section

$\lambda = \frac{B}{t} = \frac{100}{2.2} = 45.45$

where $\lambda p = 2.26 * \sqrt{\frac{Es}{fy}} = 2.26 * \sqrt{\frac{201065}{344.6}} = 54.59$

and $\lambda r = 3 * \sqrt{\frac{Es}{fy}} = 3 * \sqrt{\frac{201065}{344.6}} = 72.46$

$\lambda \leq \lambda p$ The section is compact and less than $5 * \sqrt{\frac{Es}{fy}} = 120$:. Ok

For a compact section, the compressive strength of the CFST section (pn_o) is equal to the plastic strength of section (p_p) as follows:

Pno = Pp (AISC) = (Asfy) + C2Acfc′

Pno = 344.6 * 860.64 + 344.6 * 420.64 + 0.85 * 6639.36 * 25

=599213.888 N

According to American institute of steel construction, the theoretical load carrying capacity of CFST column is given by

(a) When $\frac{P_{no}}{P_e} \leq 2.25$

$$P_n = P_{no}\left(0.658^{\frac{P_{no}}{P_e}}\right)$$

(b) When $\frac{P_{no}}{P_e} > 2.25$

$$P_n = 0.877P_e$$

Moment of Inertia steel :

$$Is\ for\ outer\ tube = \frac{(100 * 100^3 - 95.6 * 95.6^3)}{12}$$

$= 1372674.899\text{mm}^4$

$$Is\ for\ inner\ tube = \frac{(50 * 50^3 - 45.6 * 45.6^3)}{12}$$

$= 160521.8325\text{mm}^4$

Moment of Inertia concrete:

$$Ic = \frac{(95.6 * 95.6^3 - 50 * 50^3)}{12}$$

$=6439825.101$

Total Moment of Inertia = 7973021.833mm^4
Similarly, for Area of outer tube = $675\ \text{mm}^2$

Area of inner tube = $330\ \text{mm}^2$

Total area = 7919mm^2

Radius of gyration = $R_s = \sqrt{\left(\frac{Isc}{Asc}\right)}$

= 31.72845215

K=1

Slenderrness ratio $= \frac{KL}{r} = \frac{1*800}{31.72}$

= 25.21 < 40 :. Short column

C3 =0.45 +3(As/Ag) ≤ 0.9

=0.45+3(420+860/420+860+6639) =0.9 ≤ 0.9

$E_c = 0.043(Wc)^{1.5} * F'c^{0.5}$

$=0.043(2400)^{1.5} * 25^{0.5}$

=25278 Mpa

$EI\ eff = Es * Is + C3 * Ec * Ic$

=((1372674.89+160521.8325)*201065+0.9 *6439825.101*25278)

$= 4.440 * 10^{11}$Mpa

$p_e = \frac{\pi^2 EI\ eff}{(KL)^2}$

Pe=6840707 N

$$\frac{p_{no}}{p_e} = 0.085 < 2.25$$

$p_{u=p_{no}} = (0.658^{\frac{p_{no}}{p_e}})$

Pu(AISC) =561794N

2.EN 2004

For circular section

$P_{pl,Rd} = \text{Asfy} + \text{Acfc}'$

=675*344.6+330*344.6+5211*25

= 476897.7741 N

λ^- the relative slenderness ratio; when the confinement effect is considered, if the value of λ^- does not exceed 0.5.

$$\lambda^- = \sqrt{\frac{NP_{pl,Rd}}{Ncr}} \leq 0.5$$

Ec = (22000*((fc'+8)/10)^0.3

= 31475.80

$\text{EI eff} = \text{Es} * \text{Is} + 0.6 * \text{Ec} * \text{Ic}$

= ((94507.2289+808162.34961) *201065+0.6 *3791447.028*31475.80)

$= 2.53099 * 10^{11}$

$$N_{cr} = \frac{\pi^2 EI\ eff}{(KL)^2}$$

$$= \frac{\pi^2 * 2.53099 * 10^{11}}{(1*800)^2}$$

=3899141.648N

:. λ^- =0.34

EC4 code adopts simplified method to predict the capacity of CFST columns. This code gives details to estimate the confinement effect, and the confinement

effect is considered if the relative slenderness $\bar{\lambda}$ is lower than 0.5. The plastic resistance of the CFST section ($NP_{pl,Rd}$) is calculated by adding the resistance of the steel and concrete. The plastic compressive capacity of circular CFST column as:

$$N_{EC4} = \eta_a A_s f_y + A_c f_c \left(1 + \eta_c \frac{t}{D}\frac{f_y}{f_c}\right)$$

$$\eta_a = 0.25(3 + 2\bar{\lambda}) \leq 1.0$$

ηa = 0.25(3+2*0.3) =0.9

$$\eta_c = 4.9 - 18.5\bar{\lambda} + 17\bar{\lambda}^2 \geq 0$$

ηc =4.9-18.5*0.3+17*0.3^2 =0.88

$N_{EC4=}$0.9*(330*334.6+675*334.6)+(5211*25)(1+0.88*(2.2*334.6/100*25))

=47636.2648N

Finally, the plastic resistance of CFST section is multiplied by the below reduction factor (χ),

$$\chi = \frac{1}{\phi + \left(\phi^2 - \bar{\lambda}^2\right)^{0.5}} \leq 1.0$$

$$\phi = 0.5\left[1 + \alpha(\bar{\lambda} - 2) + \bar{\lambda}^2\right]$$

Where α, is an imperfection factor, equal to 0.21 for CFST columns.

Φ =0.5(1+0.21(0.34-2) +0.34^2)

=0.38

$X = \frac{1}{0.38+(0.38^2-0.34^2)^{0.5}} = 0.97$

$pu_{EC4=}$ 462337 N

For square section

$P_{pl,Rd} = Asfy + Acfc'$

=860*334.6+420*334.6+6639*25

= 607513.088 N

λ^- the relative slenderness ratio; when the confinement effect is considered, if the value of λ^- does not exceed 0.5.

$\lambda^- = \sqrt{\frac{NP_{pl,Rd}}{Ncr}} \leq 0.5$

Ec =(22000*((fc'+8)/10^0.3))

= 31475.80621

=((1372674.89+160521.8325)*201065+0.6 *6439825.101*31475.8062)

$= 4.2989 * 10^{11}$

$N_{cr} = \frac{\pi^2 EI\ eff}{(KL)^2}$

$= \frac{\pi^2 * 4.2989 * 10^{11}}{(1*800)^2}$

=6622745.899N

:. λ^- =0.3

In square section don't consider the effect of confinement , the plastic resistance of CFST section is multiplied by the below reduction factor (χ),

$$\chi = \frac{1}{\phi + \left(\phi^2 - \bar{\lambda}^2\right)^{0.5}} \leq 1.0$$

$$\phi = 0.5\left[1 + \alpha\left(\bar{\lambda} - 2\right) + \bar{\lambda}^2\right]$$

Where α, is an imperfection factor, equal to 0.21 for CFST columns.

Φ =0.5(1+0.21(0.3-2)+0.3^2)

=0.38

$X = \frac{1}{0.38+(0.38^2-0.3^2)^{0.5}} = 0.97$

$pu_{EC4=}$ *607513 N*

3.ACI code

The ACI code [30] ignores the concrete confinement effect. The ACI equation for the ultimate axial strength (PU_{AcI}) of a concrete filled circular column incorporating the contribution of the internal tube is given as

$$\mathrm{PU,(ACI)} = \left(A_{si}f_{syi}\right) + \left(A_{so}f_{syo}\right) + 0.85A_C f_C{}'$$

Where A_{so} is the cross-sectional area of the external steel tube.

A_C is the cross-sectional area of the concrete infill between both tubes,

$f_C{}'$is the unconfined cylindrical concrete strength,

and A_{si} is the cross-sectional area of the internal steel tube.

f_{syo} and f_{syi} are the yield strengths of the external and internal steel tubes, respectively.

For circular section

=0.85*25*5211 +675*344.6+330*344.6

=457353N

For square section

=0.85*25*6639 +860*344.6+420*344.6

=582619N

الخلاصة

الأعمدة المركبة المكونة من أعمدة فولاذية ثنائية الأنبوب مملوءة بخرسانة المساحيق الفعالة هي إحدى الطرق التي تجمع بين خصائص الخرسانة والفولاذ وأسرع في البناء مع قوة ضغط أفضل. تتكون هذه الطريقة من لحام أنبوبين من الفولاذ في أقسام مختلفة ولحامهما بشكل مركزي ، وملء الفجوة بينهما بمسحوق الخرسانة التفاعلي. تتكون الدراسة الحالية من جزء عملي يتضمن صب أربعة عشر عمودًا مركبًا من سبعة أقسام دائرية وسبعة أقسام مربعة بخصائص مختلفة لمعرفة أدائها المحوري. تم تقسيمها إلى ثلاث مجموعات ، المجموعة الأولى مملوءة بخرسانة المساحيق الفعالة ، المجموعة الثانية مملوءة بالخرسانة العادية والمجموعة الثالثة غير ممتلئة. جميع الأعمدة لها أبعاد مقطع عرضي (100 * 100) مم للمقطع المربع وقطر (100) مم للدائرية بسمك 2.2 مم. كانت أطوال العينات 800 مم ولكن اثنين فقط من العمود لهما 700 مم. تم فحص خصائص الأنبوب بالكود الأمريكي ، مما يحقق أداء مقبول من خلال الانثناء المحلي. تم توصيل الأنابيب الفولاذية بشكل مزدوج باللحام. تضمنت متغيرات الجزء العملي: نسبة ألياف الصلب في الخليط الخرساني حوالي 0.5٪ و 1.5٪ ، مساحة المقطع العرضي للخرسانة ، طول العمود ، إضافة روابط القص باللحام إلى الأنبوب الداخلي للعمود ونوع الخرسانة. تم تطبيق الحمل محوريًا وتركز على العمود. أظهرت نتائج العمل أن الأنابيب الفولاذية المملوءة بخرسانة المساحيق الفعالة رد الفعل تعطي مقاومة قصوى عالية مقارنة بالخرسانة العادية في حالة استخدامها. كما وجد أن الأنابيب الداخلية للأعمدة التي يتم تعزيزها بموصل القص بطولها الكلي تؤدي إلى زيادة قوة الأعمدة المملوءة بخرسانة المسحوق التفاعلي. تمت مقارنة النتائج التجريبية للقوة القصوى مع نقاط القوة في تصميم المعهد الأمريكي للإنشاءات الفولاذية (AISC) ، ومتطلبات كود البناء للخرسانة الإنشائية (ACI) ، والقانون الأوروبي .(EN 2004) أعطت معايير التصميم المذكورة توقعًا أفضل وأكثر تحفظًا للأقسام الفولاذية المربعة مقارنة بالأقسام الدائرية.

جمهورية العراق
وزارة التعليم العالي و البحث العلمي
جامعة كربلاء/ كلية الهندسة
قسم الهندسة المدنية

خرسانة المساحيق الفعالة المالئة للاعمدة الحديدية مزدوجة التجويف والتي تخضع الى احمال متكررة

رسالة مقدمة الى

قسم الهندسة المدنية في كلية الهندسة/ جامعة كربلاء

كجزء من متطلبات نيل شهادة الماجستير في علوم الهندسة المدنية – هندسة البنى التحتية

من قبل:

أحمد وفي عباس

(بكالوريوس في الهندسة المدنية – 2017)

اشراف :

أ.م.د. بهاء حسين محمد

أ.د. علي حميد ناصر

2021 م

1443 هـ